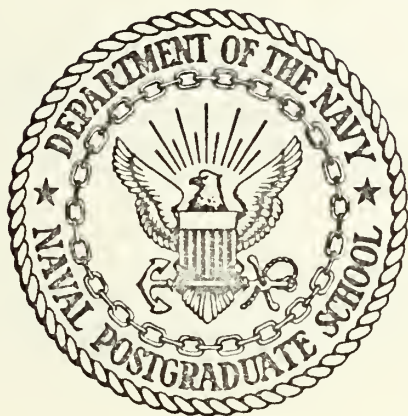


APPLICATION OF HOLOGRAPHIC INTERFEROMETRY TO
DENSITY FIELD DETERMINATION IN TRANSONIC
CORNER FLOW

Robert Anthony Kosakoski

NAVAL POSTGRADUATE SCHOOL

Monterey, California



THESIS

APPLICATION OF
HOLOGRAPHIC INTERFEROMETRY
TO
DENSITY FIELD DETERMINATION
IN TRANSONIC CORNER FLOW

by

Robert Anthony Kosakoski

Thesis Advisor

D. J. Collins

December 1972

T15-5776

Approved for public release; distribution unlimited.

Application of Holographic Interferometry
to Density Field Determination
in Transonic Corner Flow

by

Robert Anthony Kosakoski
Lieutenant, United States Navy
B.S.M.E., University of Rochester, 1965

Submitted in partial fulfillment of the
requirements for the degree of

AERONAUTICAL ENGINEER

from the

NAVAL POSTGRADUATE SCHOOL
December 1972

ABSTRACT

The successful application of holographic interferometry to the study of density fields around opaque bodies in wind tunnel experiments has been reported in the literature. The present report extends this technique to the study of the three-dimensional asymmetric flow fields encountered near the wing-fuselage junction of an aerodynamic model in the transonic flow regime. Finite fringe interferometry has been used to obtain fringe information about a partially transparent wing-body structure. A FORTRAN computer program was utilized to invert the fringe information and produce a plot of the density field around the model. The resulting asymmetric density field and shock wave structure are shown to be an accurate representation of the phenomena encountered in aerodynamic corner flow.

TABLE OF CONTENTS

I.	INTRODUCTION-----	5
II.	EXPERIMENTAL APPARATUS -----	7
	A. THE WIND TUNNEL -----	7
	B. THE HOLOGRAPHIC ARRANGEMENT -----	8
	C. THE WIND TUNNEL MODEL -----	9
III.	ANALYTICAL EVALUATION OF THE DENSITY FIELD-----	10
	A. THE BASIC EQUATION OF INTERFEROMETRY -----	10
	B. THE INTEGRAL INVERSION-----	12
	C. THE NUMERICAL PROCEDURE -----	15
IV.	EXPERIMENTAL PROCEDURE -----	18
	A. LABORATORY TECHNIQUES -----	18
	B. PHOTOGRAPHIC TECHNIQUES -----	20
	C. DATA REDUCTION -----	21
V.	EXPERIMENTAL RESULTS AND DISCUSSION -----	24
VI.	CONCLUSIONS -----	30
APPENDIX A: Reduction Of An Interferogram To Obtain		
	Fringe Shift Data-----	64
APPENDIX B: Application Of Computer Program "HOLOFER"-----		
		67
LIST OF REFERENCES -----		
		117
INITIAL DISTRIBUTION LIST -----		
		119
FORM DD-1473-----		
		120

ACKNOWLEDGEMENTS

This writer wishes to gratefully acknowledge Dr. D. J. Collins for his most valuable guidance and assistance during the course of this investigation; the Aerodynamics Division of the Naval Ship Research and Development Center, Carderock, Maryland, under Dr. R. Furey, particularly B. Ellis and O. Gilmore, for their tireless effort during the wind tunnel testing phase; the technical staff of the Department of Aeronautics under R. Besel and T. Dunton, particularly N. Leckenby and G. Middleton, for their able assistance in the fabrication and assembly of the models and equipment used in this study; and my wife and family for their noble patience and encouragement.

I. INTRODUCTION

The field of flow measurement has been revolutionized in recent years with the perfection of holography and holographic interferometry techniques. High power Q-switched and dye-switched lasers and sophisticated double-pulsing trigger mechanisms provide exposure times on the order of twenty nanoseconds, thereby "freezing" the flow during the hologram production process. The precision optical quality components and measurement techniques of Mach-Zehnder interferometry have given way to the much less restrictive requirements of holographic interferometry which provide high quality interferograms in three dimensions.

Techniques for the application of holography to interferometry have been reported by Heflinger, et al. [1], and by Brooks [2]. In the determination of the density field around a free jet in the supersonic regime, Matulka [3, 4] expressed the fringe data in a series of orthogonal polynomials and transformed them to polynomials representing density using an inversion technique reported in [5, 6]. The method was extended by Jagota [7, 8] to the determination of the three-dimensional density field around a ten-degree half angle cone in a supersonic wind tunnel. The ability to produce readable holograms in wind tunnel studies using transparent phase objects was verified by Heyer [9]. In the present report the aforementioned techniques

have been combined to study the three-dimensional density field near the wing-fuselage junction of an aerodynamic model in transonic flow. The experiment was conducted at the Naval Ship Research and Development Center, Carderock, Maryland in an eighteen inch transonic blow-down wind tunnel at a Mach number of 0.937, using a semi-transparent model of original design.

Since reasonably small variations in density were anticipated, a finite fringe technique was used in obtaining the interferograms. The horizontal finite fringe field was produced by a vertical translation of a diffusing glass in the scene beam a distance of 0.003 inches between the two exposures of the holographic plate. Fringe data obtained from the interferograms were reduced to density information using a modified form of the inversion computer program used in [7]. A self-testing procedure incorporated in the program verified the resulting density data as an accurate representation of the actual flow around the model.

II. EXPERIMENTAL APPARATUS

A. THE WIND TUNNEL

The investigation was conducted in the Naval Ship Research and Development Center blowdown supersonic wind tunnel. Transonic flow conditions were produced through incorporation of slotted upper and lower tunnel walls. The tunnel is a nominal eighteen inch blow-down-to-vacuum facility with a test section fourteen inches by eighteen inches in cross-section and twenty-nine inches in length with the slotted surfaces installed. Optical quality windows twenty-two inches in diameter in the side walls provided complete viewing of the flow in the test section as the model was rolled through 180 degrees for hologram production. A functional schematic of the wind tunnel is shown in Figure 1.

B. THE MACH NUMBER AND PRESSURE MEASUREMENT PROCEDURE

The Mach number at the test section is determined as a function of total and static pressure measurements and is maintained by carefully controlled butterfly valve settings. Total pressure is determined by recording atmospheric pressure prior to tunnel operation and accounting for the pressure loss between the plenum and the test section during operation. Static pressure is measured directly at a central wall port in the test section. Data recordings

were made on a Beckman Instruments Company 210 Digital Recorder, shown in Figure 2, and were read out on line via a Franklin Strip Tape Printer.

C. THE HOLOGRAPHIC ARRANGEMENT

The holographic arrangement is illustrated in Figure 3 and shown in photographs included as Figures 4, 5, 6, and 7. Two large wooden tables were constructed and linked together with two-by-four beams under the tunnel to form the experimental platform. Thick rubber pads were attached to the table legs to dampen possible floor vibrations. The bulk of the platform provided sufficient stability and vibration damping for the experiment. The monochromatic light source used was a KORAD K-1 pulsed ruby laser operating at a wavelength of 6943 Angstroms, together with a Pockels cell Q-switching device. The resultant effective exposure time was approximately twenty nanoseconds, eliminating the problems due to possible model vibration during hologram exposure. To maintain the laser head and output etalon at a constant temperature of 27.0 degrees Centigrade, a LAUDA constant temperature circulator Model K2R was used.

The reference beam was directed under the wind tunnel by four front surface mirrors, and the beam size was manipulated by means of lenses (Figure 3). The scene beam was routed through the test section to intersect the reference beam on the holographic plate at an angle of approximately fifty degrees. A diffuse glass, mounted on

a precision X-Y translation table in the scene beam, was used to produce light field holograms. Alignment of the Q-switched laser and system optics was accomplished using a continuous wave, low-power helium-neon laser. Reference grids were mounted accurately on the outer surfaces of the tunnel windows using a surveyor's transit. Details of the model mounting and reference grids are shown in Figure 7. To enable hologram production during daylight hours, the entire tunnel room was blacked out using drop curtains and light shields.

D. THE WIND TUNNEL MODEL

The aerodynamic model used is shown in Figures 8, 9, and 10. The metal portions of the model were stainless steel. The greater part of the modified double wedge platform wing was constructed of optical lucite, as was the portion of the fuselage at the wing root. Detailed model dimensions are shown in Figure 11. The choice of aerodynamic design provided good flow characteristics and a relatively stable lambda-type shock wave on the wing; the largely transparent construction facilitated hologram production through 180 degrees of view.

The model was rotated about its sting mount in the wind tunnel from the zero degree position, wings level, to the 180 degree position, wings level inverted. Alignment for the desired rotation angle was accomplished by manually aligning prescribed lines on the sting mount collar with a scribed mark on the sting support.

III. ANALYTICAL EVALUATION OF THE DENSITY FIELD

A. THE BASIC EQUATION OF INTERFEROMETRY

Interferograms are created when two originally coherent light beams are superimposed and projected on a viewing screen. The two rays will reinforce or annul each other, depending on their relative phase difference at the screen. This phase difference is directly a function of the optical pathlengths traversed by the two waves.

Consider a coherent beam which is split and then recombined on a viewing screen. A difference in optical pathlengths of the two component beams may be achieved by causing the beams to traverse through different media prior to recombination, with their physical pathlengths maintained equal. Each component beam will travel at a speed c_0/n where c_0 is the speed of light in a vacuum and n is the index of refraction of the medium traversed. The difference in optical pathlength is then given by

$$L = L (n_2 - n_1) = c_0 \Delta t \quad (1)$$

where Δt is the time difference of travel in the two media. If the optical pathlength is changed by an amount $N\lambda$, where λ is the wavelength of the light source and N is an integer, then the order of interference changes by an amount N . In other words, a shift of N fringes occurs in the interference pattern. The fringe shift may be expressed as

$$g = L/\lambda \quad (2)$$

where

g = fringe shift

λ = light source wavelength

L = change in optical pathlength

Substituting equation (1) into equation (2) yields

$$g = \frac{L}{\lambda} (n_2 - n_1) \quad (3)$$

The index of refraction for a given medium is a function of density. In the case of gases, since the speed of light is very nearly the same as in a vacuum, the index of refraction is well represented by the first two terms of a Taylor series expansion [10]:

$$n = 1 + \beta \frac{\rho}{\rho_s} \quad (4)$$

where β = dimensionless constant related to the Gladstone-Dale constant by $K = \beta/\rho_s$

ρ_s = reference density at 0° C, 760 mm. Hg.

The value of β for air at $\lambda = 5893$ Angstroms (deep red light) is 0.000292; variation with wavelength is very small.

For a fixed difference in the index of refraction between the two component beams the fringe shift relation becomes:

$$g = \beta \frac{L}{\lambda} \left(\frac{\rho_2 - \rho_\infty}{\rho_s} \right) \quad (5)$$

For variable density in the test section, the net change in optical pathlength is the integrated effect along the beam path, or

$$g = \frac{\beta}{\lambda \rho_s} \int_0^L (\rho - \rho_\infty) ds = Q \int_0^L f(x, y, z_c) ds \quad (6)$$

where:
$$Q = \frac{B \rho_{\infty}}{\lambda \rho_s} \quad (7)$$

$$f(x, y, z_c) = \frac{\rho(x, y, z_c)}{\rho_{\infty}} - 1 \quad (8)$$

z_c = plane of constant z

ds = incremental distance along beam path

Equation (6) is the basic integral equation for the unknown density.

With known fringe shift values from an interferogram, the equation is inverted to obtain the density along a beam path.

B. THE INTEGRAL INVERSION

The integral inversion procedure utilized in this investigation was first reported by C. D. Maldonado, et al [5, 6]. It was used subsequently by R. D. Matulka [3] and R. C. Jagota [7] to determine the density variation in an asymmetric free jet and about a cone at angle of attack in supersonic flow, respectively. The procedure involves the representation of the function $f(x, y, z_c)$ of Equation (6) in a complete set of orthogonal functions, with the expansion coefficients evaluated by use of the orthogonality condition between the functions f and g of Equation (6). The set of functions used is orthogonal over the entire (x, y) plane for every z_c and remains an orthogonal set under a rotation of the coordinate system. The coordinate system used for the inversion is shown in Figure 12. It consists of (a) a set of fixed coordinates x, y and (b) a set of moving coordinates

x', y' in which the fringe number function is defined and which rotates with respect to x, y as the viewing angle through the test section is varied.

In operator form, Equation (6) can be represented as

$$g(\xi, y', z_c) = T f(x, y, z_c) \quad (9)$$

and f is evaluated by inversely transforming the equation to obtain

$$f(x, y, z_c) = T^{-1} g(\xi, y', z_c) \quad (10)$$

This inversion is achieved by utilizing a pair of orthogonal polynomials $U_{m+2k}^{+m}(\alpha x, \alpha y)$ and $H_{m+2k}(\alpha y')$ which are related by the transform relationship

$$T[U_{2k}(\alpha x, \alpha y) e^{-\alpha^2 x'^2}] = \frac{e^{\pm i m \xi}}{[k!(m+k)!]^{1/2}} \cdot \frac{1}{2^{m+2k}} \cdot H_{m+2k}(\alpha y') \quad (11)$$

where $H_{m+2k}(\alpha y')$ are Hermite polynomials of order $m+2k$. The unknown function $f(x, y, z_c)$ is expanded in a set of functions U_{m+2k}^{+m} as

$$f(x, y, z_c) = \sum_{m=0}^{\infty} \sum_{k=0}^{\infty} \epsilon_m \left\{ C_{m+2k}^{+m}(\alpha) U_{m+2k}^{+m}(\alpha x, \alpha y) + C_{m+2k}^{-m}(\alpha) U_{m+2k}^{-m}(\alpha x, \alpha y) \right\} e^{-(\alpha^2 x^2 + \alpha^2 y^2)} \quad (12)$$

where $\epsilon_m = 1/2$ for $m = 0$, $\epsilon_m = 1$ for $m = 1, 2, 3, \dots$, and C_{m+2k}^{+m} are the unknown coefficients of the expansion. α is an arbitrary scale factor which may be considered the reciprocal of a non-dimensionalizing coefficient.

Utilizing the transform relation of Equation (11), Equation (6)

becomes

$$g(\xi, y', z_c) = \sum_{m=0}^{\infty} \sum_{k=0}^{\infty} \varepsilon_m [k!(m+k)! 2^{2(m+2k)}]^{1/2} \times [C_{m+2k}^{+m}(\alpha) e^{im\xi} + C_{m+2k}^{-m}(\alpha) e^{-im\xi}] H_{m+2k}(\alpha) e^{-\alpha^2 y'^2} \quad (13)$$

Equation (13) is subject to the orthogonality condition

$$\int_{-\pi}^{\pi} e^{\pm im\xi} e^{\mp in\xi} d\xi \int_{-\infty}^{+\infty} H_{m+2k}(\alpha y') H_{n+2l}(\alpha y') e^{-\alpha^2 y'^2} dy' = \frac{2\pi^{3/2}}{\alpha} [(m+2k)!(n+2l)! 2^{m+2k} 2^{n+2l} \delta_{mn} \delta_{(m+2k)(n+2l)}] \quad (14)$$

where δ is the Kronecker delta function. The solution of Equation

(14) applied to Equation (13) yields the series coefficients

$$C_{m+2k}^{\pm m}(\alpha) = \frac{\alpha}{2\pi^{3/2}} \left[\frac{k!(m+k)!}{(m+2k)!} \right] \int_{-\pi}^{\pi} \int_{-\infty}^{\infty} g(\xi, y', z_c) H_{m+2k}(\alpha y') e^{\mp im\xi} dy' d\xi \quad (15)$$

With the substitution of the coefficients of Equation (15), Equation (7)

becomes

$$f(x, y, z_c) = \frac{\alpha}{\pi^{3/2}} \sum_{m=0}^{\infty} \sum_{k=0}^{\infty} \varepsilon_m \frac{[k!(m+k)!]^{1/2}}{(m+2k)!} e^{-(\alpha^2 x^2 + \alpha^2 y^2)} \times \text{Re} \left[\int_{-\pi}^{\pi} \int_{-\infty}^{\infty} g(\xi, y', z_c) e^{-im\xi} H_{m+2k}(\alpha y') dy' d\xi \times U_{m+2k}^m(\alpha x, \alpha y) \right] \quad (16)$$

The functions $U_{m+2k}^{\pm m}$ are defined as

$$U_{m+2k}^{\pm m}(\alpha x, \alpha y) = (-1)^k \alpha \left[\frac{k!(\alpha^2 x^2 + \alpha^2 y^2)^m}{\pi(m+k)!} \right]^{1/2} e^{\pm im\phi} L_k^m(\alpha^2 x^2 + \alpha^2 y^2) \quad (17)$$

where $\phi = \tan^{-1}(y/x) - (\pi/2)$ and L_k^m are the associated Laguerre polynomials

$$\left[L_k^m(\alpha^2 x^2 + \alpha^2 y^2) \right]^S = \sum_{s=0}^{\infty} \frac{(m+k)!}{(k-s)!(m+s)! s!} \left[(-1)(\alpha^2 x^2 + \alpha^2 y^2) \right]^S \quad (18)$$

Insertion of Equation (17) into Equation (16) yields

$$f(x, y, z_c) = \left(\frac{\alpha}{\pi} \right)^2 \sum_{m=0}^{\infty} \sum_{k=0}^{\infty} \varepsilon_m \frac{(-1)^k k!}{(m+2k)!} (\alpha^2 x^2 + \alpha^2 y^2)^{m/2} \left[L_k^m(\alpha^2 x^2 + \alpha^2 y^2) \right. \\ \left. \times \left[B_{m+2k}^m(\alpha) \cos(m\phi) + D_{m+2k}^m(\alpha) \sin(m\phi) \right] e^{-(\alpha^2 x^2 + \alpha^2 y^2)} \right] \quad (19)$$

where

$$B_{m+2k}^m(\alpha) = \int_{-\pi}^{\pi} \int_{-\infty}^{\infty} g(\xi, y', z_c) \cos(m\xi) H_{m+2k}(\alpha y') dy' d\xi \quad (20)$$

$$D_{m+2k}^m(\alpha) = \int_{-\pi}^{\pi} \int_{-\infty}^{\infty} g(\xi, y', z_c) \sin(m\xi) H_{m+2k}(\alpha y') dy' d\xi \quad (21)$$

Equations (19), (20), and (21) are the basic equations used to obtain the density distribution from the experimentally determined fringe variations in a completely asymmetric flow field.

C. THE NUMERICAL PROCEDURE

Because the function $g(\xi, y', z_c)$ is an experimentally determined quantity the unknown coefficients $B_{m+2k}^m(\alpha)$ and $D_{m+2k}^m(\alpha)$ in the series representation of $f(x, y, z_c)$ in Equation (19) cannot be calculated analytically. It is therefore necessary to evaluate the double integrals of Equations (20) and (21) numerically. This is accomplished by noting in Figure 12 and Equation (8) that there is an area outside which the density is invariant, namely outside the test

section where the known density is ρ_{∞} . Since the function $f(x, y, z_c) = 0$ outside this circular domain, the limits of integration of $+\infty$ and $-\infty$ in Equations (20) and (21) can be replaced by finite values. The fringe distribution is then approximated by small increments over the test domain, resulting in the representation of the B and D coefficients as double series:

$$B_{m+2k}^m(\alpha) = \sum_{i=1}^{I-1} \sum_{j=0}^{J-1} g(\xi_j + \Delta \xi_j, x_i + \Delta x_i) \int_{\xi_j}^{\xi_{j+1}} \cos(m\xi) d\xi \int_{x_i}^{x_{i+1}} H_{m+2k}(\alpha x) dx \quad (22)$$

and

$$D_{m+2k}^m(\alpha) = \sum_{i=1}^{I-1} \sum_{j=0}^{J-1} g(\xi_j + \Delta \xi_j, x_i + \Delta x_i) \int_{\xi_j}^{\xi_{j+1}} \sin(m\xi) d\xi \int_{x_i}^{x_{i+1}} H_{m+2k}(\alpha x) dx \quad (23)$$

Using the derivative formula for Hermite polynomials, Equations (22)

and (23) can be manipulated to yield workable series expressions:

$$B_{m+2k}^m(\alpha) = \left[\frac{1}{2\alpha m} \cdot \frac{1}{(m+2k+1)} \right] \sum_{i=0}^{I-1} \sum_{j=0}^{J-1} g(\xi_j + \Delta \xi_j, x_i + \Delta x_i) \times \left[\sin(m\xi_{j+1}) - \sin(m\xi_j) \right] \left[H_{m+2k+1}(\alpha x_{i+1}) - H_{m+2k+1}(\alpha x_i) \right] \quad (24)$$

$$D_{m+2k}^m(\alpha) = - \left[\frac{1}{2\alpha m} \cdot \frac{1}{(m+2k+1)} \right] \sum_{i=0}^{I-1} \sum_{j=0}^{J-1} g(\xi_j + \Delta \xi_j, x_i + \Delta x_i) \times \left[\cos(m\xi_{j+1}) - \cos(m\xi_j) \right] \left[H_{m+2k+1}(\alpha x_{i+1}) - H_{m+2k+1}(\alpha x_i) \right] \quad (25)$$

Since it is impossible to sum over an infinite number of terms,

Equation (19) is necessarily expressed as the sum of a finite series:

$$f(x, y, z_c) = \left(\frac{\alpha}{\pi}\right)^2 \sum_{k=0}^K \sum_{m=0}^M \varepsilon_m (-1)^k \left[\frac{k!}{(m+2k)!} \right] (\alpha^2 x^2 + \alpha^2 y^2) \quad (26)$$

$$\times \left[\int_k^m (\alpha^2 x^2 + \alpha^2 y^2) \left[B_{m+2k}^m(\alpha) \cos(m\phi) + D_{m+2k}^m(\alpha) \sin(m\phi) \right] e^{-(\alpha^2 x^2 + \alpha^2 y^2)} \right]$$

It has been demonstrated that judicious selection of the parameters

$\Delta \xi$, Δx , K , M , and α yields density distributions with very good accuracy [3, 6].

IV. EXPERIMENTAL PROCEDURE

A. LABORATORY TECHNIQUES

In order to visualize the general flow patterns and localize shock or expansion waves about the model a series of standard Schlieren photographs were taken at varying flow Mach numbers. Pictures were produced for roll angles of 0° , 45° , and 90° at Mach numbers from 0.925 to 1.10. A representative series of Schlieren photographs is shown in Figures 13, 14, and 15. Analysis of the Schlieren photographs dictated a flow Mach number of 0.937 for the experimental study; this Mach number yielded uniform upstream flow conditions and located the lambda-type shock wave ideally near the center of the lucite section of the model wing.

The coherence length of the pulsed ruby laser was approximately ten centimeters for the output power utilized. This reduced the normally critical requirement for pathlength equality in the scene and reference beams that must be fulfilled in the classical Mach-Zehnder interferometric approach. Consequently, a length of string proved to be a sufficiently accurate measuring device to maintain the two beam pathlengths within the coherence length of the laser, a requirement for interferogram production. To compensate for the fact that the scene beam traversed approximately five inches of glass tunnel walls and lucite grids which the reference beam did not, the scene beam



was adjusted to be some 2.5 inches shorter than the reference beam. Reference beam pathlength was maintained at approximately 138 inches throughout the experiment.

Holograms produced using the basic holographic setup shown in Figure 3 exhibited clear, well-defined fringe patterns in nearly every instance. In deciding on the final arrangement, several techniques were tested to improve upon fringe pattern definition. Horizontal, vertical and diagonal translations of the diffuser plate in the scene beam were considered, varying from 0.001 inches to 0.005 inches. A vertical translation of 0.003 inches yielded clear horizontal fringes that were quite easily analyzed. The transverse mode selector aperture was varied from 1.0 mm. to 3.0 mm. in increments of 0.5 mm; best lighting of the model resulted with use of a 2.5 mm. aperture. The temperature of the cooling water circulated through the laser head and etalon was varied from 26.0°C. to 28.0°C. in increments of 0.2°C., with 27.0°C. providing the best fringe definition. Finally, a variety of beam splitters and lenses were tested prior to final selection of the best available optics arrangement for the experiment. A 2:1 reference to scene beam strength ratio was found to yield very good holograms.

Two double exposure holograms were taken for each model viewing angle. The first, labeled a double-static exposure, consisted of two exposures in a no-flow condition with a 0.003 inch vertical translation of the diffuser plate between exposures. The fringe

patterns in this hologram provided a measure of the effect of tunnel wall glass, grid plexiglass and model lucite on the subsequent double exposure. The second, or static-dynamic, exposure consisted of a no-flow exposure, a 0.003 inch diffuser translation, and finally an exposure at flow Mach number 0.937. The fringe deviations recorded in the region behind the lucite portion of the model by the double-static hologram were measured and subtracted from the fringe shifts measured in the corresponding static-dynamic hologram.

Holograms were produced on Agfa-Gaevert 8E75 holographic plates, 4 inches by 5 inches in size. As recommended by Collier, et al. [11] the development process included:

1. Five minutes in Kodak D-19 developer
2. Thirty seconds in a flowing water bath
3. Five minutes in standard rapid fixer
4. Thirty seconds in a flowing water bath
5. One and one-half minutes in Kodak Hypo Clearing agent
6. Five minutes in a flowing water bath
7. Five minutes in methanol bath
8. One minute in a flowing water bath
9. Drying

B. PHOTOGRAPHIC TECHNIQUES

Normal reconstructions of the original scene were made by illuminating the holograms with a seven milliwatt continuous wave

helium-neon laser beam at a wavelength of 6328 Angstroms. There was some slight distortion in the reconstructed scene because of the difference in wavelengths of the original scene beam and the reconstruction beam; however, the effect was almost totally negated by shrinkage of the holographic plate emulsion during the development process.

A common technique of image reconstruction was employed, utilizing a conjugate reference beam to reilluminate the exposed hologram, as shown in Figure 16. The resulting scene was recorded on photographic film. Individual points on the photograph are produced by a series of non-parallel rays originating from various source points on the diffuser plate in the scene beam. Using a reilluminating beam of small diameter has the effect of a small aperture at the focal point of the imaging lens, filtering out all but a set of nearly parallel rays, as shown in Figure 17. The real images produced in this manner have a large depth of field, permitting simultaneous projection on the film of front and rear grids, the model and the fringe patterns. The imaging lens was focused as near to the plane of the fringes as possible, producing photographs at various planes of constant z_c .

C. DATA REDUCTION

Photographic interferograms were obtained using the arrangement shown in Figure 16, with the camera viewing screen in the position of the real image. The line of sight in the plane desired was achieved by translating and elevating the hologram until common points on the

front and rear grids were aligned. The Graphic View camera, with the wide angle lens aperture set fully open at $f7.8$, was adjusted to yield the best focus on the fringe plane. Exposure times of from $1/5$ to $3/4$ seconds were used to produce workable interferogram photographs on Polaroid Type 55 P/N film.

Fringe shift analysis was accomplished on 8 inch by 10 inch enlargements of the 4 inch by 5 inch film used to record the images. The enlargements were placed face down on a light table, and the fringes, model contours and shock wave were traced on the back surface at the desired cross-sectional plane. Fringe shift values were recorded by measuring the distance between (1) the intersection of the hypothetically undeviated fringe and the cross-sectional plane and (2) the intersection of the deviated fringe with the same plane. Fringe shifts so obtained were corroborated by placing the negative in a photographic enlarger and tracing the lines of interest directly onto graph paper.

The known model fuselage diameter of 1.1 inches was compared with that measured in each individual photograph to yield magnification factors relating projected dimensions to actual dimensions. These factors were then used as corrections to the fringe shift measurements. A grid reference point located on the cross-sectional plane of interest served as the datum for all fringe shift measurements. A base point was located at the intersection of the cross-sectional plane of interest and the body longitudinal axis. Fringe shift measurements were

corrected using this base point as the new datum so that the inversion circle was properly centered on the body axis. The radius of the inversion circle was selected to be nearly equal to the semi-span of the wing. Fringe shift measurements were converted to fringe numbers using the average free stream spacing, while fringe locations were nondimensionalized using the inversion circle diameter. From the data so obtained, the radial variation of fringe number was plotted for each viewing angle. Fringe numbers at 201 equidistant points, as required for input into Mode 3 of the computer program, HOLOFER, were recorded from the resulting curves. Further details concerning this inversion computer program are outlined in Appendix B. A typical reduction of an interferogram to obtain the radial variation of fringe number at a particular cross-sectional plane is detailed in Appendix A.

V. EXPERIMENTAL RESULTS AND DISCUSSION

A pair of double exposure holograms was taken of the model at $11\frac{1}{4}$ degree intervals through a 180 degree field of view. Experimental data from the wind tunnel runs are recorded in Table I. Initial resulting density patterns indicated relatively smooth contours across adjacent intervals; the interval was therefore doubled to $22\frac{1}{2}$ degrees to simplify and speed the analysis. Fringe data were first inserted into the inversion computer program along nine lines of sight in the 180 degree field of view. A numerical comparison of views from 0 degrees to 90 degrees and from 90 degrees to 180 degrees verified to within 0.20 percent the assumption of a single plane of symmetry in the experiment. The fringe data input was then reduced to five lines of sight in a 90 degree field of view, as shown in Figure 18. The resulting output was an inverted density field along nine radial lines spanning a 180 degree field of view, with a mirror image on the opposite side of the plane of symmetry, as shown in Figure 19.

The static-dynamic photographic interferogram for the 0 degree view, along with its corresponding double-static interferogram, is shown in Figure 20. The diffraction effects caused by the presence of the lucite portions of the model are clearly visible in the double-static exposure, where the free stream fringe lines are bent and displaced toward the model axis. This displacement was measured

and subtracted from subsequent measurements made on the static-dynamic exposure, as outlined in Section IV.A. Photographic interferograms of the remainder of the static-dynamic exposures are shown in Figures 21 through 24. Clearly visible and reduceable in nearly all views were (1) the region of uniform subsonic flow, commonly called the free stream condition, (2) the transition from local subsonic to local supersonic flow, and (3) the lambda-type shock wave on the model wing. These characteristics are shown in schematic representation in Figure 25.

Contour plots of the density function, as expressed in Equation (8) of Section III.A., for successive z-planes of analysis are shown in Figures 26 and 27. The cross-sectional plane of analysis for the plot of Figure 26 was located at 186.75 mm. from the model nose along the longitudinal axis. For Figure 27, the plane of interest was 195.25 mm. from the model nose. It is apparent from both contour plots that the model went to a very small angle of attack under the loading forces produced during tunnel operation; this is evidenced by the compression of the contour lines above the model and the corresponding expansion of the contours below the model. Measurements made from photographic interferograms confirm this angle of attack to be, at most, 0.05 degrees. The closed contours above and adjacent to the wing surface in both figures may very well be the result of a vortex originating at the intersection of the wing leading edge and the



fuselage on either side of the model and traveling aft and outward over the wing surface.

A comprehensive quantitative analysis of the shock wave structure was not undertaken, with the exception of estimating the strength of the shock by comparison of fringe line separation immediately ahead of and aft of the shock wave. Fringe line separation measurements on either side of the shock wave were converted first to density information and thence to pressure information, disregarding compressibility effects. An approximate strength value of 0.207 was computed using the accepted definition of $(p_2 - p_1)/p_1$. This corresponds to a local Mach number of 1.08 in the supersonic region just ahead of the shock wave. Qualitative shock wave analysis resulted in the construction of a three-dimensional structural representation as shown in Figure 28, using input information from several interferogram viewing angles. While location of the leading and trailing edges of the lambda-type shock wave was very accurate, interior structure was largely indefinable due to "smearing" and blurring of the fringes transiting the shock wave itself.

As a preliminary step to possible future studies in this field, photographic interferograms were made from holograms produced with the aerodynamic model set at small angles of attack. Orientations included angles of attack of five and ten degrees, with roll angles varying from zero to ninety degrees. Although the holograms themselves were of very good quality, the photographic reproductions

were relatively poor due to the fact that an inferior photographic arrangement had to be used. They were therefore omitted from this report. It was inferred from the holograms, however, that a complete study at angle of attack using the basic procedures followed in the present study would be both totally feasible and rewardingly fruitful.

The original character of the experimental data prevented comparison with published results. Qualitative studies of transonic phenomena are widely available, and the general characteristics of the resulting density field and shock wave structure serve to bear out the schematics based on theoretical and mathematical models. Moreover, the self-testing mode of the inversion computer program, HOLOFER, verified the consistency and reproductibility of the resulting density distributions to within 2.0 percent through proper choice of the input parameters, primarily the slope-matching parameter α . The errors encountered in the final results are due primarily to errors in the fringe data input to the inversion program. The intrinsic presence of laser speckle, the extended pathlengths of the scene and reference beams and the unavoidable beam scattering and diffraction within the lucite model sections, created difficulty in obtaining precisely the slope of the fringe lines behind the lucite sections. Fringe spacing measurements in the free stream flow were conservatively judged accurate to within 0.5 mm. This assumption was quite reasonable since all measurements were effected with a scale graduated at half millimeter intervals. This figure of 0.5 mm.,

combined with the mean free stream fringe spacing of 5.197 mm. for all interferograms, indicated measurement accuracy to within one tenth (0.1) of a fringe. The mean systematic error of the free stream spacing in each view was computed to be a maximum of 3.9 percent. Associated with this systematic error was a random error of 2.1 percent in the measurement of fringe shifts in each view to a conservative accuracy of 0.5 mm. The resulting error for each viewing angle was therefore a maximum of 6.0 percent, found by merely adding the two types of error for each view. The minimum error limit was found by considering the error resulting from the reproduction of the same interferogram view five separate times. Statistically, with 6.0 percent error in each view, the composite error for the repeated view is 2.6 percent. As five different views, or lines of sight, were used for the data between zero and ninety degrees, the final total error in the analysis was therefore in the interval between 2.6 percent and 6.0 percent. To insure contour clarity and guard against overlapping, the maximum error figure of 6.0 percent was used in construction of the plots shown in Figures 26 and 27. In general, the rather large fringe shifts led to a very low mean fringe sensitivity value of 0.1259. This coefficient indicated a resulting density function (Equation (8)) inaccuracy of less than 1.5 percent for a fringe shift measurement misreading of 0.5 mm.

Physical limitations of beam diameter and hologram plate area dictated the choice of an inversion circle diameter somewhat smaller

than the full data circle normally used in the finite fringe procedure. This, in effect, introduced an inconsistency in reference density into the analysis since the density on the selected circle and immediately outside it was not the calculated ρ_{∞} ; the density function was therefore not zero outside the actual inversion region. To alleviate this inconsistency, a new, updated reference density was computed for each cross-sectional plane of analysis by averaging the density values on the selected circle from the first inversion process. The actual reference densities used were $\rho = 1.777$ mg/cc for the 186.75 mm. plane and $\rho = 1.642$ mg/cc for the 195.25 mm. plane. This procedure was justified since all density values between the selected circle and the full data circle were constant to within approximately fifteen percent. The updated reference densities were then used to produce the final output density field. The net effect was a scaled, uniform shift toward density function values slightly lower than those computed on the basis of the original reference density.

VI. CONCLUSIONS

The finite fringe procedure for the production of holographic interferograms has been applied successfully to the determination of the three-dimensional density distribution of the flow near the wing-fuselage junction of a partially transparent aerodynamic model in the transonic regime. Density contours accurate to within six percent enabled a thorough analysis of the flow field to be conducted, highlighting flow characteristics and the presence of the shock wave. Subsequent studies of similar models at angle of attack have been shown to be entirely feasible. Procedures used in the experiment also exhibit promise for the direct analysis of duct and inlet flows as well as comprehensive study of shock wave structure.

The inversion computer program, HOLOFER, was found to be adequate in handling a general asymmetric flow field analysis. However, it was considered quite cumbersome and difficult to modify for various experimental situations. Subsequent analysts will find the procedures advocated by Sweeney and Vest [12] for the recording and analyzing of interferograms of considerable interest. In addition, the efforts of Van Houton [13], who utilized the method proposed by Junginger and van Haeringen [14], may prove valuable in reducing computer time significantly.

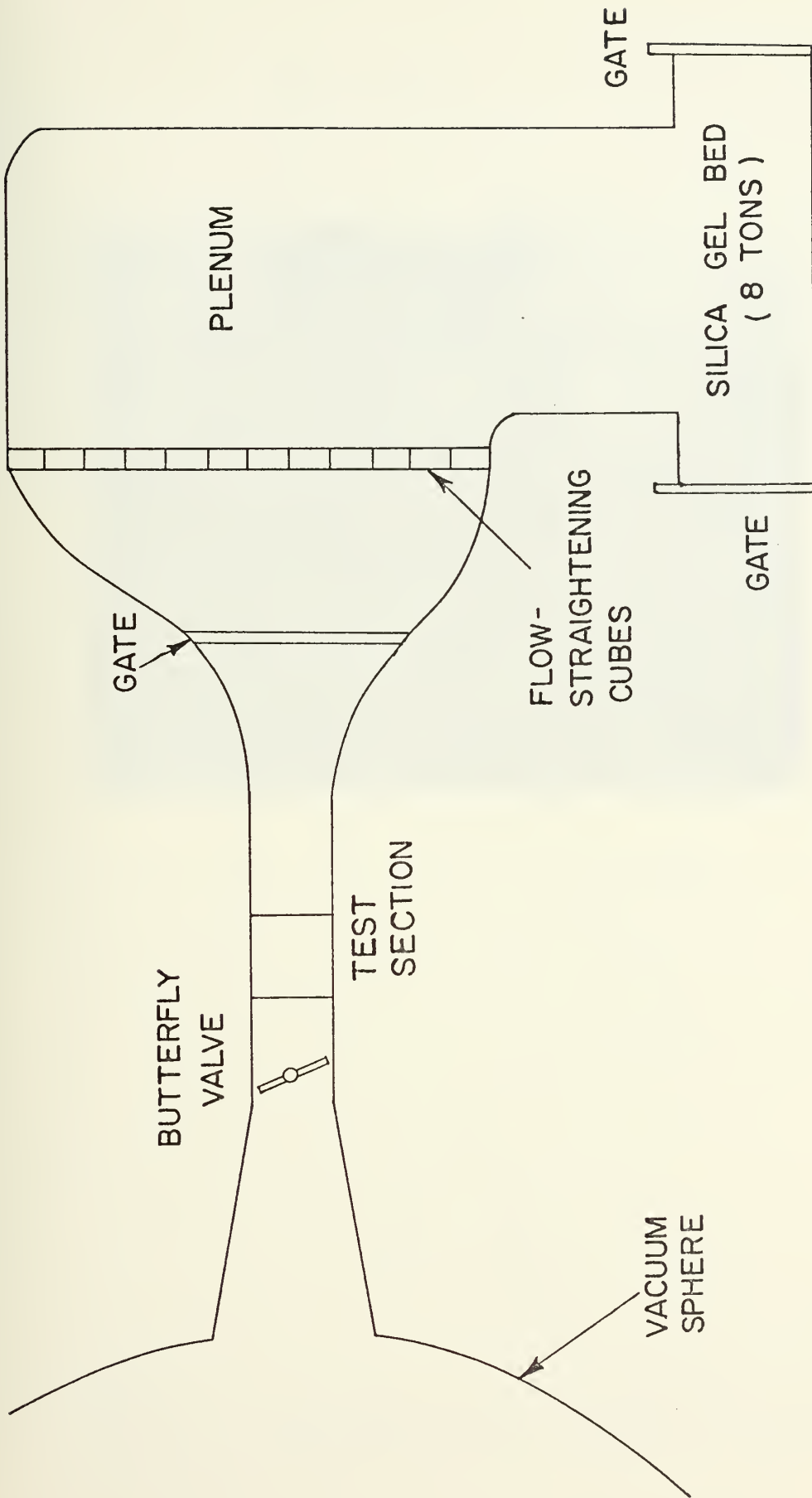


FIGURE 1. FUNCTIONAL SCHEMATIC OF NSRDC WIND TUNNEL



FIGURE 2. BECKMAN 210 DATA RECORDING SYSTEM

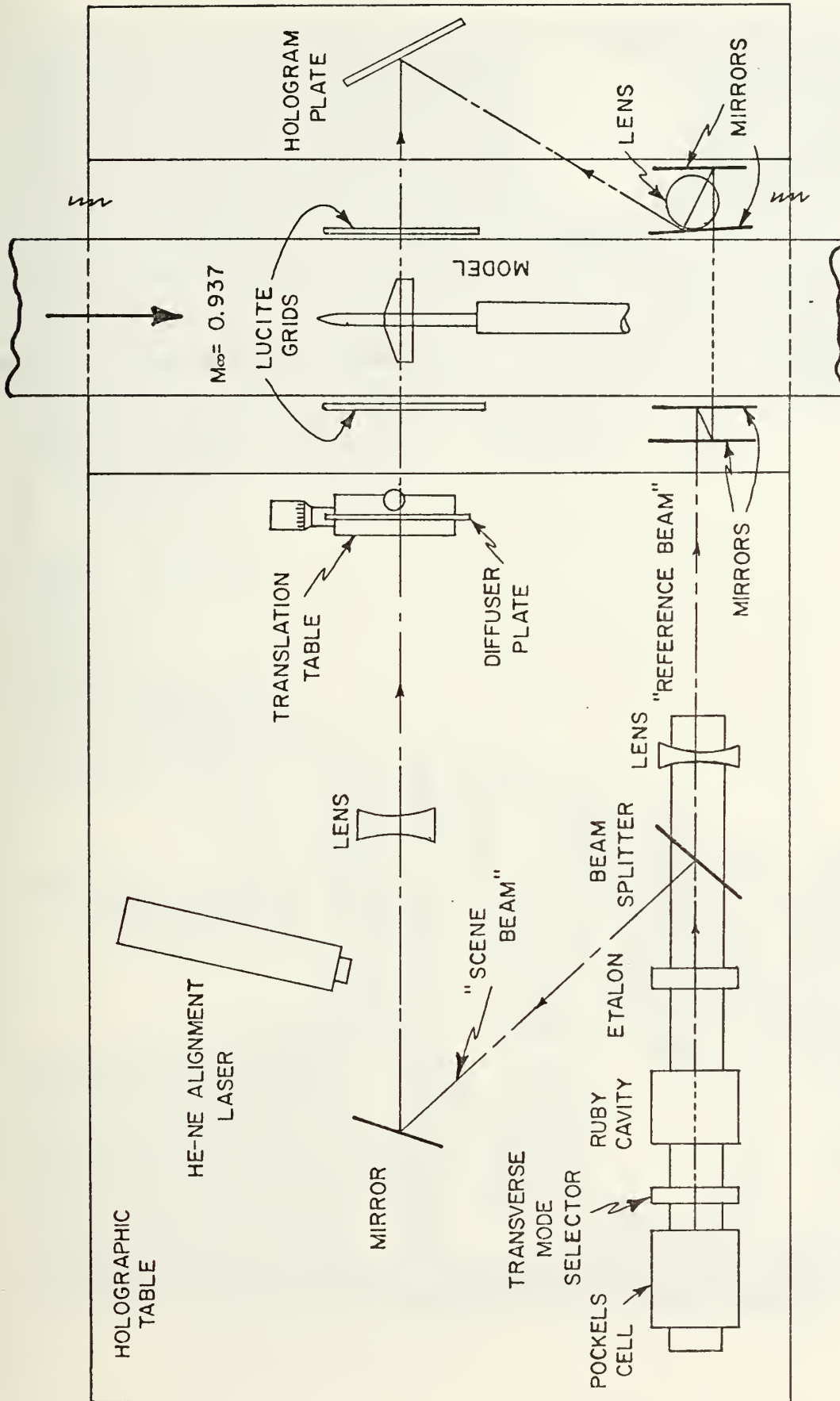


FIGURE 3. SCHEMATIC DRAWING OF THE HOLOGRAPHIC ARRANGEMENT

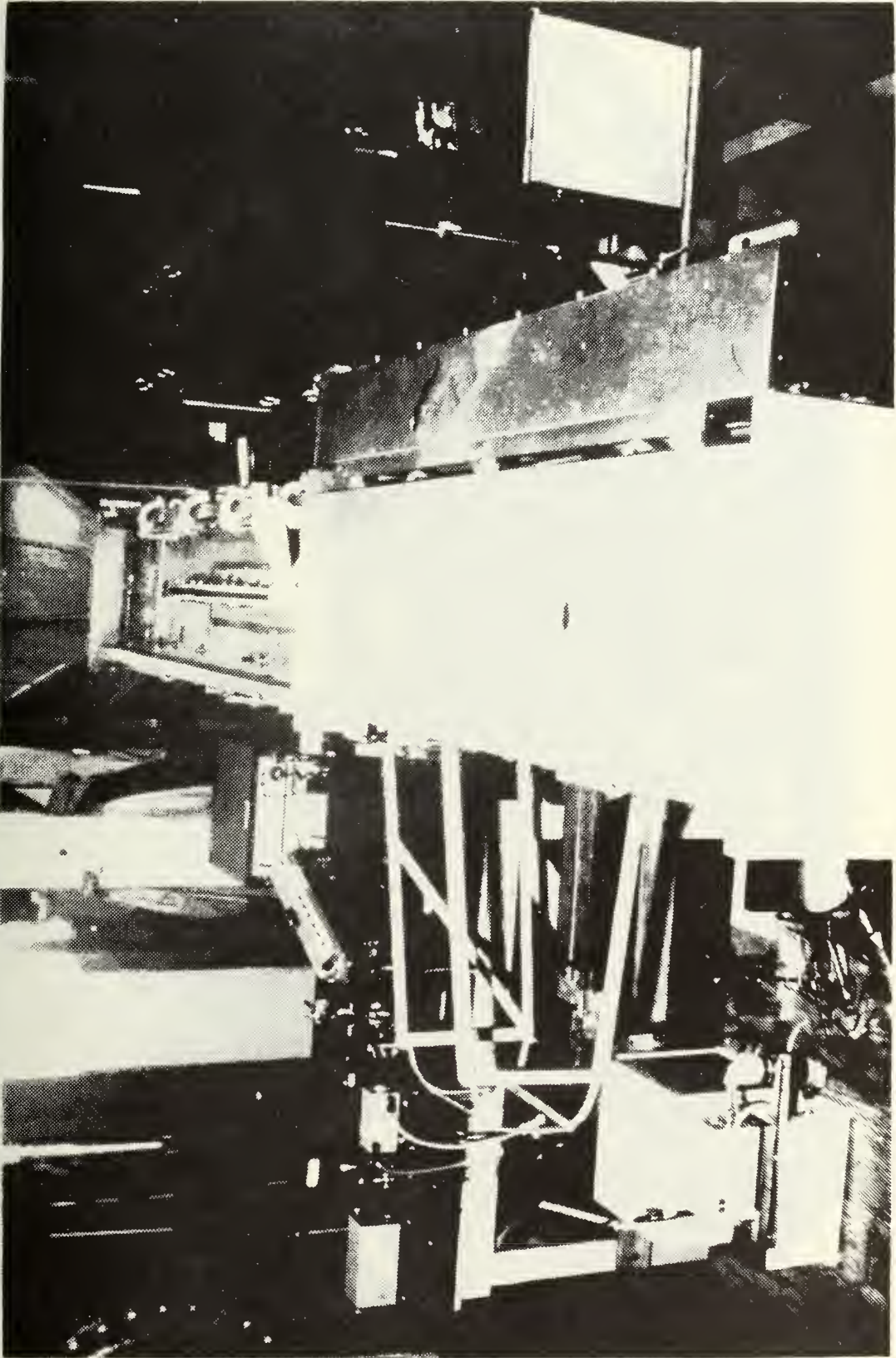


FIGURE 4. OVERHEAD VIEW OF TUNNEL AND ENTIRE HOLOGRAPHIC SYSTEM

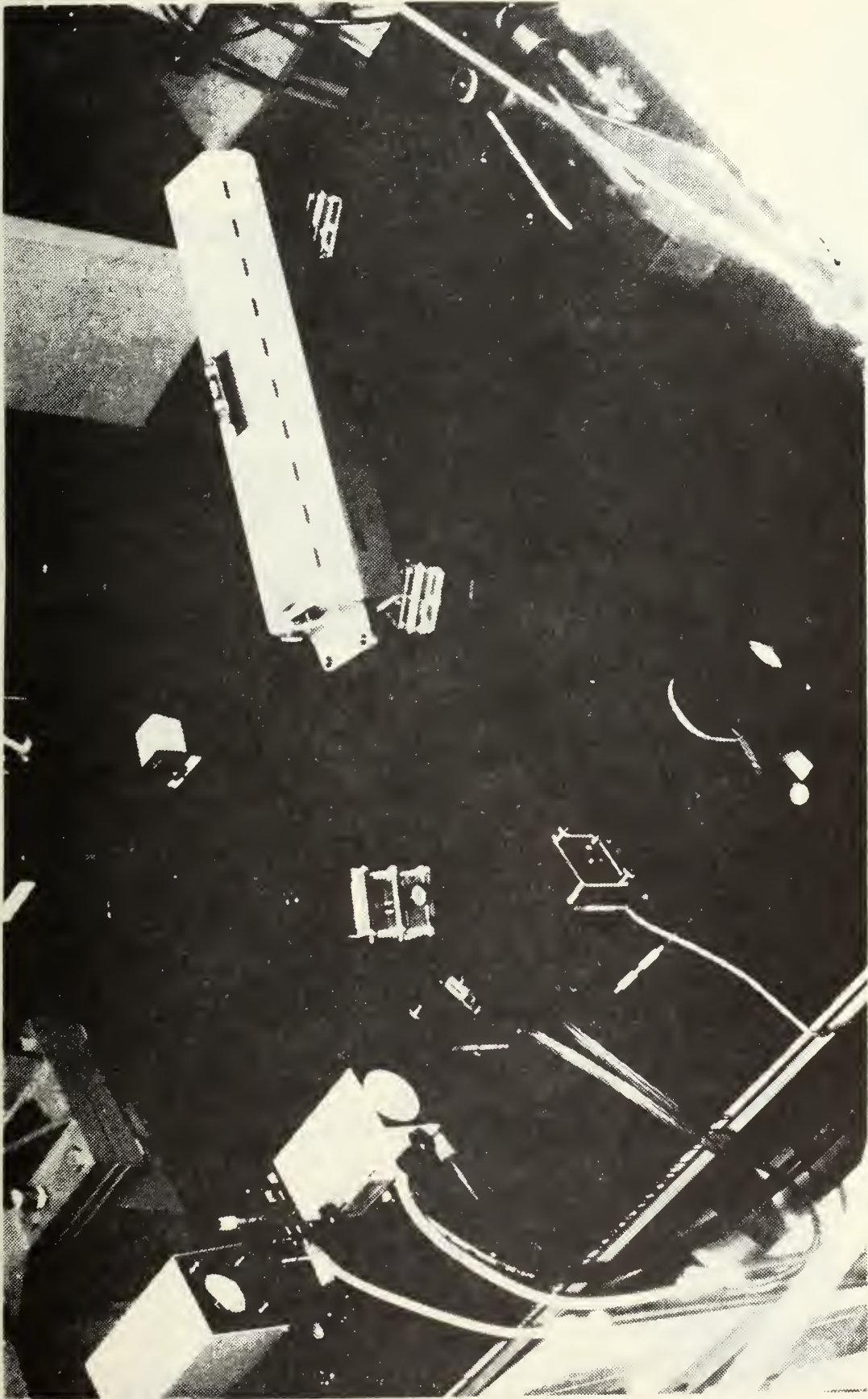


FIGURE 5. OBLIQUE VIEW OF HOLOGRAPHIC TABLE

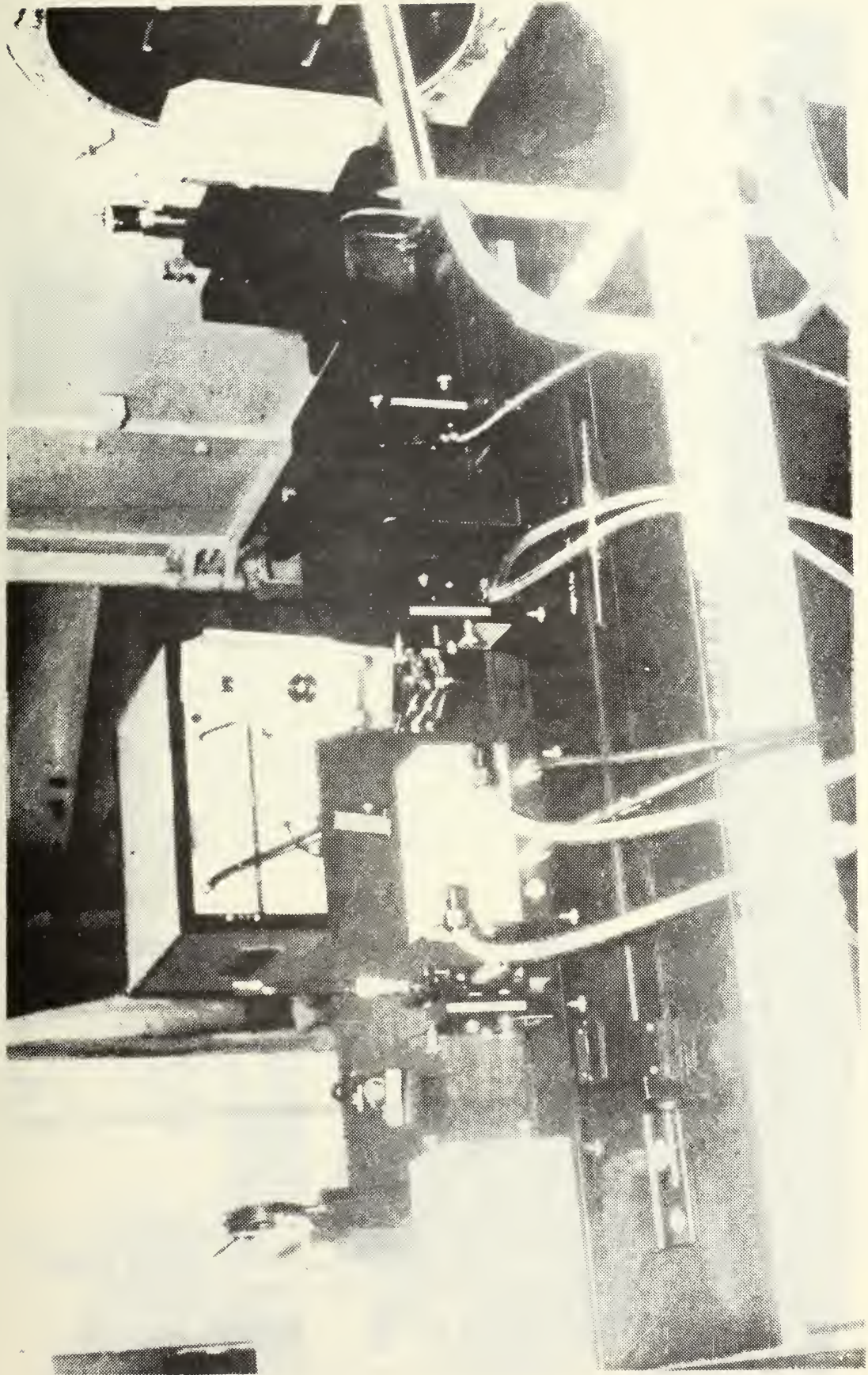


FIGURE 6. OBLIQUE VIEW OF HOLOGRAPHIC TABLE

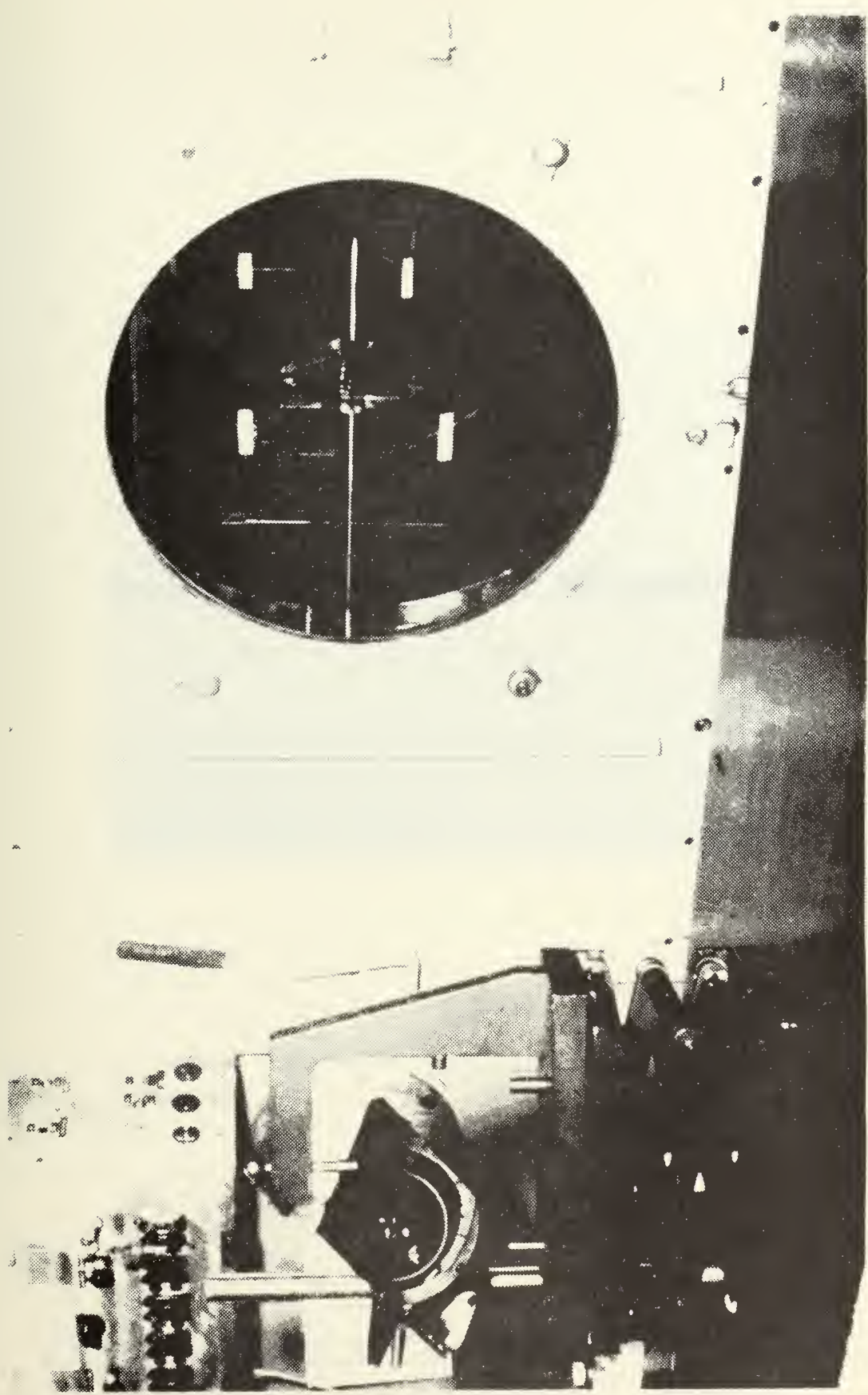


FIGURE 7. DETAIL OF MODEL MOUNTING AND REFERENCE GRIDS



FIGURE 8. AERODYNAMIC TEST MODEL: 0 DEG. ROLL ANGLE

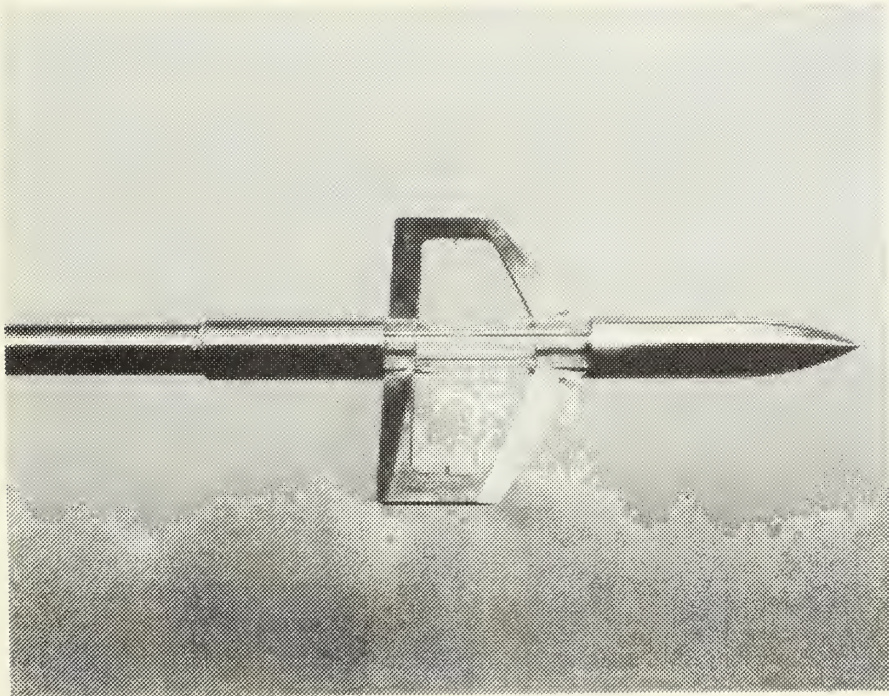


FIGURE 9. AERODYNAMIC TEST MODEL; 45 DEG. ROLL ANGLE

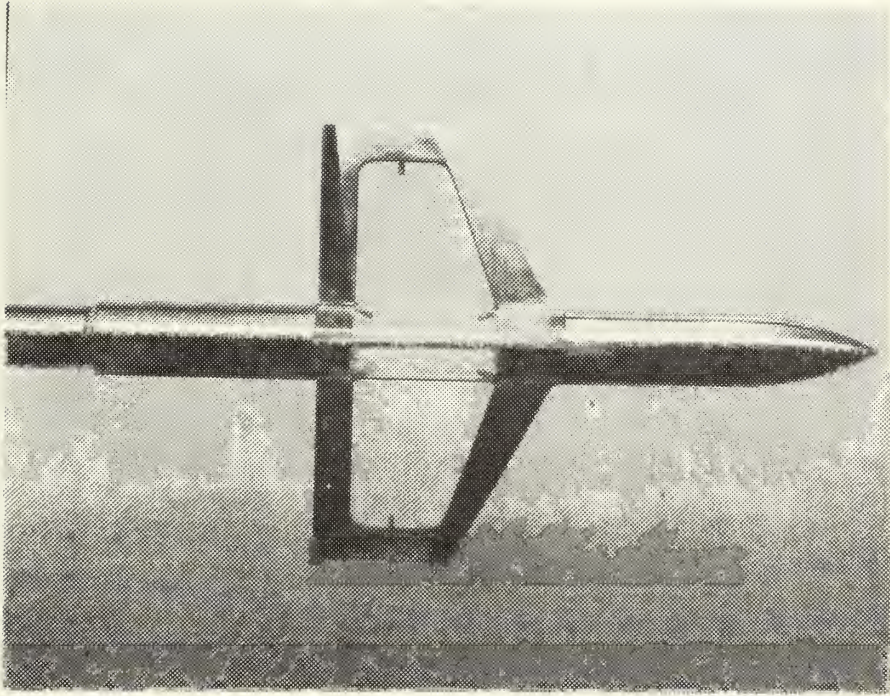
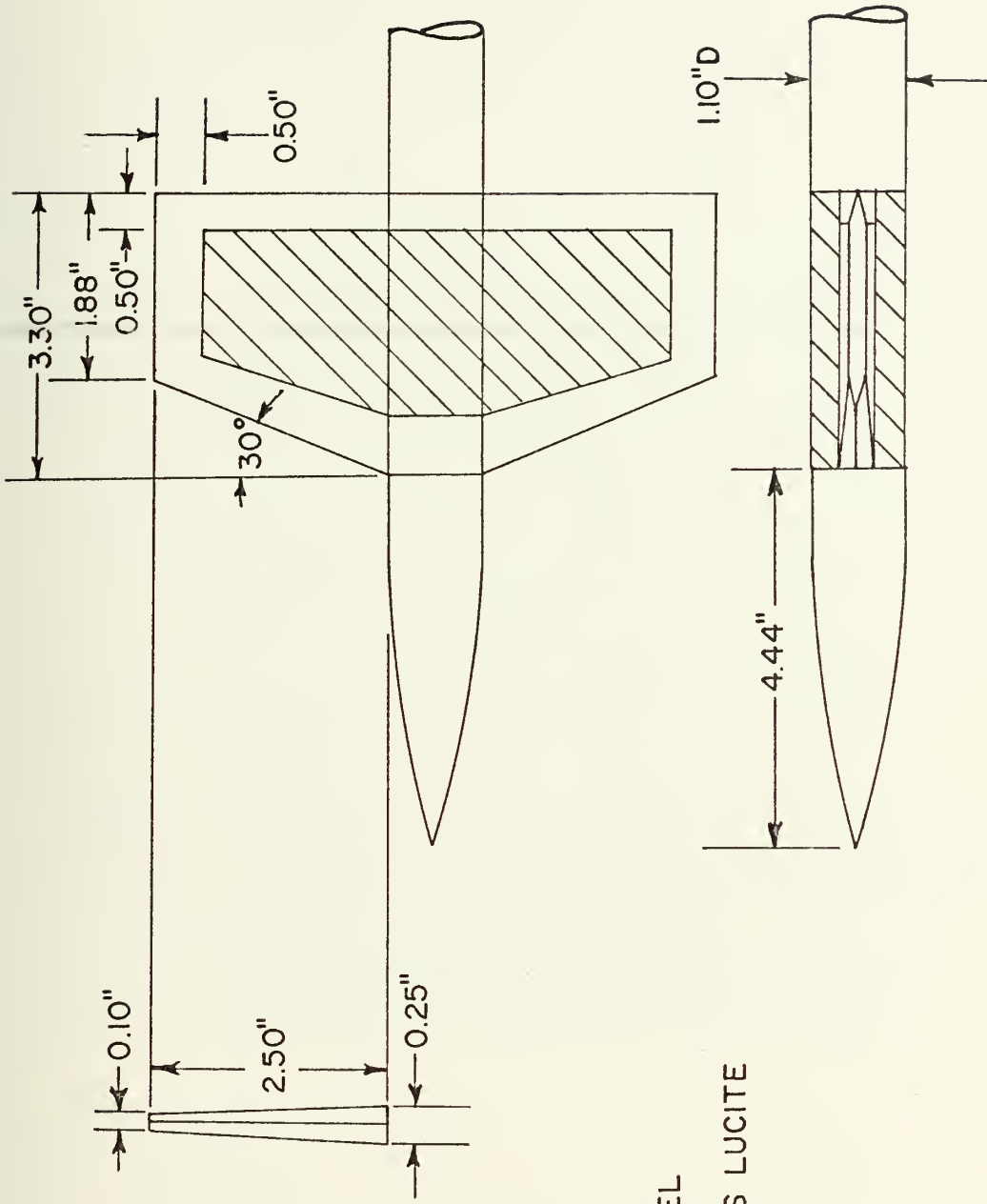


FIGURE 10. AERODYNAMIC TEST MODEL; 90 DEG. ROLL ANGLE



NO SCALE
 STAINLESS STEEL
 HATCHED AREAS LUCITE

FIGURE 11. DETAILS OF THE AERODYNAMIC TEST MODEL

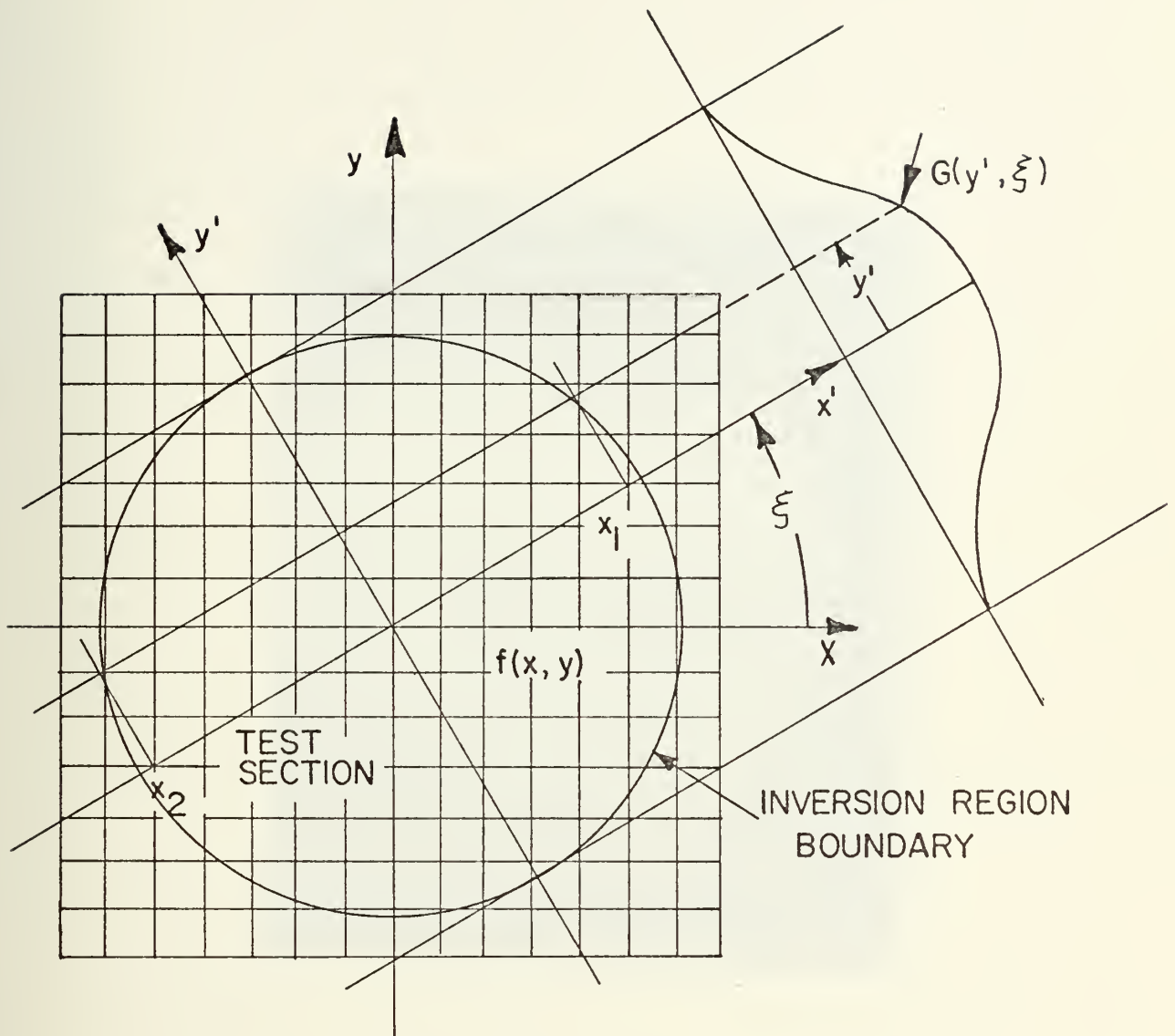


FIGURE 12. CO-ORDINATE SYSTEM USED FOR INVERSION OF FRINGE NUMBER TO DENSITY

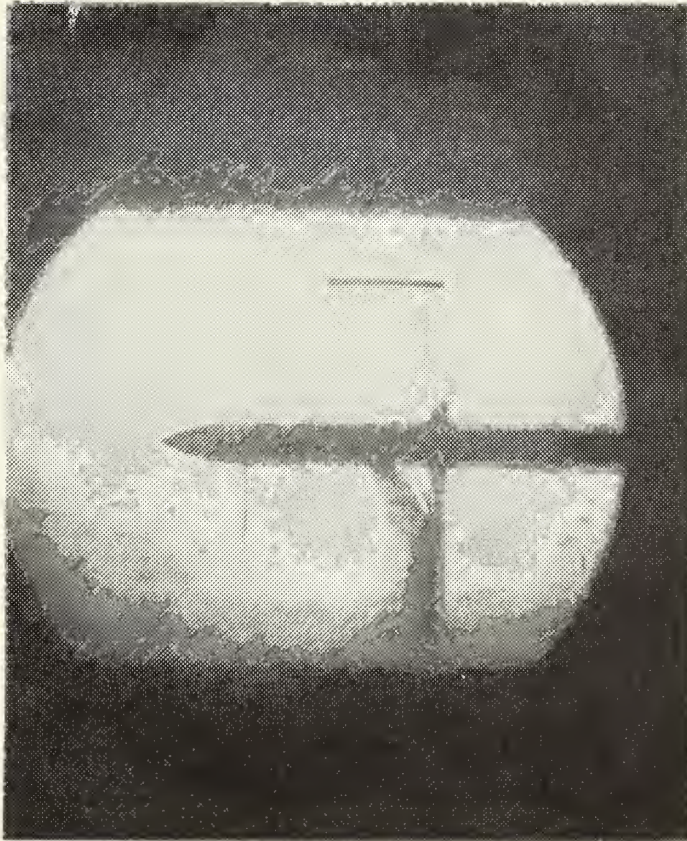


FIGURE 13. SCHLIEREN PHOTOGRAPH; 0 DEG. ROLL ANGLE,
0.967 MACH NUMBER

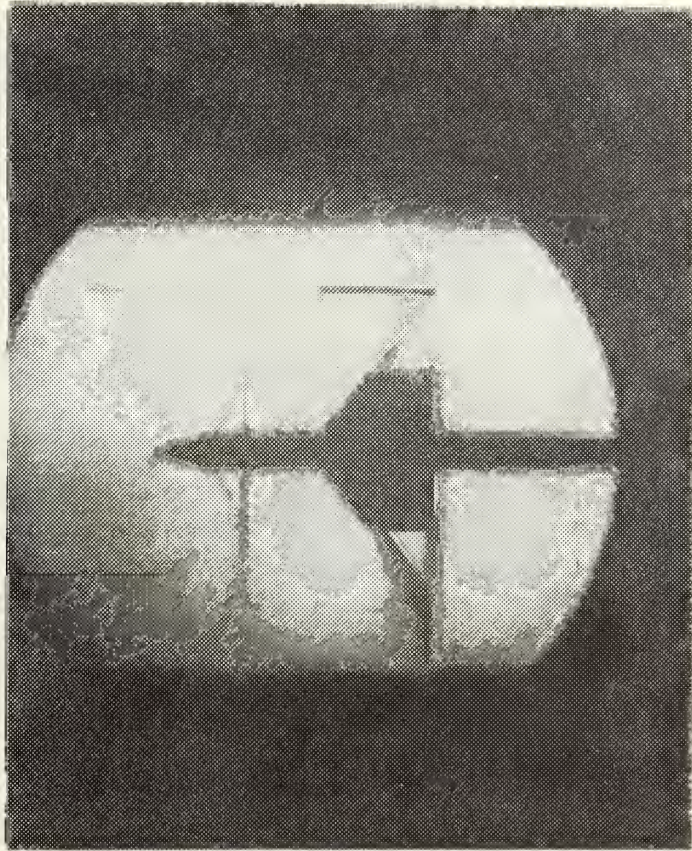


FIGURE 14. SCHLIEREN PHOTOGRAPH; 45 DEG. ROLL ANGLE.
0.967 MACH NUMBER

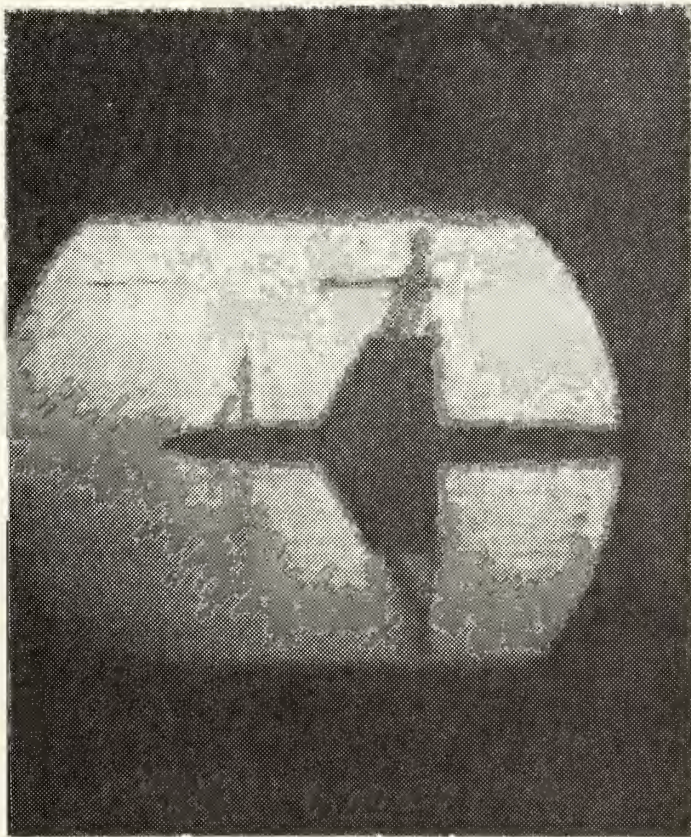


FIGURE 15. SCHLIEREN PHOTOGRAPH: 90 DEG. ROLL ANGLE,
0.967 MACH NUMBER

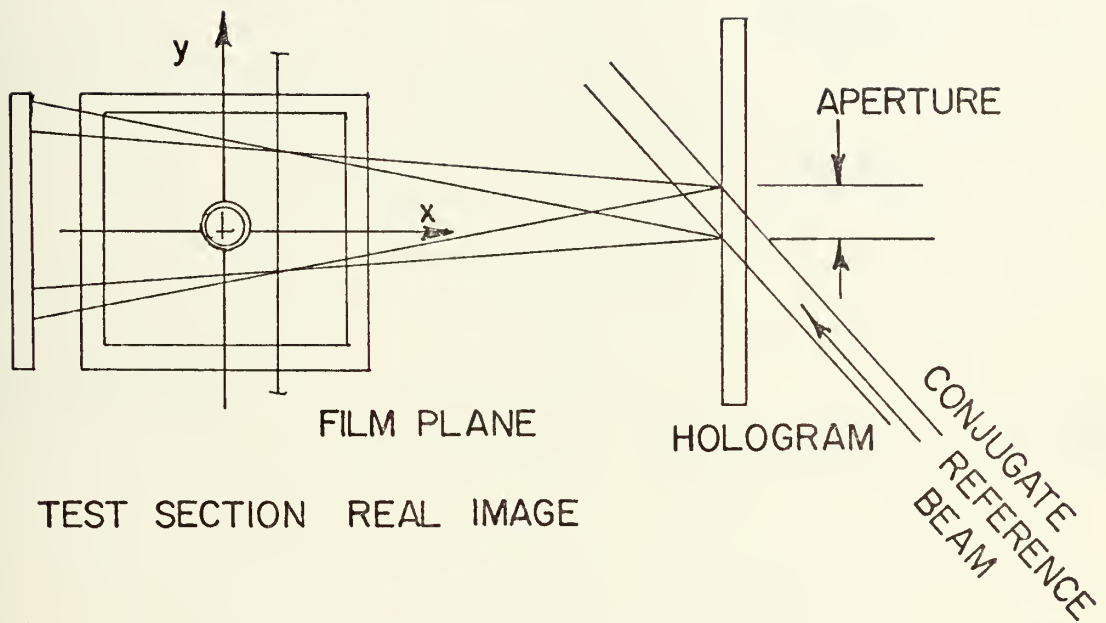


FIGURE 16. LENSLESS PHOTOGRAPHIC TECHNIQUE USING A CONJUGATE REFERENCE BEAM OF SMALL DIAMETER

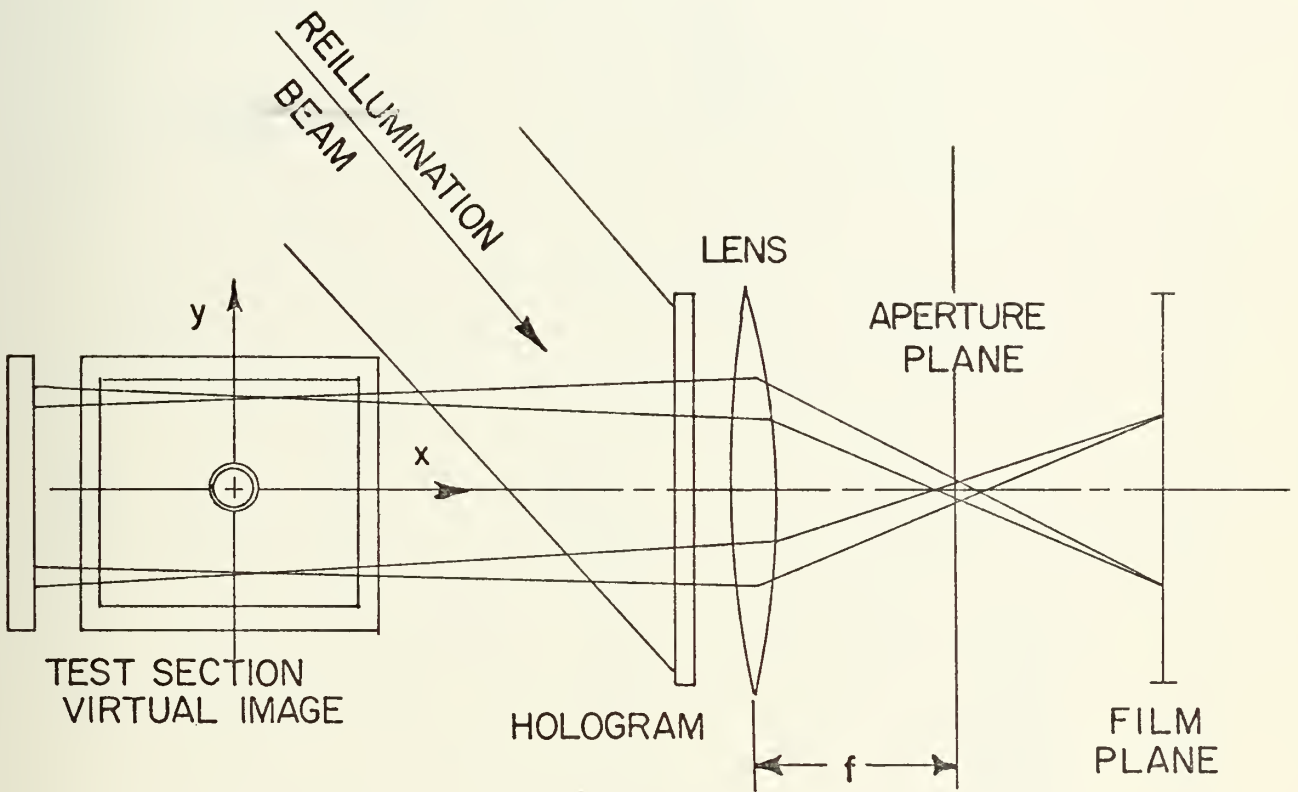


FIGURE 17. SPATIAL FILTERING TECHNIQUE FOR SELECTING PHOTOGRAPH OF CONSTANT ANGLE LINES OF LIGHT

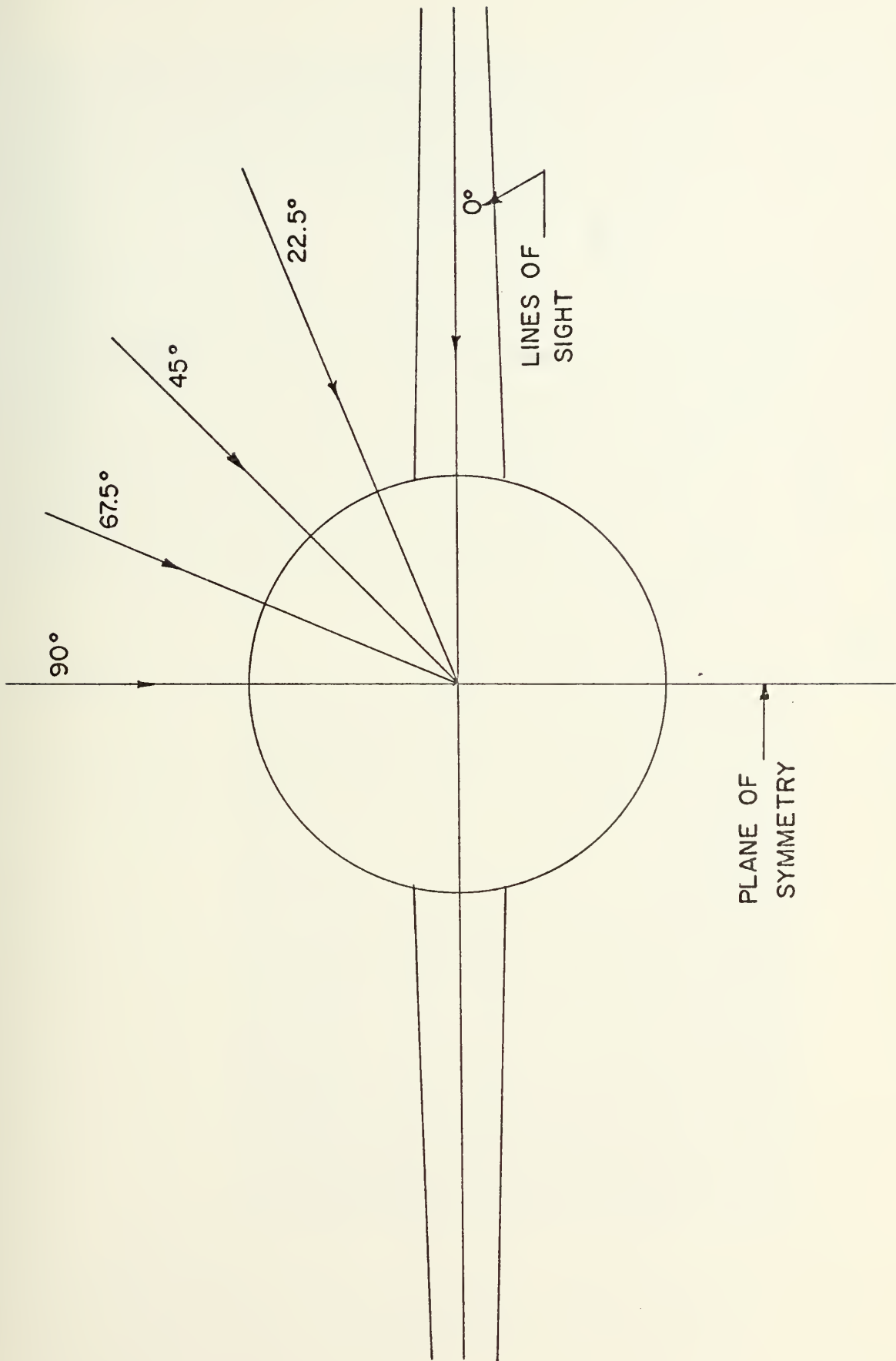


FIGURE 18. FRINGE DATA INPUT INFORMATION

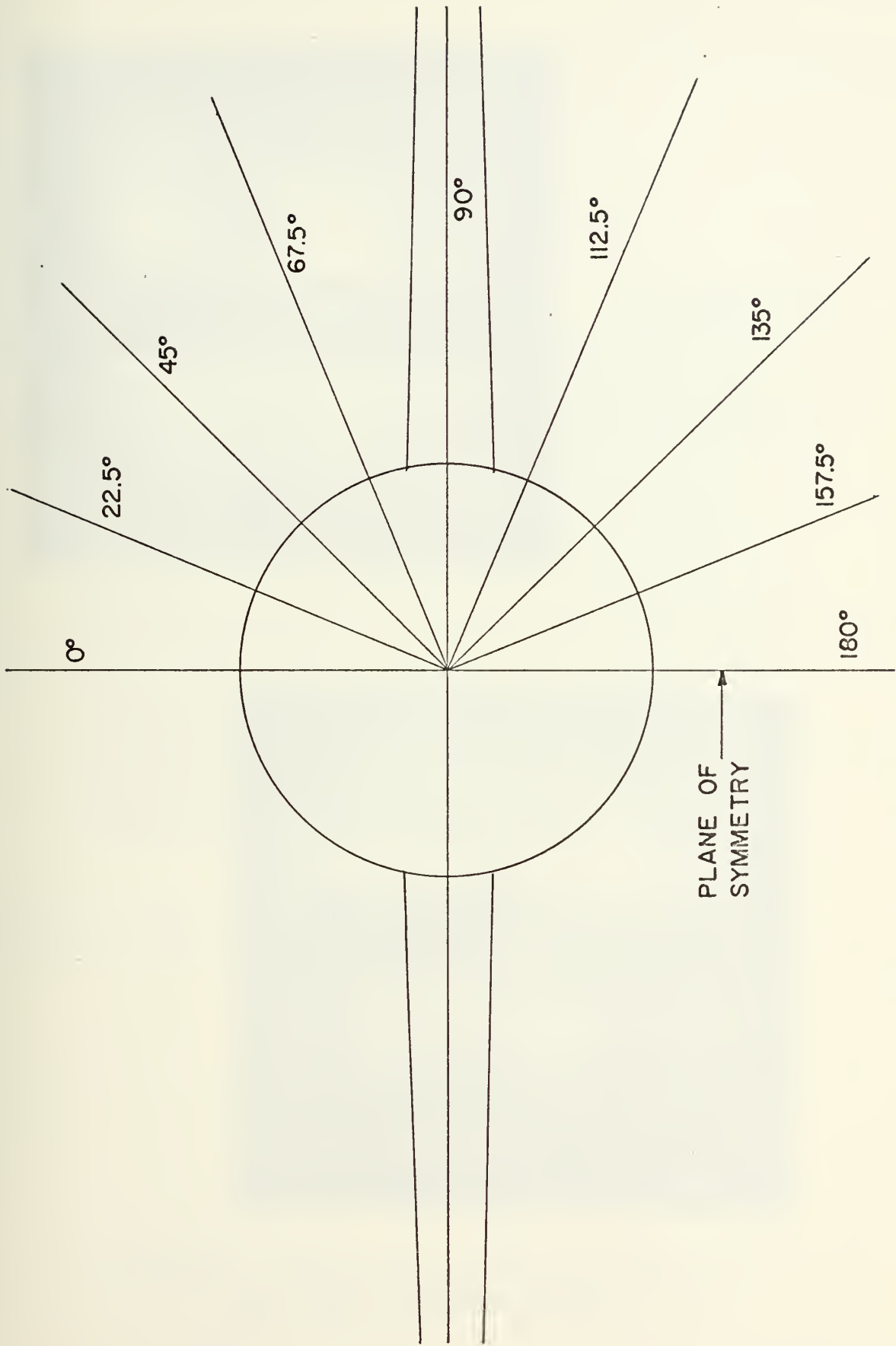
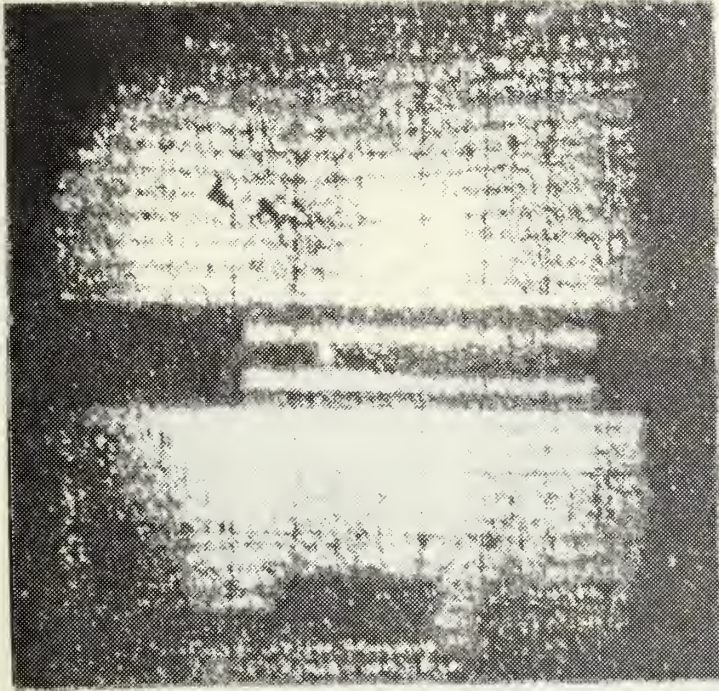
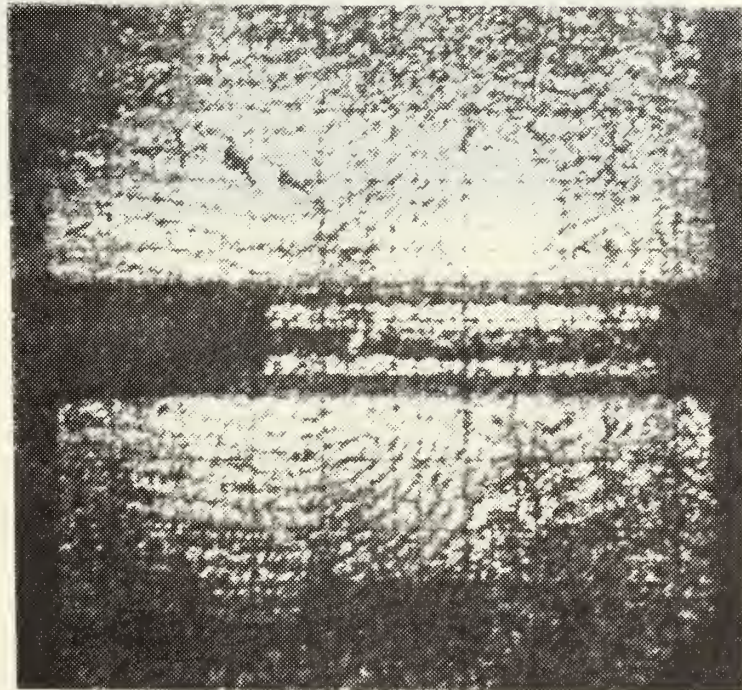


FIGURE 19. DENSITY DATA OUTPUT INFORMATION



DOUBLE-STATIC
INTERFEROGRAM



STATIC-DYNAMIC
INTERFEROGRAM

FIGURE 20. PHOTOGRAPHIC INTERFEROGRAMS
FOR 0 DEG. VIEWING ANGLE

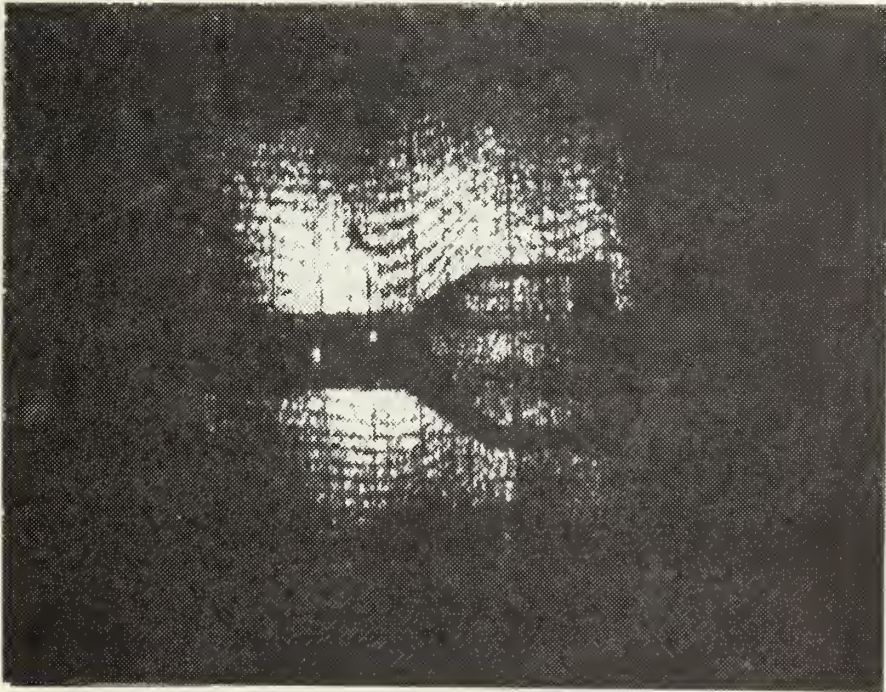


FIGURE 21. STATIC-DYNAMIC INTERFEROGRAM
FOR $22\frac{1}{2}$ DEG. VIEWING ANGLE



5

FIGURE 22. STATIC-DYNAMIC INTERFEROGRAM
FOR 45 DEG. VIEWING ANGLE

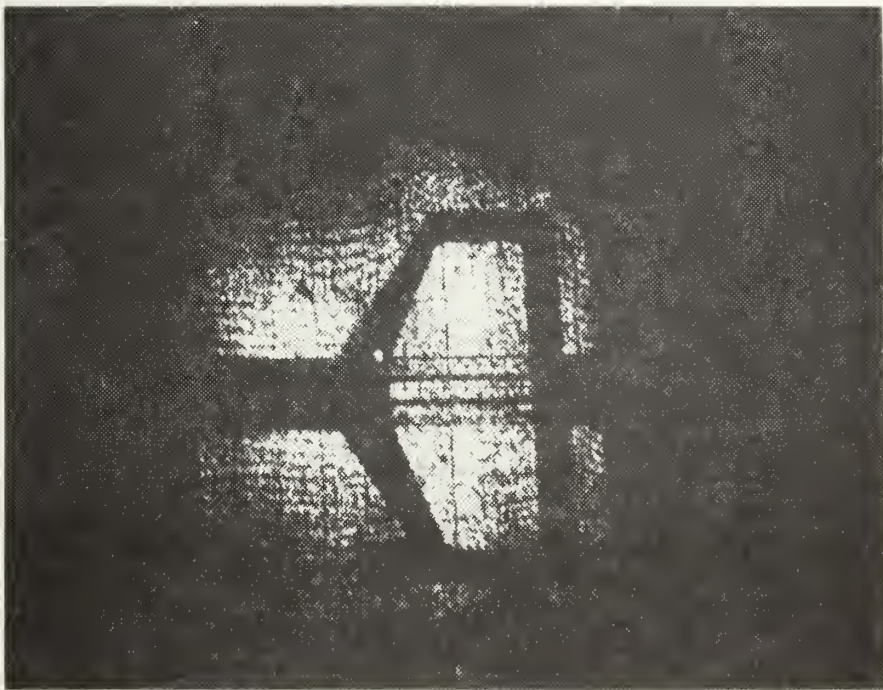


FIGURE 23. STATIC-DYNAMIC INTERFEROGRAM
FOR $67\frac{1}{2}$ DEG. VIEWING ANGLE

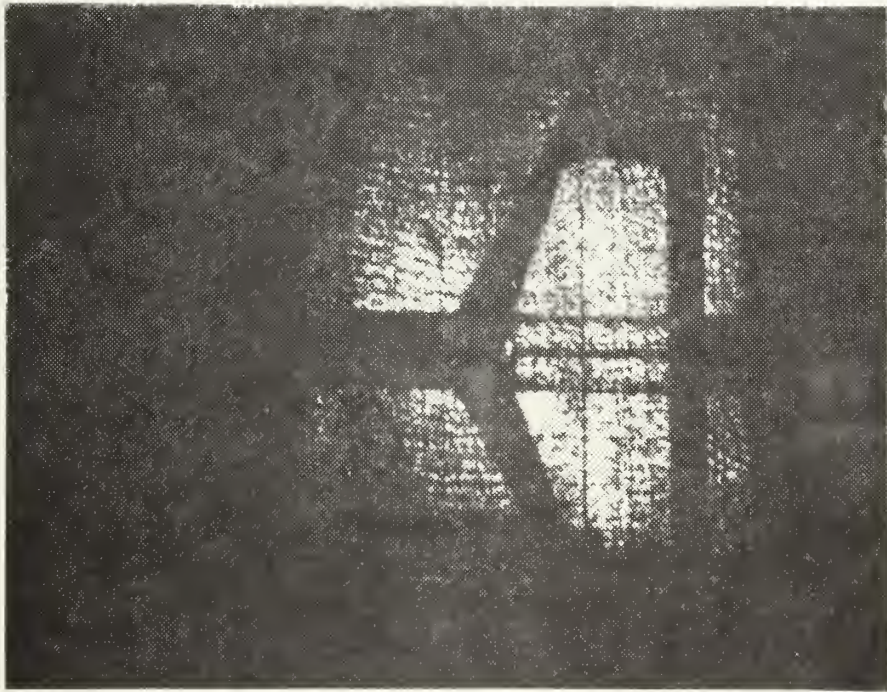


FIGURE 24. STATIC-DYNAMIC INTERFEROGRAM
FOR 90 DEG. VIEWING ANGLE

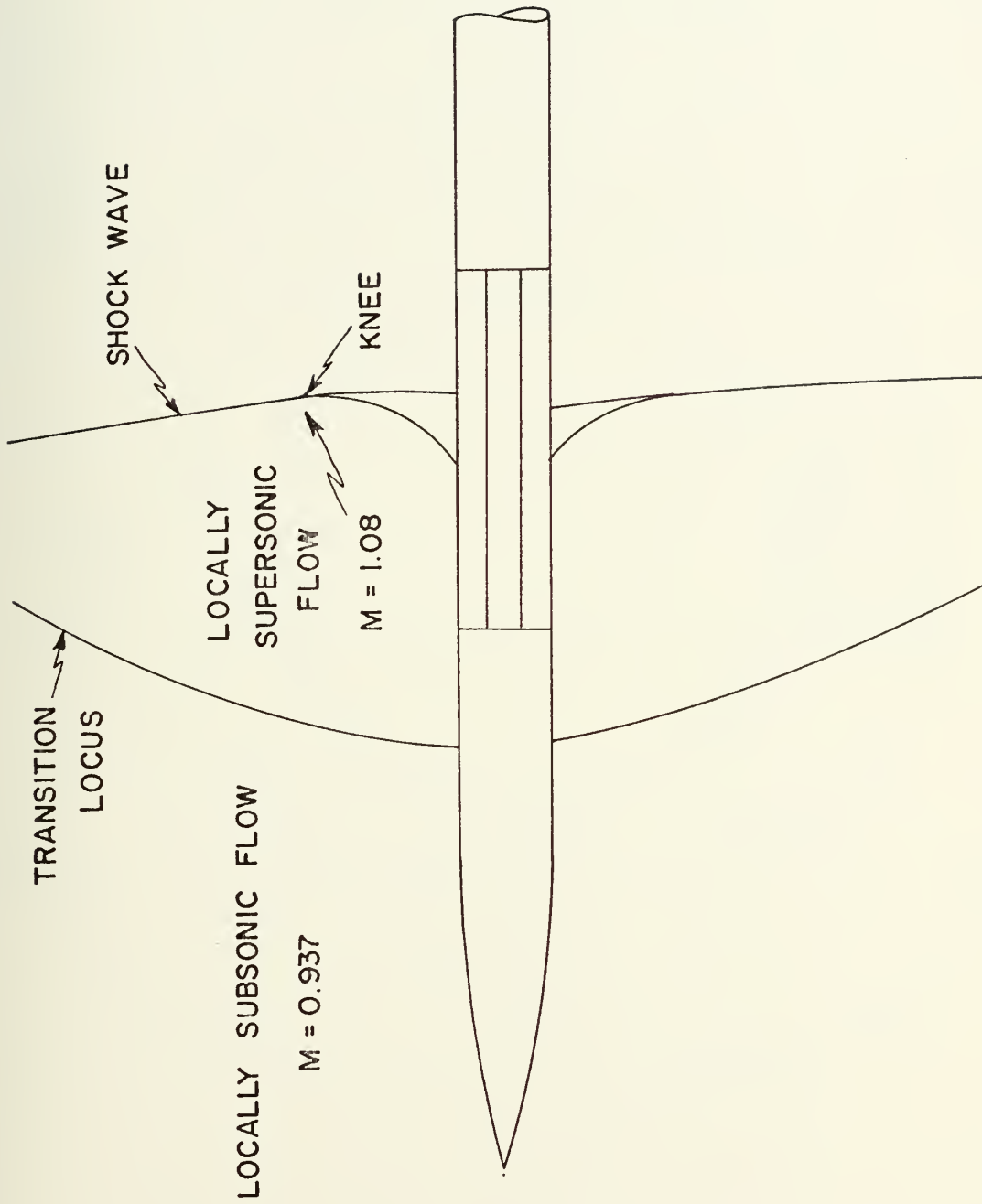


FIGURE 25.
CHARACTERISTIC TRANSONIC FLOW REGIONS; FROM SEVERAL INTERFEROGRAMS

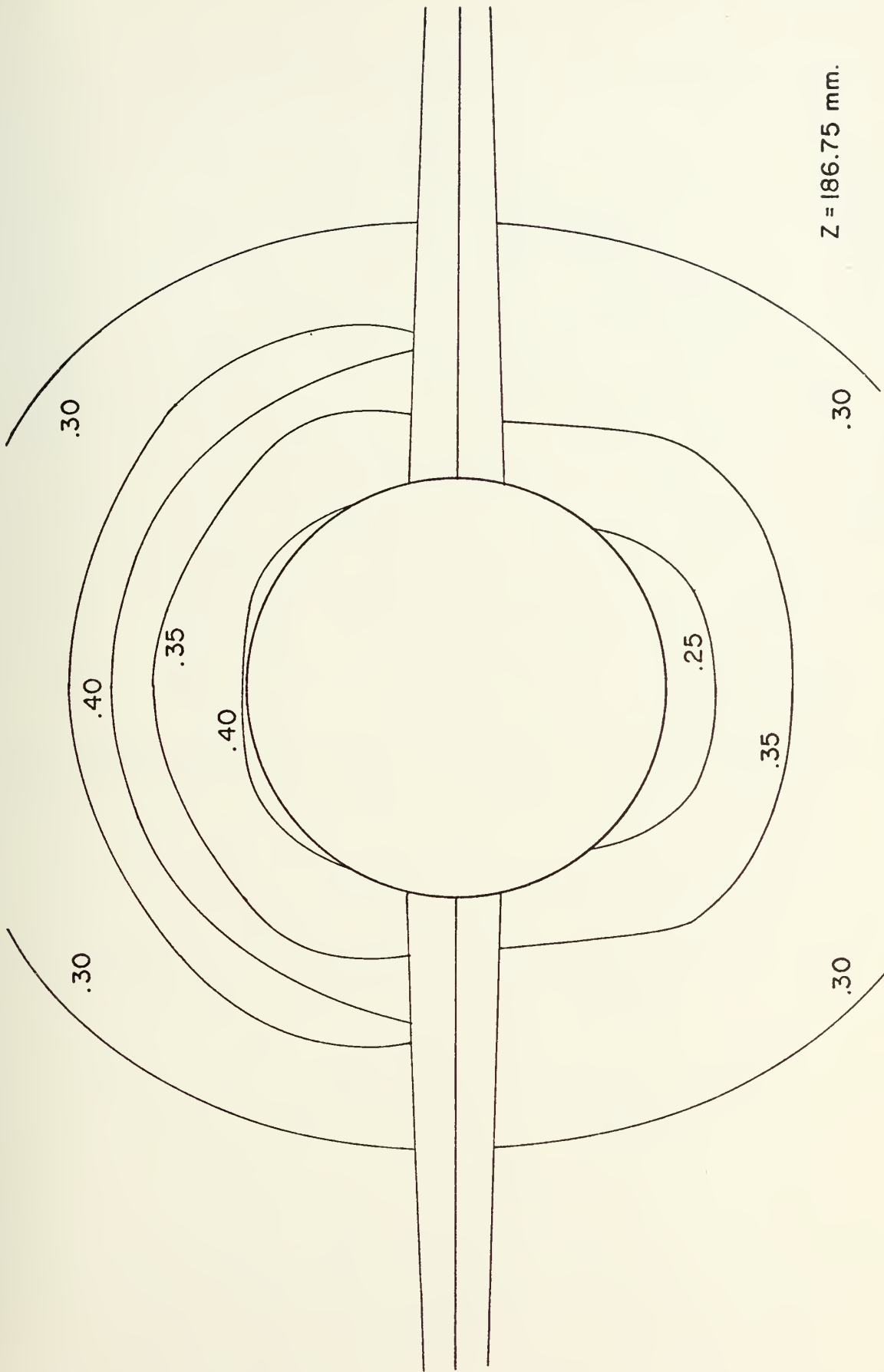


FIGURE 26. CONTOUR PLOT OF DENSITY FUNCTION, $(\rho / \rho_{\infty}) - 1$, FOR GIVEN CROSS-SECTIONAL PLANE

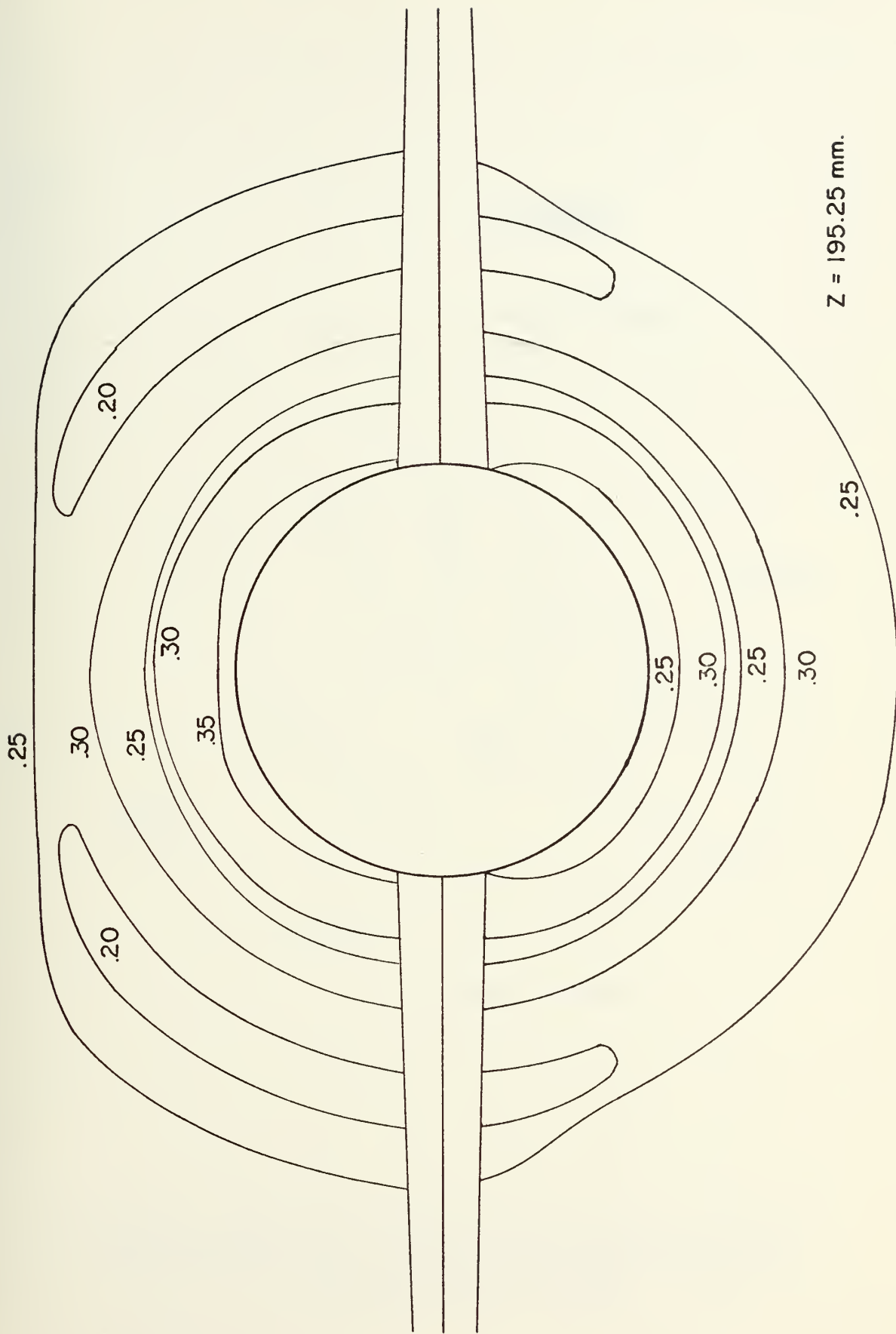


FIGURE 27.
 CONTOUR PLOT OF DENSITY FUNCTION, $(\rho / \rho_0) - 1$, FOR GIVEN CROSS-SECTIONAL PLANE
 $Z = 195.25$ mm.

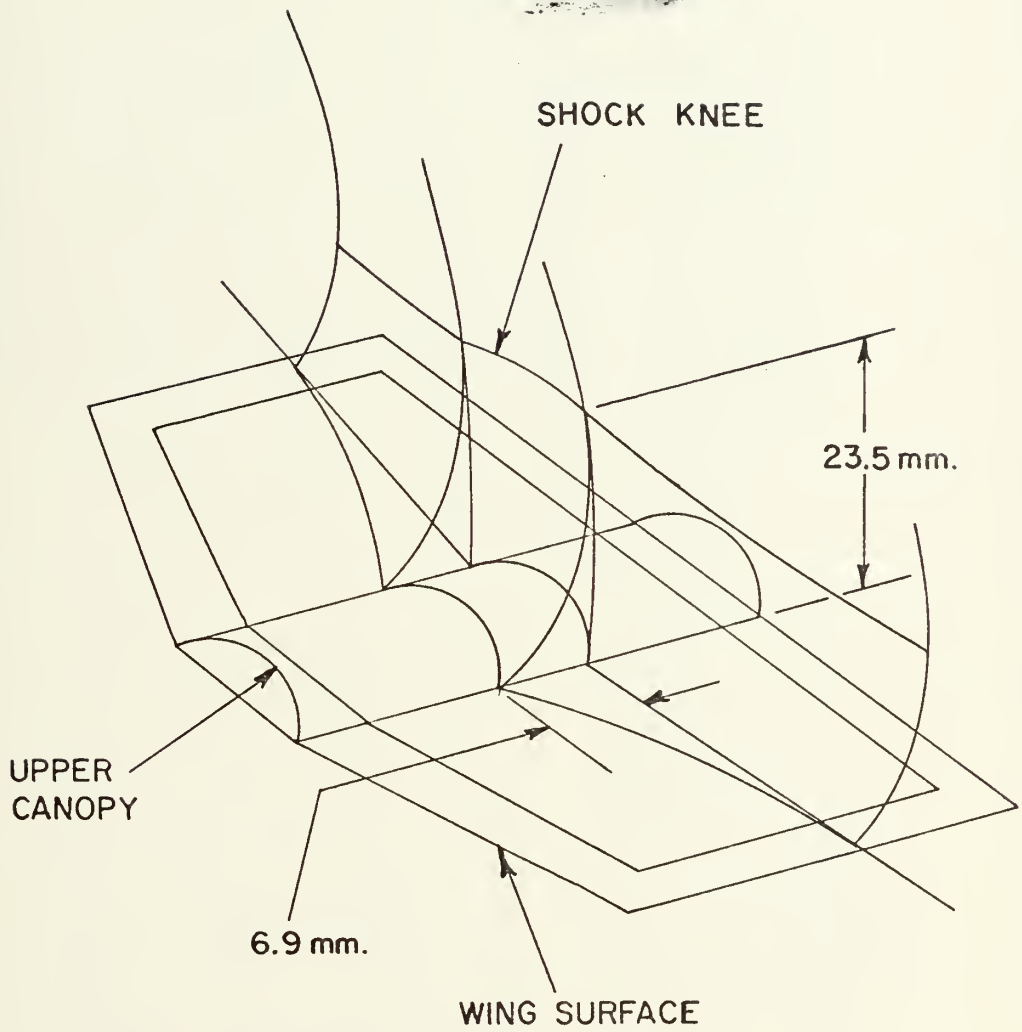


FIGURE 28. THREE DIMENSIONAL SCHEMATIC OF SHOCK WAVE STRUCTURE; CONSTRUCTED USING SEVERAL INTERFEROGRAM VIEWS

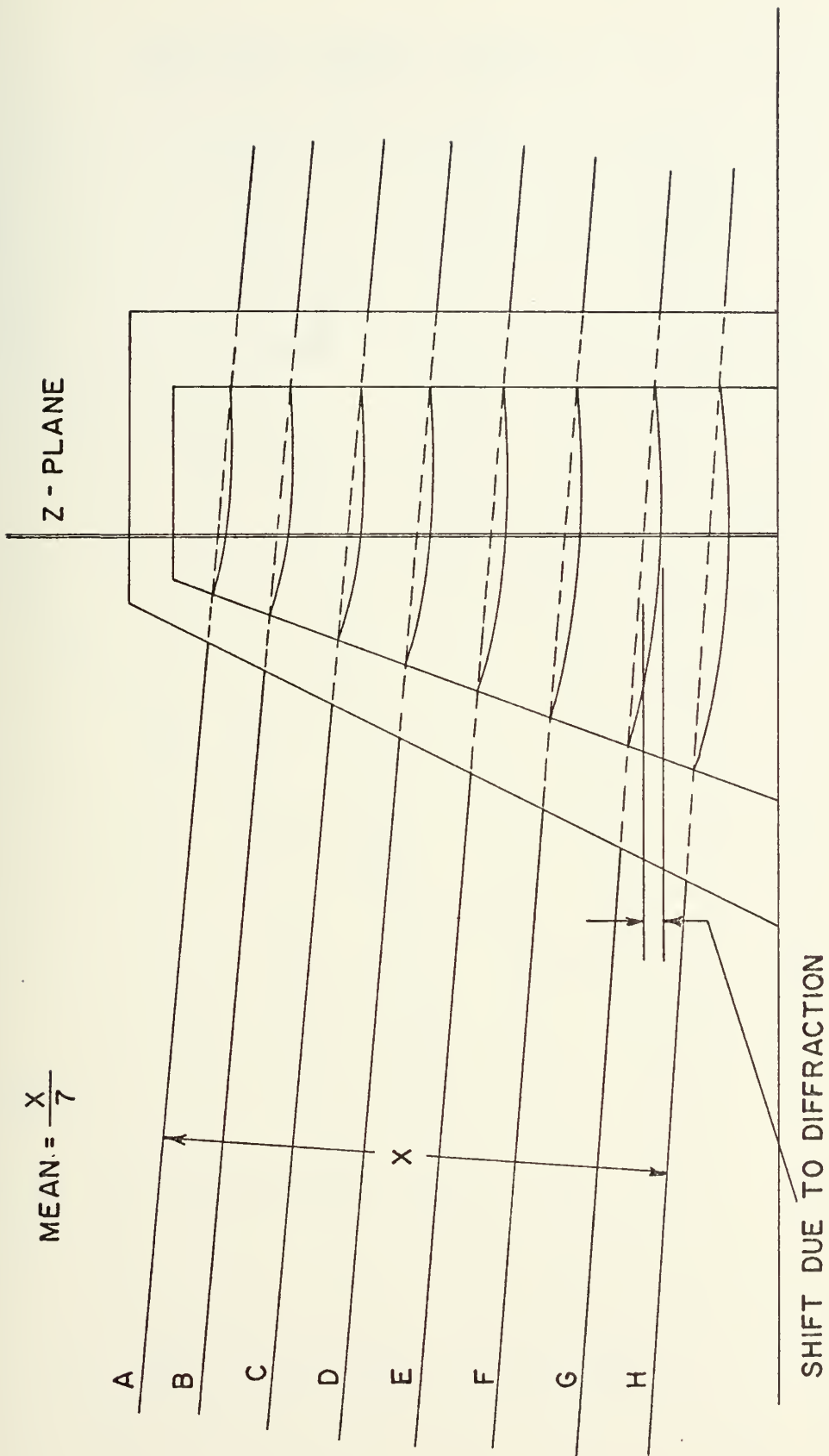


FIGURE 29. DOUBLE-STATIC HOLOGRAM REDUCTION PROCESS; $Z = 186.75$ mm.

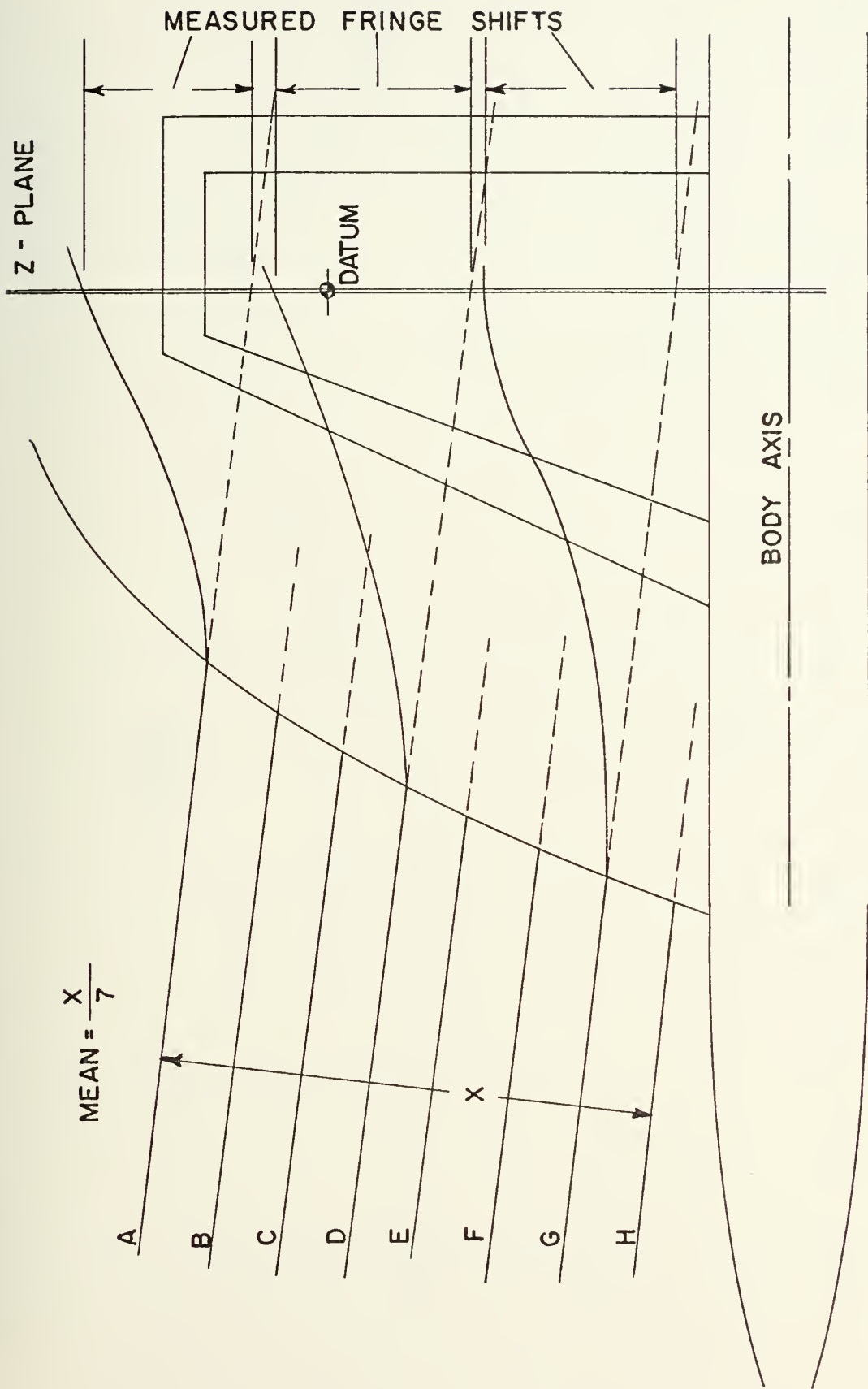


FIGURE 30. STATIC-DYNAMIC HOLOGRAM REDUCTION PROCESS; Z = 186.75 mm.

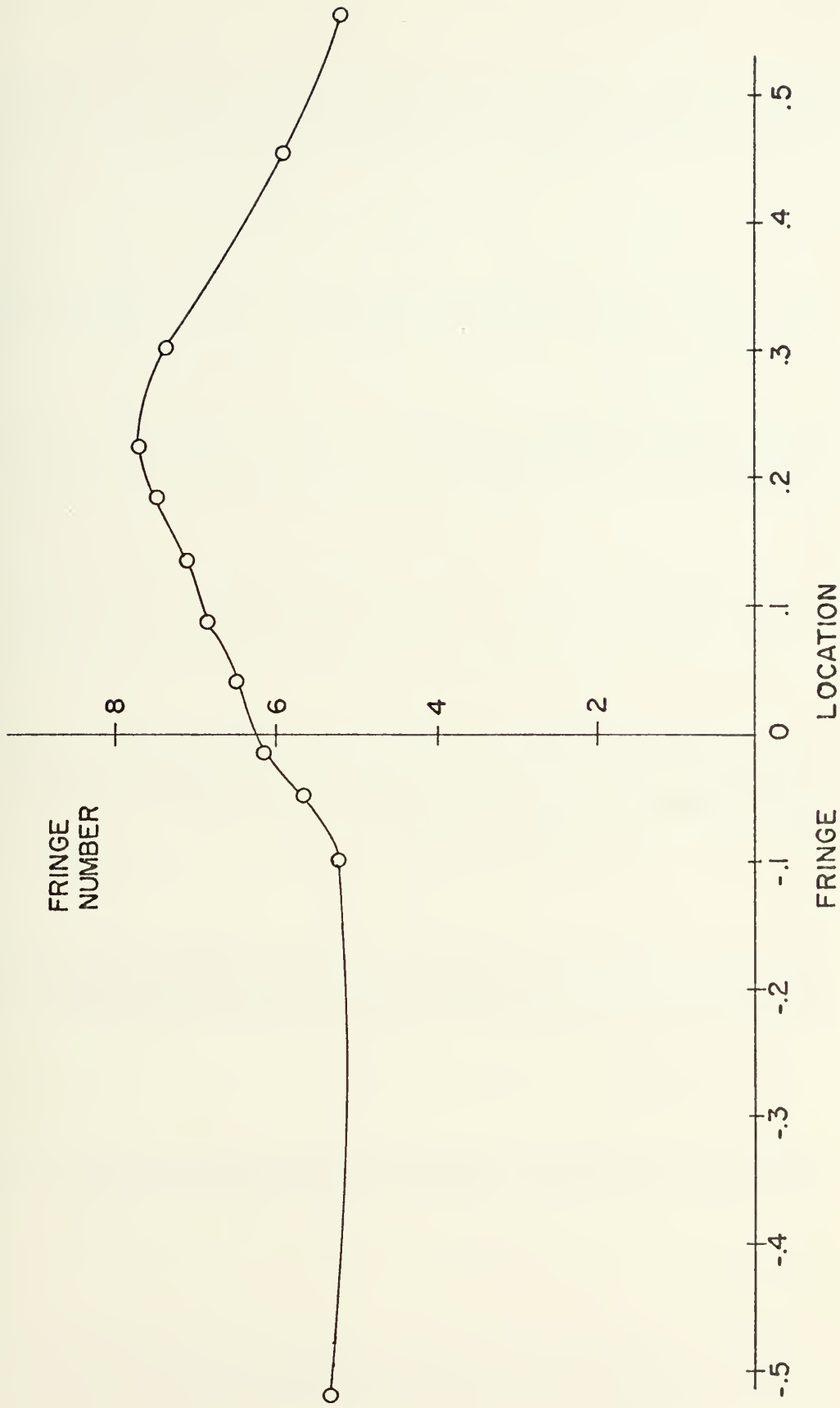


FIGURE 31. RADIAL VARIATION OF FRINGE NUMBER;
ZERO DEGREE VIEW, $Z = 186.75$ mm.

RUN NUMBER	HOLOGRAM NUMBER	DOUBLE EXPOSURE	ROLL ANGLE	P _A (psi)	P _T (psi)	T _T (deg. F)	MACH NUMBER
1	9	S/S	0.00				
2	10	S/D	0.00	14.781	14.181	64.6	.9371
3	23	S/S	11.25				
4	24	S/D	11.25	14.820	14.228	64.2	.9398
5	19	S/S	22.50				
6	20	S/D	22.50	14.784	14.187	64.6	.9361
7	15	S/S	33.75				
8	16	S/D	33.75	14.800	14.206	64.2	.9392
9	11	S/S	45.00				
10	12	S/D	45.00	14.785	14.185	64.6	.9391
11	25	S/S	56.25				
12	26	S/D	56.25	14.830	14.237	64.3	.9361
13	21	S/S	67.50				
14	22	S/D	67.50	14.787	14.195	64.3	.9365
15	17	S/S	78.75				
16	18	S/D	78.75	14.870	14.285	64.8	.9342
17	13	S/S	90.00				
18	14	S/D	90.00	14.787	14.195	64.6	.9402
19	35	S/S	101.25				
20	36	S/D	101.25	14.781	14.274	61.5	.9392
21	27	S/S	112.50				
22	28	S/D	112.50	14.875	14.281	62.5	.9371
23	37	S/S	123.75				
24	38	S/D	123.75	14.878	14.284	61.0	.9369
25	29	S/S	135.00				
26	30	S/D	135.00	14.875	14.278	62.0	.9372
27	39	S/S	146.25				
28	40	S/D	146.25	14.881	14.286	60.3	.9352
29	31	S/S	157.50				
30	32	S/D	157.50	14.875	14.276	61.8	.9350
31	41	S/S	168.75				
32	42	S/D	168.75	14.881	14.287	61.0	.9371
33	33	S/S	180.00				
34	34	S/D	180.00	14.875	14.282	62.0	.9357

TABLE I. EXPERIMENTAL DATA FOR WIND TUNNEL RUNS AT NSRDC

FRINGE I. D.	MEASURED SHIFT	CORRECTED SHIFT	FRINGE NUMBER	DISTANCE FROM DATUM	DE MAG. DISTANCE	DISTANCE FROM AXIS	NONDIMEN. LOCATION
A	25.0	21.475	3.53	-27.0	-25.1	-63.8	--.798
B	29.6	26.075	4.29	-23.2	-21.6	-59.8	--.748
C	30.4	26.875	4.42	-18.5	-17.2	-55.4	--.693
D	31.6	28.075	4.62	-13.0	-12.1	-50.3	--.623
E	35.5	31.975	5.23	- 9.5	- 8.8	-47.0	--.588
F	36.0	32.475	5.34	- 3.6	- 3.4	-41.6	--.520
G	34.0	30.475	5.23	+32.8	+30.5	- 7.7	--.096
H	36.4	32.875	5.64	+37.0	+34.4	- 3.8	--.048
I	40.0	36.475	6.26	+40.0	+37.2	- 1.0	--.013
J	41.5	37.975	6.51	+44.4	+41.3	+ 3.1	+ .039
K	43.5	39.975	6.86	+48.5	+45.2	+ 7.0	+ .088
L	45.3	41.775	7.17	+52.7	+49.1	+10.9	+ .136
M	47.4	43.875	7.53	+57.0	+53.1	+14.9	+ .186
N	48.6	45.075	7.73	+60.5	+56.3	+18.1	+ .226
O	46.8	43.275	7.42	+67.0	+62.4	+24.2	+ .303
P	38.5	34.975	5.99	+80.3	+74.8	+36.6	+ .458
Q	34.0	30.475	5.23	+89.6	+83.4	+45.2	+ .565

Mean free stream spacing = 5.96 mm.

Diffraction Correction = 3.525 mm.

Magnification factor = 1.074

Body axis location = +38.2 mm

All measurements in millimeters

- = above, + = below

TABLE II.

RECORDED DATA FOR ZERO DEGREE VIEW AT Z = 186.75 mm. FROM BODY NOSE

APPENDIX A

REDUCTION OF AN INTERFEROGRAM TO OBTAIN FRINGE SHIFT DATA

The reduction of data for a cross-sectional plane of interest involved a complete analysis of both doubly exposed holograms, and their corresponding interferograms, for each viewing angle.

For each view, or line of sight, the double-static exposure was first placed face down on a light table. The average fringe spacing was recorded on the back by measuring the perpendicular distance between two sufficiently separated fringe lines in the free stream and dividing by the number of spacings in between. The method is portrayed in Figure 29. Of primary importance was the measurement of the uniform shift of fringe lines due to the beam diffractive quality of the lucite sections of the model; this was taken to be the average distance between hypothetically unaltered fringe lines and the corresponding shifted fringes at their intersection with the z -plane.

The static-dynamic exposure was then placed face down on the light table and the fringe and model contours traced on the back, as shown in Figure 30. Again, the average free stream fringe line spacing was measured and checked against the value from the double-static exposure. A reference point, or datum, was selected at the intersection of a well-defined horizontal grid line and the z -plane of interest. Fringe shifts were computed in the following manner:

1. The distance from datum to a hypothetically undeviated fringe line at its intersection with the z-plane was measured in millimeters.
2. The distance from datum to the actual deviated, or shifted, fringe at its intersection with the z-plane was measured in millimeters. Measured shifts should be made perpendicular to the fringe direction. The present procedure is convenient and only introduces an error of about 1% in the overall level of the density field.
3. The raw fringe shift distance was then the distance in 1. above minus the distance in 2.
4. To correct for diffraction error, the uniform shift measured in the double-static exposure was then subtracted from the distance in 3.

Fringe numbers were calculated by dividing the shift for each fringe by the average free stream spacing for the exposure. Magnification factors were computed for each exposure by comparing photographically recorded model diameter with actual model diameter.

Since the datum location varied slightly from exposure to exposure, it was necessary to reference all measurements to a central point for each plane of analysis. This point was taken to be the intersection of the longitudinal axis of the model fuselage and the cross-sectional plane of interest. The intersections of shifted fringe lines with the z-plane were referenced to this fixed point and demagnified. The resulting distances were then nondimensionalized using the selected inversion circle radius. Table II contains typical data recorded for the zero degree view at the 186.75 mm. plane of interest.

A plot of fringe numbers versus nondimensionalized fringe location was produced for each viewing angle using data obtained from the interferograms. Fringe numbers at 201 equidistant points, as required for input into Mode 3 of the inversion computer program, were recorded from the resulting curves. The curve plotted using the data from Table II is shown in Figure 31.

APPENDIX B

APPLICATION OF COMPUTER PROGRAM "HOLOFER"

The computer program used in this study is designed to invert an array of fringe numbers across a field to obtain the associated density field using a special adaptation of the inversion technique first proposed by C. D. Maldonado [5, 6]. Three different modes of operation are available to the operator, as described below:

(a) Mode 1

This mode provides the basic self-testing capability of the computer program. It can either generate its own input density field using Subroutine FUNCT or read in a density field through Subroutine FREAD. The fringe number array corresponding to the input density data is first generated; this information is then used as the input for the inversion to obtain the original density distribution once again. This self-testing procedure was utilized in the present investigation to determine the best value of the scale factor, α , required to assure accurate density in the region of inversion.

(b) Mode 2

This mode generates the fringe array at regular intervals across the test field from irregularly spaced fringe values read in through Subroutine SHEET. Simulated fringe arrays may be generated

by one of the functions specified in Subroutine FUNCT if NCODE = 1 is specified. Mode 2 has not been utilized in the present investigation.

(c) Mode 3

Mode 3 operation reads in a regularly spaced array of input density values directly utilizing Subroutine READ, which is first called by Subroutine GARRAY. The parameters in the first two cards preceding the input fringe data serve to identify the size, location and symmetry of the fringe field. The following parameters were used in calculating the asymmetric density field in the present experiment:

<u>PARAMETER</u>	<u>INPUT</u>
NOF	Run Number
IMAX	201
JMAX	20
ISYM	1
JSYM	1
IMS	201
JMS	5
Z	0.0, 1.0
XO	0.0
YO	0.0
PHISYM	0.0

Amplifying details and applications of the inversion computer program are found in References [3, 7, 9]. A listing of the program is included in this appendix for reference.


```

CAL00010
CAL00020
CAL00030
CAL00040
CAL00050
CAL00060
CAL00070
CAL00080
CAL00090
CAL00100
CAL00110
CAL00120
CAL00130
CAL00140
CAL00150
CAL00160
CAL00170
CAL00180
CAL00190
CAL00200
CAL00220
CAL00230
CAL00240
CAL00250
CAL00260
CAL00270
CAL00280
CAL00290
CAL00300
CAL00310
CAL00320
CAL00330
CAL00340
CAL00350
CAL00360
CAL00370
CAL00380
CAL00390
CAL00400
CAL00410
CAL00420
CAL00430
CAL00440
CAL00450
CAL00460
CAL00470

*****HOLOVERT*****
HOLOVERT INVERTS THE FIELD AT AN ARRAY OF POINTS IN A VARIABLE
COORDINATE SYSTEM. IT SURVEYS NPTS POINTS EACH FOR A SET OF NLINS
LINES ACROSS THE FIELD.
*****
COMMON I MAX, J MAX, I IMX, J JMX, I JMX, ALPHA, SIZE, EPS, MODE, BOX, SD, IX, Z
COMMON /TAB/ I INDEX, KEXTRA, MEXTRA, KLIMIT, MLIMIT, KOUT, MOUT
COMMON /TAB2/ IPT, KPT, LPT, BND, NPTS, NLINS, RHOINF, RLAMDA, BETA
COMMON /OUT/ XP, THEO, CALC, ERR, RHO, CA, FA
COMMON /EQPAR/ A, B, C, D, E, P, Q, S, T, U, V, W, RO, RA, NO, NA, NOF, NAF
COMMON /SYM/ ISYM, JSYM, MSYM, FCU, IMS, JMS, QSYM
COMMON /IO/ CMS, IN1, IN2, IN4
DATA BL, PL, ST, EX, OH, SC, DH, BR/1H, IH+, IH*, IHX, IHO, IH-, IH//
DIMENSION RB(7), TL(62), RO(101), RA(101)
-----
DIMENSION G(5151), GA(5151), H(202, 5), SCF(73, 6), BDA(4000)
DIMENSION THEO(51, 11), CALC(51, 11), ERR(51), RHO(51)
DIMENSION CA(51), FA(51, 11), AR(42), XP(51), YP(51)
CMS=0.
-----
REWIND 3
IN1=5
IN2=5
IN4=5
IF (CMS.NE.1.) GO TO 20
IN1=1
IN2=2
IN4=4
IF (CMS.EQ.1.) REWIND 4
READ (IN4, 89) (AR(I), I=1, 42)
IMAX=AR(1) *2
IF (JMAX.LE.0) JMAX=1
KLIMIT=AR(3)
MLIMIT=AR(4)
KEXTRA=AR(5)
MEXTRA=AR(6)
JSYM=AR(14)
ALPHA=AR(17)
SIZE=AR(8)
EPS=AR(9)
MODE=AR(13)
DGN=AR(17)
RHOINF=AR(10)
RLAMDA=AR(11)*1.E-8
BETA=AR(12)

```

C
C
C
C
C
C

C

C

20

CAL00480
 CAL00490
 CAL00500
 CAL00510
 CAL00520
 CAL00530
 CAL00540
 CAL00550
 CAL00560
 CAL00570
 CAL00580
 CAL00590
 CAL00600
 CAL00610
 CAL00620
 CAL00630
 CAL00640
 CAL00650
 CAL00660
 CAL00670
 CAL00680
 CAL00690
 CAL00700
 CAL00710
 CAL00720
 CAL00730
 CAL00740

NPTS=AR(15)
 NLINS=AR(16)
 SD=AR(18)
 PHIZ=AR(19)
 DELPHI=AR(20)
 YPZERO=AR(21)
 YPRNG=AR(22)
 XPZERO=AR(23)
 XPRNG=AR(24)
 NOF=AR(25)
 NAF=AR(26)
 IPT=AR(27)
 KPT=AR(28)
 LPT=AR(29)
 BND=AR(30)
 A=AR(31)
 B=AR(32)
 C=AR(33)
 D=AR(34)
 E=AR(35)
 P=AR(36)
 S=AR(37)
 T=AR(38)
 U=AR(39)
 V=AR(40)
 W=AR(41)
 Q=AR(42)

WRITE(6,90)
 WRITE(6,98)
 WRITE(6,91)
 WRITE(6,92)
 WRITE(6,93)
 WRITE(6,94)
 WRITE(6,95)
 WRITE(6,96)
 WRITE(6,97)
 WRITE(6,98)
 FORMAT(//)//
 FORMAT(/5X,/,
 1, MEXTRA *, /3X, 6F10.0)
 1, BETA *, /3X, 2F10.3, * ALPHA *, /3X, 2F10.3, * SIZE *, EPS., * RHO-INF * LAMBDA *, SET00340
 1, STD DEV *, /2X, 5F10.0, * MODE * LINES * DIAGNOS *, SET00360
 1, XPRNGE *, /4X, 6F10.3)
 1, MAP BND *, /2X, 6F10.0)

90
 91
 92
 93
 94
 95


```

96 1, FORMAT (/5X, '* A * B * C * D * E *', SET00420
97 1, FORMAT (/5X, '* S * T * U * V * W *', SET00440
98 1, FORMAT (/3X, 75A1)
   IF (DGN.GE.4) WRITE (6, 89) (AR(I), I=1, 42)
   NNN=2
   IF (MODE.LT.0) NNN=1
   IF (MODE.GT.5) NNN=3
   IF (MODE.GT.5) MODE=MODE-10
   NGP=0
   IF (KLIMIT.LT.KEXTRA) KEXTRA=KLIMIT
   IF (MLIMIT.LT.MEXTRA) MEXTRA=MLIMIT
   IF (IPT.LT.0) NGP=IPT
   IF (IPT.LT.0) IPT=-IPT
   ISYM=2.1-(FLOAT(JSYM)/2.-FLOAT(JSYM/2))*2
   IF (JSYM.EQ.0) ISYM=1
   IF (JSYM.GT.JMAX) ISYM=2
   IF (ISYM.EQ.1) JMAX=((JMAX+1)/2)*2
   RJMX=JMAX
   MSYM=JSYM
   IF ((MSYM.EQ.0).OR.(MSYM.GT.JMAX)) MSYM=1
   FCU=ISYM*JSYM#JMAX
   IF ((JSYM.GT.JMAX).OR.(JSYM.EQ.0)) FCU=JMAX
   QSYM=FCU/RJMX
   IMS=(IMAX+ISYM-1)/ISYM
   JMS=JMAX
   IF (ISYM.EQ.1) JMS=(JMAX/2+1)/2
   IF (JSYM.EQ.0) JMS=JMAX/2
   MODE=ABS(AR(13))
   XO=0.
   YO=0.
   ZD=0.
   PHISYM=0.
   HS=SIZE/2.
   RHOS=1.286
   BOX=RHOINF*BETA/RHOS/RLAMDA
   RPTS=NPTS
   XPR=0.
   IF (NPTS.GT.1) XPR=XPRNG/(RPTS-1.)/2.
   XPM=-XPR
   PIE=3.141592653589793
   MONE=1
   WRITE (6, 58) IMAX, JMAX, IMS, JMS, ISYM, MSYM, QSYM, FCU, /
   FORMAT (3X, 'IMAX, JMAX, IMS, JMS, ISYM, MSYM, QSYM, FCU, /
   7I5, 2F7.3/)
1  NTWO=2
   IX=IMAX+JMAX

```

```

CAL00750
CAL00760
CAL00770
CAL00780
CAL00790
CAL00800
CAL00810
CAL00820
CAL00830
CAL00840
CAL00850
CAL00860
CAL00870
CAL00880
CAL00890
CAL00900
CAL00910
CAL00920
CAL00930
CAL00940
CAL00950
CAL00960
CAL00970
CAL00980
CAL00990
CAL01000
CAL01010
CAL01020
CAL01030
CAL01040
CAL01050
CAL01060
CAL01070
CAL01080
CAL01090
CAL01100
CAL01110
CAL01120
CAL01130
CAL01140
CAL01150
CAL01160
CAL01170

```

58


```

NF=INI
IF ((MODE.EQ.1.) .AND. (NOF.EQ.8) .AND. (DGN.GE.1.)) WRITE (6,69)
IF ((MODE.EQ.1.) .AND. (NOF.EQ.8)) CALL FREAD (NO,RO,NF,ZD)
Z=ZD
IF (DGN.GE.1.) WRITE (6,68)
CALL GARRAY (G,GA,NOF,DGN,MONE,XO,YO,PHISYM)
LM=1
IF ((LPT.EQ.0) .AND. (BND.EQ.0)) LM=0
IIMX=IMAX+1
JJMX=JMAX+1
IJMX=IMAX*JMAX
NBD=1
IF (JSYM.EQ.0) NBD=2
KBD=KLIMIT*NBD
DO 15 IJ=1, IJMX
GA(IJ)=0
IF (NAF.EQ.0) GO TO 16
NF=IN2
IF ((NAF.EQ.8) .AND. (DGN.GE.1.)) WRITE (6,69)
IF (NAF.EQ.8) CALL FREAD (NA,RA,NF,ZD)
MST=MODE
MODE=1
IF (DGN.GE.1.) WRITE (6,68)
IF (NAF.NE.0) CALL GARRAY (GA,G,NAF,DGN,NTWO,XO,YO,PHISYM)
MODE=MST
DO 6 IJ=1, IJMX
G(IJ)=G(IJ)+GA(IJ)
RLINS=NLINS
IF (NAF.EQ.8) WRITE (6,88) NA,(RA(L),L=1,NA)
IF (NOF.EQ.8) WRITE (6,87) NO,(RO(I),I=1,NO)
IF (LM.EQ.0) GO TO 14
RB(1)=-1.7
DO 1 I=2,7
RB(I)=RB(I-1)+.5
TPIE=2.*PIE
MPIE=-PIE
DYP=0.
DXP=0.
IF (NLINS.GT.1) DYP=YPRNG/(RLINS-1.)
IF (NPTS.GT.1) DXP=XPRNG/(RPTS-1.)
IF ((DGN.GE.1.) .AND. (NPN.EQ.2)) WRITE (6,64)
IF (NPN.EQ.2) CALL BDGEN (G,H,SCF,DGN,NBD,BDA,KBD)
DO 5 J=1,NLINS
IF (DGN.GE.1.) WRITE (6,67) J
RJM=J-1
PHI=PHIZ+DELP+I*RJM
YP(J)=YPZERO+DYP*RJM
PSI=(PHI+90.)*PIE/180.

```

15

6
16

1

CAL01180
CAL01190
CAL01200
CAL01210
CAL01220
CAL01230
CAL01240
CAL01250
CAL01260
CAL01270
CAL01280
CAL01290
CAL01300
CAL01310
CAL01320
CAL01330
CAL01340
CAL01350
CAL01360
CAL01370
CAL01380
CAL01390
CAL01400
CAL01410
CAL01420
CAL01430
CAL01440
CAL01450
CAL01460
CAL01470
CAL01480
CAL01490
CAL01500
CAL01510
CAL01520
CAL01530
CAL01540
CAL01550
CAL01560
CAL01570
CAL01580
CAL01590
CAL01600
CAL01610
CAL01620
CAL01630
CAL01640
CAL01650

CAL01660
 CAL01670
 CAL01680
 CAL01690
 CAL01700
 CAL01710
 CAL01720
 CAL01730
 CAL01740
 CAL01750
 CAL01760
 CAL01770
 CAL01780
 CAL01790
 CAL01800
 CAL01810
 CAL01820
 CAL01830
 CAL01840
 CAL01850
 CAL01860
 CAL01870
 CAL01880
 CAL01890
 CAL01900
 CAL01910
 CAL01920
 CAL01930
 CAL01940
 CAL01950
 CAL01960
 CAL01970
 CAL01980
 CAL01990
 CAL02000
 CAL02010
 CAL02020
 CAL02030
 CAL02040
 CAL02050
 CAL02060
 CAL02070
 CAL02080
 CAL02090
 CAL02100
 CAL02110
 CAL02120
 CAL02130

```

TAU=PSI-PHISYM
IF (LPT.EQ.0) GO TO 9
WRITE (6,78) (ST,I=1,124)
IF (LPT.GT.1) WRITE (6,74) (ST,I=1,95)
IF ((CMS.EQ.1.) .AND. (LPT.GT.1)) READ (5,79) ZZ
WRITE (6,86) Z,PHI,YP(J)
WRITE (6,85) Z,PHI,YP(J)
WRITE (6,76) Z,PHI,YP(J)
IF (MODE.EQ.1) WRITE (6,83) (RB(I),I=1,7)
IF (MODE.GT.1) WRITE (6,80) (RB(I),I=1,7)
WRITE (6,81) (DH,I=1,54),(PL,I=1,13)
IC=0
DO 3 I=1,NPTS
  RIM=I-1
  THEO(I,J)=0.
  CA(I)=0.
  FA(I,J)=0.
  ERR(I)=0.
  CALC(I,J)=0.
  RH(I)=XPZERO+DXP*RIM
  XPI=ABS(XP(I))
  IF (XPI.LT.1.E-13) XP(I)=0.
  RS=SQRT(XP(I)**2+YP(J)**2)/HS
  ITH=(RS.GT.1.) GO TO 13
  ITH=ATANM(YP(J),XP(I))
  IF (XPI.EQ.0.) ITH=0.
  SIG=TAU-PIE/2.+ITH
  IF (SIG.GT.PIE) SIG=SIG-TPIE
  IF (SIG.LT.MPIE) SIG=SIG+TPIE
  SIGI=SIG
  XS=RS*COS(SIG)
  IF (DGN.GE.1.) WRITE (6,44) SIG
  FORMAT (1,SIG=,E10.3)
  YS=RS*SIN(SIG)
  IF (DGN.GE.5) WRITE (6,57) PHI,DELPHI,PSI,TAU,THI,SIG,SIGI,XS,YS
  I FORMAT (1,ANGLES=,10E10.3)
  RI=I
  F=0.
  IF (DGN.GE.2.) WRITE (6,66) I
  CALL FUNCT (XS,YS,FA(I,J),NAF,DGN,NTWO)
  IF (MODE.EQ.1) CALL FUNCT (XS,YS,F,NOF,DGN,MONE)
  THEO(I,J)=F
  IF (NNN.GE.2) REWIND 3
  IF (NNN.GE.2) CALL FIELD (RS,SIGI,SOLN,NBD,BDA,DGN,KBD)
  IF (NNN.EQ.1) CALL FIELD2 (RS,SIGI,SOLN,G,H,SCF,DGN)
  CA(I)=SOLN/BOX/HS
  CALC(I,J)=CA(I)-FA(I,J)

```

9

44

57

CAL02140
 CAL02150
 CAL02160
 CAL02170
 CAL02180
 CAL02190
 CAL02200
 CAL02210

CAL02260
 CAL02270
 CAL02280
 CAL02290
 CAL02300
 CAL02310
 CAL02320
 CAL02330
 CAL02340
 CAL02350
 CAL02360
 CAL02370
 CAL02380
 CAL02390
 CAL02400
 CAL02410
 CAL02420
 CAL02430
 CAL02440
 CAL02450
 CAL02460
 CAL02470
 CAL02480
 CAL02490
 CAL02500
 CAL02510
 CAL02520
 CAL02530
 CAL02540
 CAL02550
 CAL02560
 CAL02570
 CAL02580
 CAL02590
 CAL02600
 CAL02610

```

RHO(I)=RHOINF*(CALC(I,J)+1.)
ERR(I)=CA(I)
IF (MODE.EQ.1) ERR(I)=(CALC(I,J)-THEO(I,J))
IF (MODE.GT.1) THEO(I,J)=FA(I,J)
IF (LPT.EQ.0) GO TO 3
LC=0
TL(I)=BL
TTL=0
IF ((XP(I).GT.XPM).AND.(XP(I).LT.XPR)) TTL=1.
IF (IC.EQ.5) IC=0
IF (IC.EQ.0) TL(I)=PL
DO 2 L=2,62
  TL(L)=BL
  IF ((I.EQ.1).OR.(TTL.EQ.1).OR.(I.EQ.NPTS)) TL(L)=PL
  IF (LC.EQ.13) LC=0
  IF ((IC.EQ.0).AND.(LC.EQ.0)) TL(L)=PL
  LC=LC+1
  TL(2)=PL
  TL(22)=PL
  TL(62)=PL
  IC=IC+1
  RLW=(CA(I)+1.)*20.+2.5
  LW=RLW
  IF (LW.GT.62) LW=62
  IF (LW.LT.2) LW=2
  TL(LW)=SC
  RLY=(FA(I,J)+1.)*20.+2.5
  LY=RLY
  IF (LY.GT.62) LY=62
  IF (LY.LT.2) LY=2
  IF (NAF.NE.0) TL(LY)=ST
  RLX=(THEO(I,J)+1.)*20.+2.5
  LX=RLX
  IF (LX.GT.62) LX=62
  IF (LX.LT.2) LX=2
  IF (MODE.EQ.1) TL(LX)=OH
  RLZ=(CALC(I,J)+1.)*20.+2.5
  LZ=RLZ
  IF (LZ.GT.62) LZ=62
  IF (LZ.LT.2) LZ=2
  TL(LZ)=EX
  WRITE (6,82)MOUT,KOUT,INDEX,THEO(I,J),ERR(I),CALC(I,J),RHO(I),
1XP(I),(TL(L),L=1,62)
  IF ((NPTS.LE.20).AND.(I.NE.NPTS)) WRITE (6,79)
  CONTINUE
IF (LPT.NE.0) WRITE (6,81) (DH,I=1,54),(PL,I=1,13)
TMAX=0.
TMIN=0.

```

13

2

3


```

CAL02620
CAL02630
CAL02640
CAL02650
CAL02660
CAL02670
CAL02680
CAL02690
CAL02700
CAL02710
CAL02720
CAL02730
CAL02740
CAL02750
CAL02760
CAL02770
CAL02780
CAL02790
CAL02800
CAL02810
CAL02820
CAL02830
CAL02840
CAL02850
CAL02860
CAL02870
CAL02880
CAL02890
CAL02900
CAL02910
CAL02920
CAL02930
CAL02940
CAL02950
CAL02960
CAL02970
CAL02980
CAL02990
CAL03000
CAL03010
CAL03020
CAL03030
CAL03040
CAL03050
CAL03060
CAL03070
CAL03080
CAL03090

IE=0
BE=0.
EB=0.
DO 4 I=1,NPTS
  TH=THEO(I,J)      TMAX=TH
  IF (TH.GT.TMIN)   TMIN=TH
  ER=ABS(CALC(I,J)-TH)
  IF (ER.LE.BE) GO TO 4
BE=ER
IE=I
CONTINUE
TMM=TMAX-TMIN
EB=RHOINF*(CALC(IE,J)-THEO(IE,J))
IF (TMM.NE.0.) BE=(CALC(IE,J)-THEO(IE,J))*100./TMM
IF ((MDE.EQ.1).AND.(LPT.NE.0)) WRITE (6,75) EB,XP(IE),BE
IF ((DELPHI.NE.0.) YP(J)=PHI
CONTINUE
IF (BND.EQ.0.) GO TO 14
IF (LPT.EQ.1) WRITE (6,78) (ST,I=1,124)
IF (LPT.GT.1) WRITE (6,74) (ST,I=1,95)
IF ((CMS.EQ.1).AND.(LPT.GT.1)) READ (5,79) ZZ
IF (DGN.GE.1.) WRITE (6,63)
CALL MAP (NPTS,NLINS,CALC,NOF,Z,BND)
IF (NAF.EQ.0) GO TO 10
NAO=10*NOF+NAF
IF ((DGN.GE.1).AND.(NGP.EQ.-3)) WRITE (6,62)
IF (NGP.EQ.-3) CALL GPUNCH (Z,XO,YO,PHISYM,NAO,IMAX,JMAX,G)
DO 7 IJ=1,IJMX
  G(IJ)=G(IJ)-GA(IJ)
  IF (IPT.LE.0) GO TO 11
  IF ((IPT.EQ.1).OR.(IPT.EQ.3)) WRITE (6,78) (ST,I=1,124)
  IF ((IPT.EQ.2).OR.(IPT.GE.4)) WRITE (6,74) (ST,I=1,95)
  IF ((CMS.EQ.1).AND.((IPT.EQ.2).OR.(IPT.GE.4))) READ (5,79) ZZ
  CALL GPRINT (G,MONE)
  IF (NGP.EQ.-1) CALL GPUNCH (Z,XO,YO,PHISYM,NOF,IMAX,JMAX,G)
  IF (IPT.EQ.3) WRITE (6,78) (ST,I=1,124)
  IF (IPT.GE.4) WRITE (6,74) (ST,I=1,95)
  IF ((CMS.EQ.1).AND.((IPT.GE.4))) READ (5,79) ZZ
  IF (IPT.GE.3) CALL GPRINT (GA,NTWO)
  IF (KPT.LE.0) GO TO 12
  IF ((KPT.EQ.1).OR.(KPT.EQ.3)) WRITE (6,78) (ST,I=1,124)
  IF ((KPT.EQ.2).OR.(KPT.GE.4)) WRITE (6,74) (ST,I=1,95)
  IF ((CMS.EQ.1).AND.((KPT.EQ.2).OR.(KPT.GE.4))) READ (5,79) ZZ
  IF (DGN.GE.1.) WRITE (6,61)
  CALL GPLOTT (G,GA,JMS)
  WRITE (6,73) (EX,I=1,124)
  AGAIN=ST
11
12

```



```

89 IF (CMS.NE.1.) READ(5,60) AGAIN
88 IF (AGAIN.EQ.BL) GO TO 20
WRITE (6,77)
FORMAT (6F12.7)
1 POINTS) WAS: /7(11F10.3//) THE INPUT DATA FOR ADD-ON FUNCTION NO.8 (' ,I3,
87 1 POINTS) WAS: /7(11F10.3//) THE INPUT DATA FOR THE TEST FUNCTION NO.8, (' ,I3,
86 1 POINTS) WAS: /7(11F10.3//) THE INVERTED CROSS SECTION FOR: '
85 10X, 'Z =', F8.3, ' CM.', /10X, 'PHI=', F8.3, ' DEGREES' /10X,
14HY, '=', F8.3, ' CM.', /44X, '0 = ORIGINAL FUNCTION' /
270X, '*' = ADD-ON FUNCTION')
84 10X, 'Z =', F8.3, ' CM.', /10X, 'PHI=', F8.3, ' DEGREES' /10X,
83 10X, 'Z =', F8.3, ' CM.', /10X, 'PHI=', F8.3, ' DEGREES' /10X,
14HY, '=', F8.3, ' CM.', /44X, '0 = ORIGINAL FUNCTION' /
270X, '*' = ADD-ON FUNCTION')
82 10X, 'Z =', F8.3, ' CM.', /10X, 'PHI=', F8.3, ' DEGREES' /10X,
14HY, '=', F8.3, ' CM.', /44X, '0 = ORIGINAL FUNCTION' /
270X, '*' = ADD-ON FUNCTION')
81 10X, 'Z =', F8.3, ' CM.', /10X, 'PHI=', F8.3, ' DEGREES' /10X,
80 14HY, '=', F8.3, ' CM.', /44X, '0 = ORIGINAL FUNCTION' /
270X, '*' = ADD-ON FUNCTION')
79 10X, 'Z =', F8.3, ' CM.', /10X, 'PHI=', F8.3, ' DEGREES' /10X,
78 14HY, '=', F8.3, ' CM.', /44X, '0 = ORIGINAL FUNCTION' /
77 270X, '*' = ADD-ON FUNCTION')
76 10X, 'Z =', F8.3, ' CM.', /10X, 'PHI=', F8.3, ' DEGREES' /10X,
75 14HY, '=', F8.3, ' CM.', /44X, '0 = ORIGINAL FUNCTION' /
74 270X, '*' = ADD-ON FUNCTION')
69 10X, 'Z =', F8.3, ' CM.', /10X, 'PHI=', F8.3, ' DEGREES' /10X,
68 14HY, '=', F8.3, ' CM.', /44X, '0 = ORIGINAL FUNCTION' /
67 270X, '*' = ADD-ON FUNCTION')
66 10X, 'Z =', F8.3, ' CM.', /10X, 'PHI=', F8.3, ' DEGREES' /10X,
65 14HY, '=', F8.3, ' CM.', /44X, '0 = ORIGINAL FUNCTION' /
64 270X, '*' = ADD-ON FUNCTION')
63 10X, 'Z =', F8.3, ' CM.', /10X, 'PHI=', F8.3, ' DEGREES' /10X,
62 14HY, '=', F8.3, ' CM.', /44X, '0 = ORIGINAL FUNCTION' /
61 270X, '*' = ADD-ON FUNCTION')
60 10X, 'Z =', F8.3, ' CM.', /10X, 'PHI=', F8.3, ' DEGREES' /10X,
14HY, '=', F8.3, ' CM.', /44X, '0 = ORIGINAL FUNCTION' /
270X, '*' = ADD-ON FUNCTION')
M
CAL03230
CAL03240
CAL03250
CAL03260
CAL03270
CAL03280
CAL03290
CAL03300
CAL03310
CAL03320
CAL03330
CAL03340
CAL03350
CAL03360
CAL03370
CAL03380
CAL03390
CAL03400
CAL03410
CAL03420
CAL03430
CAL03440
CAL03450
CAL03460
CAL03470
CAL03480
CAL03490
CAL03500
CAL03510
CAL03520
SUB00010
SUB00020

```

```

C000001
C

```



```

SUBROUTINE BDGEN (G,H,SCF,DGN,NBD,BDA,KBD) .
C
C BDGEN EVALUATES THE B AND D COEFFICIENTS FOR ALL M AND K, AND WRITES
C THE ARRAY LINEARLY ON DISK.
C
COMMON IMAX,JMAX,IIMX,JJMX,IJMX,ALPHA,SIZE,EPS,MODE,BOX,SD,IX,Z
COMMON /TAB/ INDEX,KEXTRA,MEXTRA,KLIMIT,MLIMIT,KOUT,MOUT
COMMON /SYM/ ISYM,MSYM,FCU,IMS,JMS,QSYM
DIMENSION G(IJMX),H(IIMX,5),SCF(JJMX,6),BDA(KBD)
C INITIALIZE THE VALUES:
INDEX=0
KL2=NBD*KLIMIT
REWINDD 3
JJMX6=JJMX*6
IIMX2=(IIMX+1)/2
PIE=3.141592653589793
RIMAX=IMAX
KLIMP=KLIMIT+1
DX=2./RIMAX
RJMAX=JMAX
DXI=2.*PIE/FCU
C INITIALIZE THE MODIFIED HERMITE POLYNOMIAL ARRAY; VECTORS:
C (1)=H1, (2)=H2, (3)=ALPHA*X(I), (4)=HM+2 STORED, (5)=HM+1 STORED
DO 1,II=1,IIMX2
RII=II
IIM=IIMX-II+1
H(II,3)=ALPHA*(RII*DX-DX-1.)
H(IIM,3)=-H(II,3)
H(II,1)=2.*H(II,3)
H(II,2)=(H(II,3)*H(II,1)-1.)/3.
H(IIM,1)=-H(II,1)
H(IIM,2)=H(II,2)
H(II,5)=H(IIM,2)
H(IIM,4)=H(II,1)
H(IIM,4)=H(IIM,1)
SIGN=1.
C INITIALIZE THE SIN/COS ARRAY:
DO 2,J=1,JJMX
RJM=J-1
SCF(J,1)=0.
SCF(J,2)=1.
SCF(J,3)=SIN(RJM*DXI-PIE/2.)
SCF(J,4)=COS(RJM*DXI-PIE/2.)
SCF(J,5)=0.
SCF(J,6)=0.
MS=0
C COMMENCE THE M LOOP:
SUB00030
SUB00040
SUB00050
SUB00060
SUB00070
SUB00080
SUB00090
SUB00100
SUB00110
SUB00120
SUB00130
SUB00140
SUB00150
SUB00160
SUB00170
SUB00180
SUB00190
SUB00200
SUB00210
SUB00220
SUB00230
SUB00240
SUB00250
SUB00260
SUB00270
SUB00280
SUB00290
SUB00300
SUB00310
SUB00320
SUB00330
SUB00340
SUB00350
SUB00360
SUB00370
SUB00380
SUB00390
SUB00400
SUB00410
SUB00420
SUB00430
SUB00440
SUB00450
SUB00460
SUB00470
SUB00480
SUB00490
SUB00500

```



```

SUB00510
SUB00520
SUB00530
SUB00540
SUB00550
SUB00560
SUB00570
SUB00580
SUB00590
SUB00600
SUB00610
SUB00620
SUB00630
SUB00640
SUB00650
SUB00660
SUB00670
SUB00680
SUB00690
SUB00700
SUB00710
SUB00720
SUB00730
SUB00740
SUB00750
SUB00760
SUB00770
SUB00780
SUB00790
SUB00800
SUB00810
SUB00820
SUB00830
SUB00840
SUB00850
SUB00860
SUB00870
SUB00880
SUB00890
SUB00900
SUB00910
SUB00920
SUB00930
SUB00940
SUB00950
SUB00960
SUB00970

DO 7 MP=1,MLIMIT
RM=MP-1
RM=M
SIGN=-SIGN
IF (DGN.LE.-4) WRITE (6,88) SCF(1,1),SCF(2,1),SCF(1,2),SCF(2,2)
TEST FOR SYMMETRY SKIPS:
IF (MS.EQ.MSYM) MS=0
TOTAL=0.
MS=MS+1
IF (MS.NE.1) GO TO 6
C COMMENCE THE K LOOP:
DO 5 KP=1,KLIMIT
K=KP-1
PK=KP
RK=K
INDEX=INDEX+1
C CALL THE B & D COEFFICIENTS AND WRITE THEM ON DISK:
CALL BD (M,K,G,H,SCF,B,D,JJMX6)
IF (DGN.EQ.3.) WRITE (6,89) M,K,B,D
IF (DGN.LE.-2) WRITE (6,89) M,K,B,D
IF (DGN.LE.-4) WRITE (6,88) H(1,1),H(1,2),H(1,4),H(1,5)
KK=K*NBD+1
K2=KP*NBD
BDA(K2)=B
BDA(KK)=B
C GENERATE THE NEXT ORDER OF THE SET OF HERMITE POLYNOMIALS FOR NEW K:
ORDER=M+2*KP+1
HA=SQRT((PK+RM))/ORDER
HB=2.*SQRT((PK+1.))*((ORDER+1.))/(ORDER+2.)
DO 5 II=1,IIMX2
IIM=IIMX-II+1
H(II,1)=2.*(H(II,3)*H(II,2)-HA*H(II,1))
H(II,M,1)=SIGN*H(II,1)
H(II,2)=HB*(H(II,3)*H(II,1)-ORDER*H(II,2))
C ADVANCE THE SIN/COS ARRAY FOR THE NEXT M:
DO 3 J=1,JJMX
IF (DGN.LE.-5) WRITE (6,87) (SCF(J,NT),NT=1,6)
FORMAT (1, SIN/COS MXI:8E10.3)
STEMP=SCF(J,1)
SCF(J,1)=SCF(J,4)+STEMP*SCF(J,3)
SCF(J,2)=SCF(J,2)-STEMP*SCF(J,3)
DO 4 J=1,JMAX
SCF(J,5)=SCF(J+1,1)-SCF(J,1)
SCF(J,6)=SCF(J+1,2)-SCF(J,2)
WRITE (3) (BDA(I),I=1,KBD)
IF (DGN.LE.-3) WRITE (6,88) (BDA(I),I=1,10)
IF (JSYM.GT.JMAX) RETURN
RM=RM+1

```



```

C REGENERATE THE HERMITE ARRAY FOR NEW M, K=0:
DO 7 II=1, IIMX2
IIM=IIMX-II+1
H(II,2)=H(II,4)*SQRT(RM)/(RM+1.)
H(II,1)=H(II,5)*(RM+2.)
H(IIM,1)=-SIGN*H(II,1)
H(II,2)=2.*SQRT(RM+1)*H(II,3)*H(II,1)-(RM+1.)*H(II,2)
H(II,2)=H(II,2)/(RM+2.)/(RM+3.)
H(II,4)=H(II,1)
H(II,5)=H(II,2)
FORMAT (' M=', I4, ', K=', I4, ', B=', E10.4, ', D=', E10.4)
89 FORMAT (2X, 10E10.3)
88 RETURN
END
C000002
C

```

```

SUBROUTINE FIELD (RS,SIG,SOLN,NBD,BDA,DGN,KBD)
SUB01140
SUB01150
SUB01160
SUB01170
SUB01180
SUB01190
SUB01200
SUB01210
SUB01220
SUB01230
SUB01240
SUB01250
SUB01260
SUB01270
SUB01280
SUB01290
SUB01300
SUB01310
SUB01320
SUB01330
SUB01340
SUB01350
SUB01360
SUB01370
SUB01380
SUB01390
SUB01400
SUB01410
SUB01420
SUB01430

C FIELD EVALUATES THE VALUE OF THE FIELD FUNCTION AT A PARTICULAR
C POINT DESIGNATED IN CYLINDRICAL COORDINATES, BY USING THE INVERSION
C EQUATION OF MALDONADO. ET.AL. FIELD USES THE ARRAY OF B & D
C COEFFICIENTS GENERATED IN SUBROUTINE BDGEN.
COMMON IMAX, JMAX, IIMX, JIMX, IJMX, ALPHA, SIZE, EPS, MODE, BOX, SD, IX, Z
COMMON /TAB/ INDEX, KEXTRA, MEXTRA, KLIMIT, MLIMIT, KOUT, MOUT
COMMON /SYM/ ISYM, JSYM, MSYM, FCU, IMS, JMS, QSYM
DIMENSION BDA(KBD), STK(52), STM(52)
C INITIALIZE THE VALUES:
INDEX=0
MTIMER=0
KOUT=0
MOUT=0
MMAX=0
KMAX=0
TOTAL=0.
JJMX6=JJMX*6
REWIND 3
AR=ALPHA*RS
ARG=AR**2
EXPON=EXP(-ARG)
PIE=3.141592653589793
APP=ALPHA/PIE/PIE
M=0
RM=M
RIMAX=IMAX
DX=2./RIMAX

```


SUB01920
 SUB01930
 SUB01940
 SUB01950
 SUB01960
 SUB01970
 SUB01980
 SUB01990
 SUB02000
 SUB02010
 SUB02020
 SUB02030
 SUB02040
 SUB02050
 SUB02060
 SUB02070
 SUB02080
 SUB02090
 SUB02100
 SUB02110
 SUB02120
 SUB02130
 SUB02140
 SUB02150
 SUB02160
 SUB02170
 SUB02180
 SUB02190
 SUB02200
 SUB02210
 SUB02220
 SUB02230
 SUB02240
 SUB02250
 SUB02260
 SUB02270
 SUB02280
 SUB02290
 SUB02300
 SUB02310
 SUB02320
 SUB02330
 SUB02340
 SUB02350
 SUB02360
 SUB02370
 SUB02380
 SUB02390

```

TOTAL=TOTAL+ADD
IF (DGN.GT.-5) GO TO 5
STOT=TOTAL*EXPON*APP/BOX/SIZE
WRITE (6,89) M,K,STOT,ADD,BRAKET,P,ARM,B,CMS,D,SMS
ESTABLISH CHECK AS THE RELATIVE SIZE OF THE M,K TERM OF THE SERIES:
CHECK=ABS(ADD)
IF (TOTAL.GT.EPS) CHECK=ABS(ADD/TOTAL)
ADVANCE THE K INDEX:
K=K+1
RK=K
DO 10 KA=1,KEXTRA
KB=KEXTRA-KA+1
STK(KB+1)=STK(KB)
STK(2)=TOTAL
ORDER=M+2*K+1
GENERATE THE NEXT ORDER OF LAGUERRE POLYNOMIAL FOR NEW K:
PM=PP
P=PP
PP=PP*(ORDER-ARG)-PM*SQRT(RK*(RM+RK))
PP=PP/SQRT((RK+1.)*(RM+RK+1.))
SET K TIMER TO PROVIDE EXTRA K TERMS AFTER CHECK < EPS:
KTIMER=KTIMER+1
IF (K.GE.KLIMIT) GO TO 6
IF (CHECK.GE.EPS) KTIMER=0
IF (KTIMER.LE.KEXTRA) GO TO 3
GO TO 7
KOUT=KOUT+1
IF (KEXTRA.EQ.0) GO TO 7
TOTAL=0
DO 11 KA=1,KEXTRA
TOTAL=TOTAL+STK(KA+1)
RKX=KEXTRA
TOTAL=TOTAL/RKX
END OF K LOOP: ADVANCE M:
M=M+1
RM=M
STP=SMS
SMS=SMS*CMI+CMS*SMI
SMS=CMS*CMI-STP*SMI
IF (K.GT.KMAX) KMAX=K
FM=FM*RM
DO 12 MA=1,MEXTRA
MB=MEXTRA-MA+1
STM(MB+1)=STM(MB)
STM(2)=TOTAL
SET M TIMER FOR EXTRA M TERMS:
IF (MS.EQ.1) MTIMER=MTIMER+1
IF (JSYM.GT.JMAX) GO TO 9

```

C 5
 C
 10
 C
 C
 6
 11
 C
 7
 12
 C

SUB02400
SUB02410
SUB02420
SUB02430
SUB02440
SUB02450
SUB02460
SUB02470
SUB02480
SUB02490
SUB02500
SUB02510
SUB02520
SUB02530
SUB02540
SUB02550
SUB02560
SUB02570
SUB02580

```

13 IF (K.GT.KEXTRA) MTIMER=0
   IF (M.GE.MLIMIT) GO TO 13
   IF (MTIMER.LE.MEXTRA) GO TO 2
   IF (MEXTRA.EQ.0) GO TO 9
   TOTAL=0.
   DO 14 MA=1,MEXTRA
   TOTAL=TOTAL+SIM(MA+1)
   RMX=MEXTRA
   TOTAL=TOTAL/RMX
   END OF M LOOP; COMPUTE OUTPUT SOLN.
9   MOUT=M-1
   IF (KOUT.EQ.0) KOUT=KMAX-1
   SOLN=TOTAL*EXPON*APP/2.
   FORMAT (1,M=,I4,/,K=,I4,/, SUBTOTAL=,9E10.3)
   FORMAT (2X,10E10.3)
   RETURN
END
C000003
C

```

SUB02590
SUB02600
SUB02610
SUB02620
SUB02630
SUB02640
SUB02650
SUB02660
SUB02670
SUB02680
SUB02690
SUB02700
SUB02710
SUB02720
SUB02730
SUB02740
SUB02750
SUB02760
SUB02770

```

SUBROUTINE BD (M,K,G,H,SCF,B,D,JJMX6)
C
C
C   BD EVALUATES THE FIRST (B) AND SECOND (D) COEFFICIENTS IN THE
C   INVERSION EQUATION, FOR A PARTICULAR SET OF INDEXES M & K.
C   BD MAKES USE OF THE HERMITE POLYNOMIAL ARRAY GENERATED BY
C   SUBROUTINE FIELD AS M & K ADVANCE.
C
COMMON IMAX,JMAX,IIMX,JJMX,IJMX,ALPHA,SIZE,EPS,MODE,BOX,SD,IX,Z
COMMON /SYM/ ISYM,JSYM,MSYM,FCU,IMS,JMS,QSYM
DIMENSION G(IJMX),SCF(JJMX6),H(IIMX)
PIE=3.141592653589793
B=0.
D=0.
RM=M
RK=K
RJMAX=JMAX
JJMX4=4*JJMX
DXI=2.*PIE/FCU
FORMAT(1X,I10,/)
IF (JSYM.LE.0) GO TO 4
S=DXI
DO 1 J=1,JMAX
DO 1 I=1,IJMX
IJ=IMAX*(J-1)+I

```

SUB02780
SUB02790
SUB02800
SUB02810
SUB02820
SUB02830
SUB02840

```

200

```



```

1 DH=H(I,I)-H(I)
  B=B+G(I,J)*S*DH
  B=B*QSYM/2.
  RETURN
2 DO 3 J=1,JMAX
  JS=J+JJMX4
  S=SCF(JS)/RM
  DO 3 I=1,I MAX
  II=I+1
  IJ=I MAX*(J-1)+I
  DH=H(II)-H(I)
  B=B+G(I,J)*S*DH
  B=B*QSYM
  RETURN
3 IF (M.NE.O) GO TO 6
  S=DXI
  DO 5 J=1,JMAX
  DO 5 I=1,I MAX
  II=I+1
  IJ=I MAX*(J-1)+I
  DH=H(II)-H(I)
  B=B+G(I,J)*S*DH
  B=B/2.
  RETURN
4 DO 7 J=1,JMAX
  JS=J+JJMX4
  J2=JS+JJMX
  S=SCF(JS)/RM
  C=SCF(J2)/RM
  DO 7 I=1,I MAX
  II=I+1
  IJ=I MAX*(J-1)+I
  DH=H(II)-H(I)
  B=B+G(I,J)*S*DH
  FORMAT (' BD:',4I5,10F6.2)
  RETURN
5 END
6 C000004
  C

```

```

SUB02850
SUB02860
SUB02870
SUB02880
SUB02890
SUB02900
SUB02910
SUB02920
SUB02930
SUB02940
SUB02950
SUB02960
SUB02970
SUB02980
SUB02990
SUB03000
SUB03010
SUB03020
SUB03030
SUB03040
SUB03050
SUB03060
SUB03070
SUB03080
SUB03090
SUB03100
SUB03110
SUB03120
SUB03130
SUB03140
SUB03160
SUB03170
SUB03180
SUB03190
SUB03200
SUB03210
SUB03220
SUB03230
SUB03240

```

```

SUBROUTINE FIELD2 (RS,SIG,SOLN,G,H,SCF,DGN)
C
C FIELD2 COMPUTES THE SAME INVERSION AS SUBROUTINE FIELD, EXCEPT THAT
C THE COEFFICIENTS B AND D ARE COMPUTED INDIVIDUALLY AS USED BY
C CALLING BD. DISK STORAGE IS NOT REQUIRED, BUT COMPUTING TIME IS
C MUCH GREATER. FIELD2 IS UTILIZED BY SPECIFYING A NEGATIVE MODE ON
SUB03250
SUB03260
SUB03270
SUB03280
SUB03290
SUB03300

```



```

C THE INPUT PARAMETER. VALUE OF THE FIELD FUNCTION AT A PARTICULAR
C FIELD EVALUATES THE VALUE OF THE FIELD FUNCTION AT A PARTICULAR
C POINT DESIGNATED IN CYLINDRICAL COORDINATES, BY USING THE INVERSION
C EQUATION OF MALDONADO, ET AL. FIELD CALLS SUBROUTINES BD & GARRAY.
C
COMMON IMAX, JMAX, IIMX, JJMX, IJMX, ALPHA, SIZE, EPS, MUDE, BOX, SD, IX, Z
COMMON /TAB/ INDEX, KEXTRA, MEXTRA, KLIMIT, MLIMIT, KOUT, MOUT
COMMON /SYM/ ISYM, JSYM, MSYM, FCU, IMS, JMS, QSYM
DIMENSION G(IJMX), H(IIMX,5), SCF(JJMX,6)
C INITIALIZE THE VALUES:
INDEX=0
MTIMER=0
KOUT=0
MOUT=0
MMAX=0
KMAX=0
TOTAL=0.
JJMX6=JJMX*6
IJMX2=(IIMX+1)/2
ARG=ALPHA*RS
ARG=AR**2
EXPON=EXP(-ARG)
PIE=3.141592653589793
APP=ALPHA/PIE/PIE
M=0
RM=M
RIMAX=IMAX
DX=2./RIMAX
RJMAX=JMAX
DXI=2.*PIE/FCU
C INITIALIZE THE MODIFIED HERMITE POLYNOMIAL ARRAY; VECTORS:
(1)=H1, (2)=H2, (3)=ALPHA*X(I), (4)=HM+2 STORED, (5)=HM+1 STORED
DO 1 I1=1, IIMX2
RII=IIMX-I1+1
IIM=IIMX-I1+1
H(I1,3)=ALPHA*(RII*DX-DX-1.)
H(IIM,3)=-H(I1,3)
H(I1,1)=2.*H(I1,3)
H(I1,2)=(H(I1,3))*H(I1,1)
H(IIM,1)=-H(I1,2)
H(I1,5)=H(I1,2)
H(IIM,5)=H(I1,2)
H(I1,4)=H(I1,1)
H(IIM,4)=H(I1,1)
SIGN=1.
FM=1.
C INITIALIZE THE SIN/COS ARRAY:
SUB03310
SUB03320
SUB03330
SUB03340
SUB03350
SUB03360
SUB03370
SUB03380
SUB03390
SUB03400
SUB03410
SUB03420
SUB03430
SUB03440
SUB03450
SUB03460
SUB03470
SUB03480
SUB03490
SUB03500
SUB03510
SUB03520
SUB03530
SUB03540
SUB03550
SUB03560
SUB03570
SUB03580
SUB03590
SUB03600
SUB03610
SUB03620
SUB03630
SUB03640
SUB03650
SUB03660
SUB03670
SUB03680
SUB03690
SUB03700
SUB03710
SUB03720
SUB03730
SUB03740
SUB03750
SUB03760
SUB03770
SUB03780

```


SUB03790
 SUB03800
 SUB03810
 SUB03820
 SUB03830
 SUB03840
 SUB03850
 SUB03860
 SUB03870
 SUB03880
 SUB03890
 SUB03900
 SUB03910
 SUB03920
 SUB03930
 SUB03940
 SUB03950
 SUB03960
 SUB03970
 SUB03980
 SUB03990
 SUB04000
 SUB04010
 SUB04020
 SUB04030
 SUB04040
 SUB04050
 SUB04060
 SUB04070
 SUB04080
 SUB04090
 SUB04100
 SUB04110
 SUB04120
 SUB04130
 SUB04140
 SUB04150
 SUB04160
 SUB04170
 SUB04180
 SUB04190
 SUB04200
 SUB04210
 SUB04220
 SUB04230
 SUB04240
 SUB04250
 SUB04260

```

11 DO J=1,JJM
    RJM=J-1
    SCF(J,1)=0.
    SCF(J,2)=1.
    SCF(J,3)=SIN(RJM*DXI-PIE)
    SCF(J,4)=COS(RJM*DXI-PIE)
    SCF(J,5)=0.
    SCF(J,6)=0.
    MS=0
    C 11 COMMENT THE M LOOP:
    2 SIGN=-SIGN
    K=0
    RK=K
    ARM=1.
    IF (M.NE.0) ARM=AR**M
    KTIMER=0
    SIGNK=-1.
    C 12 COMPUTE THE K=0 & K=1 ORDERS OF LAGUERRE POLYNOMIAL FOR GIVEN M:
    PM=0.
    P=SQRT(1./FM)
    PP=(RM+1.-ARG)*SQRT(1./FM/(RM+1.))
    C 13 ADVANCE THE SIN/COS ARRAY FOR NEW M:
    DO I=1,JJM
      SCF(J,1)=SCF(J,1)*SCF(J,2)+SCF(J,2)*SCF(J,3)
      SCF(J,2)=SCF(J,2)*SCF(J,1)-SCF(J,3)
      DO I=1,JMAX
        SCF(J,5)=SCF(J+1,1)-SCF(J,1)
        SCF(J,6)=SCF(J+1,2)-SCF(J,2)
      C 14 TEST FOR SYMMETRY SKIPS:
      IF (MS.EQ.MSYM) MS=0
      TOTAL=0.
      MS=MS+1
      IF (MS.NE.1) GO TO 7
      RMS=COS(RMS)
      SMS=SIN(RMS)
      C 15 COMMENT THE K LOOP:
      INDEX=INDEX+1
      SIGNK=-SIGNK
      C 16 CALL THE B & D COEFFICIENTS AND COMPUTE THE M,K SUMMATION TERM:
      IF (DGN.LE.-2.) WRITE (6,89) M,K,B,D
      BRAKET=B
      IF (RM.EQ.0.) GO TO 4
      BRAKET=B*CMS+D*SMS
      ADD=SIGNK*BRAKET*P*ARM
      TOTAL=TOTAL+ADD
      C 17 ESTABLISH CHECK AS THE RELATIVE SIZE OF THE M,K TERM OF THE SERIES:

```



```

SUB04270
SUB04280
SUB04290
SUB04300
SUB04310
SUB04320
SUB04330
SUB04340
SUB04350
SUB04360
SUB04370
SUB04380
SUB04390
SUB04400
SUB04410
SUB04420
SUB04430
SUB04440
SUB04450
SUB04460
SUB04470
SUB04480
SUB04490
SUB04500
SUB04510
SUB04520
SUB04530
SUB04540
SUB04550
SUB04560
SUB04570
SUB04580
SUB04590
SUB04600
SUB04610
SUB04620
SUB04630
SUB04640
SUB04650
SUB04660
SUB04670
SUB04680
SUB04690
SUB04700
SUB04710
SUB04720
SUB04730
SUB04740

CHECK=ABS(ADD)
IF (TOTAL.GT.EPS) CHECK=ABS(ADD/TOTAL)
C ADVANCE THE K INDEX:
K=K+1
RK=K
ORDER=M+2*K+1
C GENERATE THE NEXT ORDER OF LAGUERRE POLYNOMIAL FOR NEW K:
PM=PP
P=PP
PP=PP*(ORDER-ARG)-PM*SQRT(RK*(RM+RK))
PP=PP/SQRT((RK+1.)*(RM+RK+1.))
C GENERATE THE NEXT ORDER OF THE SET OF HERMITE POLYNOMIALS FOR NEW K:
HA=SQRT(RK*(RK+RM))/ORDER
HB=2.*SQRT((RK+1.)*(RM+RK+1.))/(ORDER+1.)/(ORDER+2.)
DO 5 I=1,IIMX2
IIM=IIMX-I+1
H(I,1)=2.*(H(I,3)*H(I,2)-HA*H(I,1))
H(I,1)=SIGN*H(I,1)
H(I,2)=HB*(H(I,3)*H(I,1)-ORDER*H(I,2))
C SET K TIMER TO PROVIDE EXTRA K TERMS AFTER CHECK < EPS:
KTIMER=KTIMER+1
IF (K.GE.KLIMIT) GO TO 6
IF (CHECK.GE.EPS) KTIMER=0
IF (KTIMER.LE.KEXTRA) GO TO 3
GO TO 7
C END OF K LOOP: ADVANCE M AND COMPUTE NEW TOTAL:
KOUT=KOUT+1
M=M+1
IF (K.GT.KMAX) KMAX=K
RM=M
FM=FM*RM
C REGENERATE THE HERMITE ARRAY FOR NEW M, K=0:
DO 8 I=1,IIMX2
IIM=IIMX-I+1
H(I,2)=H(I,4)*SQRT(RM)/(RM+1.)
H(I,1)=H(I,5)*H(I,2)
H(I,1)=-SIGN*H(I,1)
H(I,2)=2.*SQRT(RM+1.)*H(I,1)-(RM+1.)*H(I,2)
H(I,4)=H(I,1)
H(I,5)=H(I,2)
C SET M TIMER FOR EXTRA M TERMS:
IF (M.EQ.1) MTIMER=MTIMER+1
IF (JSYM.GT.JMAX) GO TO 9
IF (K.GT.KEXTRA) MTIMER=0
IF (M.GE.MLIMIT) GO TO 9
IF (MTIMER.LE.MEXTRA) GO TO 2
C END OF M LOOP: COMPUTE OUTPUT SOLN.

```


SUB000390
 SUB000400
 SUB000410
 SUB000420
 SUB000430
 SUB000440
 SUB000450
 SUB000460
 SUB000470
 SUB000480
 SUB000490
 SUB000500
 SUB000510
 SUB000520
 SUB000530
 SUB000540
 SUB000550
 SUB000560
 SUB000570
 SUB000580
 SUB000590
 SUB000600
 SUB000610
 SUB000620

```

DO 1 I=1,IMS
RI=I
II=I MAX+1-I
R=(RI-.5)*DELR-HS
CALL GOLF (R,XI,GIJ,NOF,DGN,NUMB)
G(I,J)=GIJ
IF (ISYM.EQ.2) G(II,J)=GIJ
IF (ISYM.EQ.2) GO TO 1
G(II,J3)=GIJ
IF (JSYM.EQ.0) GO TO 1
G(I,J2)=GIJ
G(II,J4)=GIJ
CONTINUE
GO TO 4
IF (MODE.GT.2) GO TO 3
CALL SHEET (G,GA,XO,YO,PHISYM,NOF)
GO TO 4
CALL READ (Z,XO,YO,PHISYM,NOF,IMAX,JMAX,G)
IF (DGN.GE.2) WRITE (6,39)
RETURN
FORMAT (' GARRAY RETURNS' )
END
C000006
C

```

1
 2
 3
 4
 39

SUB000630
 SUB000640
 SUB000650
 SUB000660
 SUB000670
 SUB000680
 SUB000690
 SUB000700
 SUB000710
 SUB000720
 SUB000730
 SUB000740
 SUB000750
 SUB000760
 SUB000770
 SUB000780
 SUB000790
 SUB000800
 SUB000810
 SUB000820
 SUB000830
 SUB000840

```

SUBROUTINE GOLF (R,XI,GIJ,NOF,DGN,NUMB)
C
C GOLF COMPUTES THE FUNCTION G(R,XI) FOR A PARTICULAR LINE OF SIGHT
C FROM A KNOWN FUNCTION CONTAINED IN SUBROUTINE FUNCT.
C
COMMON IMAX,JMAX,IIMX,JJMX,IJMX,ALPHA,SIZE,EPS,MODE,BOX,SD,IX,Z
ZERO=0.
LMAX=IMAX*3
RLMAX=LMAX
DELXP=SIZE/RLMAX
SXI=SIN(XI)
CXI=ICOS(XI)
DELYS=DELXP*CXI
DELYS=DELXP*SXI
XP=DELXP*.5-SIZE/2.
XS=XP*CXI-R*SXI
YS=XP*SXI+R*CXI
GIJ=0.
DO 1 L=1,LMAX
RL=L
CALL FUNCT(XS,YS,F,NOF,DGN,NUMB)
GIJ=GIJ+F

```

C
 C
 C
 C

SUB00850
SUB00860
SUB00870
SUB00880
SUB00890
SUB00900
SUB00910
SUB00920
SUB00930
SUB00940
SUB00950
SUB00960
SUB00970
SUB00980

```

1  XS=XS+DELXS
   YS=YS+DELYS
   IF (GIJ.NE.0.) GIJ=GIJ*DELXP*BOX
   IF ((SD.EQ.0.) OR.(NUMB.EQ.1)) GO TO 2
   IF (DGN.GE.3) WRITE (6,28) IX
   CALL GAUSS (IX,SD,ZERO,RV)
   GIJ=GIJ+RV
2  IF (DGN.GE.3) WRITE (6,29) R,XI,GIJ
   RETURN
29  FORMAT (1, R=,F8.3,1, XI=,F8.3,1, GIJ=,F8.3)
28  FORMAT (1, GAUSS, IX=,I8)
   END
C000007
C

```

SUB00990
SUB01000

```

C  SUBROUTINE FUNCT (XS,YS,F,NOF,DGN,NUMB)
CP67USERID 1395BOXJ
C
C  FUNCT EVALUATES AS INPUT FUNCTION AT POSITION (X,Y) IN THE TEST
C  SECTION COORDINATE SYSTEM. NOF IDENTIFIES THE EQUATION USED.
C
COMMON IMAX,JMAX,IIMX,JJMX,IJMX,ALPHA,SIZE,EPS,MODE,BOX,SD,IX,Z
CCOMMON /EQPAR/ A,B,C,D,E,P,Q,S,T,U,V,W,RO,RA,NO,NA,N1,N2
DIMENSION RO(101),RA(101)
AA=A
BB=B
CC=C
DD=D
EE=E
PP=P
IF (NUMB.LE.1) GO TO 50
AA=S
BB=T
CC=U
DD=V
EE=W
PP=O
PIE=3.141592653589793
HS=SIZE/2.
R=SQRT((XS**2+YS**2)/HS)
F=0.
IF (R.GT.1.) GO TO 11
IF (NOF.LE.0) GO TO 11

```

SUB01020
SUB01030
SUB01040
SUB01050
SUB01060
SUB01070
SUB01080
SUB01090
SUB01100
SUB01110
SUB01120
SUB01130
SUB01140
SUB01150
SUB01160
SUB01170
SUB01180
SUB01190
SUB01200
SUB01210
SUB01220
SUB01230
SUB01240
SUB01250
SUB01260
SUB01270
SUB01280

```

C 1. AXISYMMETRIC GAUSSIAN:

```


SUB01290
 SUB01300
 SUB01310
 SUB01320
 SUB01330
 SUB01340
 SUB01350
 SUB01360
 SUB01370
 SUB01380
 SUB01390
 SUB01400
 SUB01410
 SUB01420
 SUB01430
 SUB01440
 SUB01450
 SUB01460
 SUB01470
 SUB01480
 SUB01490
 SUB01500
 SUB01510
 SUB01520
 SUB01530
 SUB01540
 SUB01550
 SUB01560
 SUB01570
 SUB01580
 SUB01590
 SUB01600
 SUB01610
 SUB01620
 SUB01630
 SUB01640
 SUB01650
 SUB01660
 SUB01670
 SUB01680
 SUB01690
 SUB01700
 SUB01710
 SUB01720
 SUB01730
 SUB01740
 SUB01750
 SUB01760

```

1 IF (NOF.GT.1) GO TO 2
  F=AA*EXP(-1.*(R*HS/BB)**2)
  GO TO 11
C
2 2. ADJUSTABLE RECTANGULAR STEP FUNCTION:
  IF (NOF.GT.2) GO TO 3
  F=PP
  IF ((ABS(XS-DD).LE.BB).AND.(ABS(YS-EE).LE.CC)) F=AA
  GO TO 11
C
3 3. DISPLACABLE ELLIPTICAL GAUSSIAN:
  IF (NOF.GT.3) GO TO 4
  F=AA*EXP(-1.*(((XS-DD)/BB)**2+((YS-EE)/CC)**2))
  GO TO 11
C
4 4. CONSTANT:
  IF (NOF.GT.4) GO TO 5
  F=AA
  GO TO 11
C
5 5. ADJUSTABLE AND DISPLACABLE ELLIPTIC RAMP FUNCTION:
  IF (NOF.GT.5) GO TO 6
  RBC=SQRT(((XS-DD)/BB)**2+((YS-EE)/CC)**2)
  F=0
  IF (RBC.LT.1.) F=AA*((1.-RBC)**PP)
  GO TO 11
C
6 6. DISPLACABLE ELLIPTIC STEP FUNCTION:
  IF (NOF.GT.6) GO TO 7
  RBC=SQRT(((XS-DD)/BB)**2+((YS-EE)/CC)**2)
  F=0
  IF (RBC.LT.1.) F=AA
  GO TO 11
C
7 7. CIRCULAR COSINE-SQUARED FUNCTION OF BB MAXIMA:
  IF (NOF.GT.7) GO TO 8
  F=AA*COS((2.*BB-1.)*PIE*R/2.)**2
  GO TO 11
C
8 8. NUMERICAL FUNCTION: REQUIRES AN INPUT ARRAY READ IN BY
  SUBROUTINE FREAD; N FOLLOWED BY N POINT VALUES. (101 MAX)
  A CONSTANT VALUE AA IS ADDED TO THE FUNCTION.
  IF (NOF.GT.8) GO TO 9
  IF (NUMB.LE.1) N=NO
  IF (NUMB.GT.1) N=NA
  NM=N-1
  NMM=N-2
  RN=N

```


SUB01770
 SUB01780
 SUB01790
 SUB01800
 SUB01810
 SUB01820
 SUB01830
 SUB01840
 SUB01850
 SUB01860
 SUB01870
 SUB01880
 SUB01890
 SUB01900
 SUB01910
 SUB01920
 SUB01930
 SUB01940
 SUB01950
 SUB01960
 SUB01970
 SUB01980
 SUB01990
 SUB02000
 SUB02010
 SUB02020
 SUB02030

```

RI=R*(RN-1.)+1.
IR=INT(RI)
RIR=FLOAT(IR)
DI=R-I-RIR
IF (NUMB.LE.1) F=RO(IR)
IF (NUMB.GT.1) F=RA(IR)
IF ((IR.NE.N).AND.(NUMB.LE.1)) F=F+DI*(RO(IR+1))-RO(IR)
IF ((IR.NE.N).AND.(NUMB.GT.1)) F=F+DI*(RA(IR+1))-RA(IR)
F=F*AA+BB
GO TO 11
  
```

C 9. SPECIAL FUNCTION: MAY BE WRITTEN FOR THE OCCASION AND
 C INSERTED IN SUBROUTINE SPFUN
 C IF (NOF.GT.9) GO TO 10
 C CALL SPFUN (XS,YS,F)
 C GO TO 11

C EQUATIONS NO. 10 AND BEYOND ARE SET TO ZERO.
 C F=0.

```

C 10  

C 11  

C 99 IF (DGN.GE.4) WRITE (6,99) XS,YS,F  

  C 99 FORMAT (' F8.3', F8.3, ' ', F=' ', F8.3)  

  C RETURN  

  C END  

  C C000008  

  C C
  
```

SUB02040
 SUB02050
 SUB02060
 SUB02070
 SUB02080
 SUB02090
 SUB02100
 SUB02110
 SUB02120
 SUB02130
 SUB02140
 SUB02150
 SUB02160

C SUBROUTINE SPFUN (XS,YS,F)
 C SPFUN IS A SPECIAL ROUTINE FOR EQ'N NO. 9. ANY FUNCTION MAY BE
 C ENTERED.
 C COMMON /EQPAR/ A,B,C,D,E,P,Q,S,T,U,V,W,RO,RA,NG,NA,N1,N2
 C DIMENSION RO(101),RA(101)
 C F=0.
 C IF ((ABS(XS).LE.B).AND.(ABS(YS).LE.C)) F=A
 C RETURN
 C END
 C C000009
 C C


```

SUBROUTINE SHEET (G,D,XO,YO,PHISYM,NOF)
SHEET READS IRREGULARLY SPACED VALUES OF THE LINE INTEGRAL, AS
OBTAINED FROM HOLOGRAPHIC INTERFEROGRAMS. THE INTEGRAL LINES MAY BE
DEFINED EITHER BY GRID INTERCEPT POSITIONS, OR BY ANGLE AND RADIUS
ABOUT THE CENTER OF THE LABORATORY COORDINATE SYSTEM CENTER. LINES
MUST BE ENTERED IN CONSECUTIVE ORDER FROM LOWEST (NEG.) TO HIGHEST
(POS.) RADIUS. DATA MAY BE SIMULATED BY SPECIFYING NCODE=1.
FOLLOWED BY APERTURE POSITIONS FOR A FUNCTION NUMBER IN 'SUBFUNCT'.
C          COMMON I MAX, J MAX, I J MAX, J J MAX, ALPHA, SIZE, EPS, MODE, BOX, SD, IX, Z
C          /SYM/ ISYM, JSYM, MSYM, FCU, IMS, JMS, QSYM
C          COMMON /IO/ CMS, IN1, IN2, IN4
C          DIMENSION G(I MAX, J MAX), D(I MAX, J MAX), XI(303), RR(303)
C          DIMENSION XG(303), XD(303), YG(303), YD(303), XY(303)
C          NAR=303
C          PI E=3.141592653589793
C          TPI E=-PI E
C          MPI T=PI E/2.
C          ZERO THE ARRAYS:
C          DO 1 J=1, J MAX
C          DO 1 I=1, I MAX
C          G(I, J)=0.
C          D(I, J)=0.
C          DC 2 I=1, NAR
C          XG(I)=0.
C          XD(I)=0.
C          YG(I)=0.
C          XY(I)=0.
C          XI(I)=0.
C          RR(I)=0.
C          READ THE BASIC DATA:
C          IF (CMS.EQ.1.) REWIND 1
C          READ (IN1,59) NOF, NCODE
C          READ (IN1,58) Z, XO, YO, PHISYM, XMN, YMN, YMX, YMN
C          READ (IN1,59) JM
C          RIMX=I MAX
C          DR=SIZE/RIMX
C          R=(-DR-SIZE)/2.
C          RZ=SQRT(XO**2+YO**2)
C          GAM=ATANM(YO, XO)
C          IP=3- ISYM
C          BT=JSYM
C          DAN=PI E*TP/BT
C          HS=SIZE/2.
SUB02170
SUB02180
SUB02190
SUB02200
SUB02210
SUB02220
SUB02230
SUB02240
SUB02250
SUB02260
SUB02270
SUB02280
SUB02290
SUB02300
SUB02310
SUB02320
SUB02330
SUB02340
SUB02350
SUB02360
SUB02370
SUB02380
SUB02390
SUB02400
SUB02410
SUB02420
SUB02430
SUB02440
SUB02450
SUB02460
SUB02470
SUB02480
SUB02490
SUB02500
SUB02510
SUB02520
SUB02530
SUB02540
SUB02550
SUB02560
SUB02570
SUB02580
SUB02590
SUB02600
SUB02610
SUB02620
SUB02630
SUB02640

```



```

SUB02650
SUB02660
SUB02670
SUB02680
SUB02690
SUB02700
SUB02710
SUB02720
SUB02730
SUB02740
SUB02750
SUB02760
SUB02770
SUB02780
SUB02790
SUB02800
SUB02810
SUB02820
SUB02830
SUB02840
SUB02850
SUB02860
SUB02870
SUB02880
SUB02890
SUB02900
SUB02910
SUB02920
SUB02930
SUB02940
SUB02950
SUB02960
SUB02970
SUB02980
SUB02990
SUB03000
SUB03010
SUB03020
SUB03030
SUB03040
SUB03050
SUB03060
SUB03070
SUB03080
SUB03090
SUB03100
SUB03110
SUB03120

MXY=1
IF((XMX.NE.0.).OR.(XMN.NE.0.).OR.(YMX.NE.0.).OR.(YMN.NE.0.))MXY=0
IF (MXY.EQ.1) GO TO 3
XMX=XO+HS
YMX=YO+HS
XMN=XO-HS
YMN=YO-HS
C COMMENTE THE READ AND FILL LOOP:
DO 12 J=1,JM
  READ (IN1,59)IM
  MN=0
  XH=0.
  YH=0.
C READ THE LINES, DETERMINE CODE, CALCULATE RADIUS & ANGLE FOR CODE 1:
DO 5 I=1,IM
  IF(NCODE.LE.0)READ(IN1,58) XD(I),YD(I),XG(I),YG(I),D(I),J),RR(I),
  1 XI(I),XY(I)
  IF(NCODE.GE.1)CALL SIM(XD(I),YD(I),XG(I),YG(I),RR(I),XI(I),
  1 XY(I),XO,YO,PHISYM,XMX,XMN,YMX,YMN,NOF,I,IM)
  IF (XY(I).EQ.3.) GO TO 5
  IF (XD(I).NE.0.).OR.(YD(I).NE.0.)) XY(I)=1.
  IF (XG(I).NE.0.).OR.(YG(I).NE.0.)) XY(I)=1.
  IF ((RR(I).NE.0.).OR.(XI(I).NE.0.)).AND.(XY(I).EQ.0.)) XY(I)=2.
  IF ((XY(I).EQ.0.).AND.(D(I),J).NE.0.)) XY(I)=2.
  IF (XY(I).NE.1.) GO TO 4
  DEN=SQRT((XG(I)-XD(I))*2+(YG(I)-YD(I))*2)
  IF (DEN.EQ.0.) XY(I)=4.
  IF (XY(I).EQ.4.) GO TO 4
  RR(I)=((XO-XD(I))*-(YG(I)-YD(I))-((XG(I)-XD(I))*-(YO-YD(I)))/DEN
  XI(I)=ATANM((YG(I)-YD(I)),(XG(I)-XD(I)))
  XIM=XI(I)
  IF (XY(I).EQ.2.) XIM=XI(I)
  XIN=XIM
  IF(XY(I).EQ.2.) RR(I)=RR(I)+RZO*SIN(GAM-XI(I))
  CONTINUE
C COMPUTE MAX AND MIN ANGLE INDEXES FOR APERATURE POSITION LOCATION:
DO 6 I=1,IM
  IF((XY(I).NE.1.).OR.(XY(I).NE.2.)) GO TO 6
  IF (XI(I).GT.XIM) XIM=XI(I)
  IF (XI(I).GT.XIM) IMT=XI(I)
  IF (XI(I).LT.XIN) XIN=XI(I)
  IF (XI(I).LE.XIN) INT=XI(I)
  CONTINUE
C DETERMINE APERATURE LOCATION:
LPR=0
XID=XI(IMT)-XI(INT)
IF(ABS(XID).LT.00001) LPR=1
XIH=(XI(IMT)+XI(INT))/2.

```


SUB03130
 SUB03140
 SUB03150
 SUB03160
 SUB03170
 SUB03180
 SUB03190
 SUB03200
 SUB03210
 SUB03220
 SUB03230
 SUB03240
 SUB03250
 SUB03260
 SUB03270
 SUB03280
 SUB03290
 SUB03300
 SUB03310
 SUB03320
 SUB03330
 SUB03340
 SUB03350
 SUB03360
 SUB03370
 SUB03380
 SUB03390
 SUB03400
 SUB03410
 SUB03420
 SUB03430
 SUB03440
 SUB03450
 SUB03460
 SUB03470
 SUB03480
 SUB03490
 SUB03500
 SUB03510
 SUB03520
 SUB03530
 SUB03540
 SUB03550
 SUB03560
 SUB03570
 SUB03580
 SUB03590
 SUB03600

```

RRH=10000.
XH=RRH*COS(XIH)
YH=RRH*SIN(XIH)
IF (LPR.EQ.1) GO TO 7
YTX=-RR(IMT)*SIN(XI(IMT))-YO
XTX=RR(IMT)*SIN(XI(IMT))-XO
XTN=RR(IMT)*COS(XI(IMT))-XO
UA=TAN(XI(IMT))
UC=TAN(XI(IMT))
UB=YTX-UA*XTX
UC=YTN-UC*XTN
XH=XH*UA+UB
YH=SQRT((XH-XO)**2+(YH-YO)**2)
XIH=ATANM((YH-YO),(XH-XO))
CONTINUE
7 C FILL THE ANGLE AND RADIUS FOR ANY CODE 3 OR 4 LINES:
DO 9 I=1,IM
IF(XY(I).NE.3.) GO TO 8
BAS=SQRT(RRH**2-RR(I)**2)
XI(I)=XIH-ATANM(RR(I),BAS)
GO TO 9
8 XI(I)=ATANM((YH-YD(I)),(XH-XD(I)))
RR(I)=RRH*SIN(XI(I)-XIH)
CONTINUE
9 C ANGLES AND RADII ARE NOW FILLED FOR ALL POINTS IN THIS LINE.
C VACATE THE SET OF VECTORS TO BE USED AS TEMPORARY STORAGE:
DO 10 I=1,IM
XD(I)=0.
YD(I)=0.
XG(I)=0.
YG(I)=RR(I)
XY(I)=D(I,J)
RR(I)=0.
D(I,J)=0.
XI(I)=0.
10 C CONVERT THE LINE TO REGULAR RADII USING INTERPOLATION:
RR(1)=R+DR
CALL SPLINE(YG,XY,IM,RR(1),D(1,J))
DO 11 I=2,IMAX
RI=I
RR(I)=R+DR*RI
CALL SPLINN(YG,XY,IM,RR(I),D(I,J))
11 C GENERATE THE VECTOR OF ANGLES FOR THIS COLUMN AND STORE IN G ARRAY:
DO 12 I=1,IMAX
BAS=SQRT(RRH**2-RR(I)**2)
G(I,J)=XIH-ATANM(RR(I),BAS)

```


SUB03610
 SUB03620
 SUB03630
 SUB03640
 SUB03650
 SUB03660
 SUB03670
 SUB03680
 SUB03690
 SUB03700
 SUB03710
 SUB03720
 SUB03730
 SUB03740
 SUB03750
 SUB03760
 SUB03770
 SUB03780
 SUB03790
 SUB03800
 SUB03810
 SUB03820
 SUB03830
 SUB03840
 SUB03850
 SUB03860
 SUB03870
 SUB03880
 SUB03890
 SUB03900
 SUB03910
 SUB03920
 SUB03930
 SUB03940
 SUB03950
 SUB03960
 SUB03970
 SUB03980
 SUB03990
 SUB04000
 SUB04010
 SUB04020
 SUB04030
 SUB04040
 SUB04050
 SUB04060
 SUB04070
 SUB04080

```

12 YG(I)=0.XY(I)
C D(I,J)=XY(I)
C XY(I)=0.
C COLUMNS ARE NOW ALL REGULARLY FILLED.
C NEXT, INTERPOLATE EACH ROW REGULARLY OVER THE ANGLES.
C DO 23 I=1,IMAX
C EXPAND THE DATA TO 2 SETS TO ESTABLISH SMOOTH INTERPOLATION.
  JM3=3*JM
  II=IMAX+1-I
  IF (JSYM.NE.0) GO TO 14
  DO 13 J=1,JMS
  J2=J+JMS
  J3=J2+JMS
  XD(J)=D(I,J)
  XD(J2)=D(I,J)
  XD(J3)=D(I,J)
  XG(J)=G(I,J)-PIE-PHISYM
  XG(J2)=G(I,J)-PIE-PHISYM
  XG(J3)=G(I,J)-PHISYM
  GO TO 16
13 DO 15 J=1,JMS
  J1=JMS+1-J
  J2=JMS+J
  J3=JM3+1-J
  XD(J1)=D(I,J)
  XD(J2)=D(I,J)
  XD(J3)=D(I,J)
  XG(J1)=G(I,J)-2.*(G(I,J)-PHISYM)-PIE-PHISYM
  XG(J2)=G(I,J)-PIE-PHISYM
  XG(J3)=G(I,J)+2.*(DAN+PHISYM-G(I,J))-PIE-PHISYM
  CONTINUE
15 JM2=2*JMS
16 JP=JMS/2
  DO 17 J=1,JM2
  XD(J)=XD(J+JP)
  XG(J)=XG(J+JP)
  JJS=JM2+1
  DO 18 J=JJS,JM3
  XD(J)=0.
  XG(J)=0.
17 FIND THE SMALLEST ANGLE
  XY(1)=1.
  SA=XG(1)
  DO 19 J=1,JM2
  IF (XG(J).GE.SA) GO TO 19
  SA=XG(J)
  XY(1)=J
  CONTINUE
18 C
19

```



```

C   FIND THA MAX ANGLE IN THE ROW:
XY(JM2)=JM2
SB=XG(JM2)
DO 20 J=1, JM2
IF (XG(J).LE.SB) GO TO 20
SB=XG(J)
XY(JM2)=J
CONTINUE THE ORDER OF INCREASING ANGLE IN THE ROW
C   DETERMINE THE ORDER OF INCREASING ANGLE IN THE ROW
SB=XG(JM2)
JJ=2
JSA=XY(JJ-1)
SA=XG(JJ-1)
JTS=0
DO 22 J=1, JM2
IF (XG(J).LE.SA) GO TO 22
IF (XG(J).GT.SB) GO TO 22
SB=XG(J)
XY(JJ)=J
JTS=1
CONTINUE JM2=JJ
IF (JTS.EQ.0) JM2=JJ
JJ=JJ+1
IF (JJ.LE.JM2) GO TO 21
DO 23 J=1, JM2
JX=XY(J)
YD(J)=XD(JX)
INTERPOLATE:
DXI=2.*PIE/FCU
XI(J)=DXI/2.-PIE-PHISYM
CALL SPLINE (XG,YD,JM2,XI(J),G(I,J))
DO 24 J=2, JMS
XI(J)=XI(J-1)+DXI
CALL SPLINN (XG,YD, JM2, XI(J), G(I, J))
DO 25 J=1, JMS
XIJ=XI(J)
XU=XXM
IF ((XIJ.GE.0.).AND.(XIJ.LT.PIE)) XU=XMN
YU=YMN
IF ((XIJ.GE.MPI).AND.(XIJ.LT.PIT)) YU=YMX
XL=XMN
IF ((XIJ.GE.0.).AND.(XIJ.LT.PIE)) XL=XMX
YL=YMX
IF ((XIJ.GE.MPI).AND.(XIJ.LT.PIT)) YL=YMN
SXIJ=SIN(XIJ)
CXIJ=COS(XIJ)
RMN=(XO-XL)*SXIJ-(YO-YU)*CXIJ
RMX=(XO-XU)*SXIJ-(YO-YU)*CXIJ
SUB04090
SUB04100
SUB04110
SUB04120
SUB04130
SUB04140
SUB04150
SUB04160
SUB04170
SUB04180
SUB04190
SUB04200
SUB04210
SUB04220
SUB04230
SUB04240
SUB04250
SUB04260
SUB04270
SUB04280
SUB04290
SUB04300
SUB04310
SUB04320
SUB04330
SUB04340
SUB04350
SUB04360
SUB04370
SUB04380
SUB04390
SUB04400
SUB04410
SUB04420
SUB04430
SUB04440
SUB04450
SUB04460
SUB04470
SUB04480
SUB04490
SUB04500
SUB04510
SUB04520
SUB04530
SUB04540
SUB04550
SUB04560

```



```

25 C DO 25 I=1, IMAX
      IF (RR(I).LT.RMN) G(I,J)=0.
      IF (RR(I).GT.RMX) G(I,J)=0.
      CONTINUE
      EXPAND SYMMETRY SECTOR INTO AN ORTHOGONAL INTERVAL.
      DO 26 J=1, JMS
        J2=JMAX/2+1-J
        J3=JMAX/2+J
        J4=JMAX+1-J
        DO 26 I=1, IMAX
          II=IMAX+1-I
          G(I,J2)=G(I,J)
          G(II,J3)=G(I,J)
          G(II,J4)=G(I,J)
        RETURN
      FOR EVEN SYMMETRY, AVERAGE THE GARRAY COLUMNS.
      IMS=(2*IMAX+1)/2
      DO 28 J=1, JMAX
        DO 28 I=1, IMS
          II=IMAX+1-I
          GST=(G(I,J)+G(II,J))/2.
          G(I,J)=GST
          G(II,J)=GST
        RETURN
      FORMAT (5I5)
      END
C000010
C

C000011
C
      FUNCTION ATANM(Y,X)
      C COMPUTES THE ARCTAN OF Y/X BETWEEN -PI AND +PI.
      C
      PIE=3.141592653589793
      PI2=PIE/2.
      ATANM=SIGN(PI2,Y)
      IF(X.NE.0.) ATANM=ATAN(Y/X)
      IF(X.GE.0.) RETURN
      IF(Y.GE.0.) ATANM=PIE+ATANM
      IF(Y.LT.0.) ATANM=-PIE+ATANM
      RETURN
      END
C000011
C
SUB04570
SUB04580
SUB04590
SUB04600
SUB04610
SUB04620
SUB04630
SUB04640
SUB04650
SUB04660
SUB04670
SUB04680
SUB04690
SUB04700
SUB04710
SUB04720
SUB04730
SUB04740
SUB04750
SUB04760
SUB04780
SUB04790
SUB04800
SUB04810
SUB04820
SUB04830
SUB04840
SUB04850
SUB04860
SUB04870
SUB04880
SUB04890
SUB04900
SUB04910
SUB04920
SUB04930
SUB04940
SUB04950
SUB04960
SUB04970
SUB04980
SUB04990
SUB05000
SUB05010

```


SUB000510
 SUB000520
 SUB000530
 SUB000540
 SUB000550
 SUB000560
 SUB000570
 SUB000580
 SUB000590
 SUB000600
 SUB000610
 SUB000620
 SUB000630
 SUB000640
 SUB000650
 SUB000660
 SUB000670
 SUB000680
 SUB000690
 SUB000700
 SUB000710
 SUB000720
 SUB000730

```

3  XI=-180.+DXI*(RJ-.5)
   IGB=(J-1)*IMAX+IB
   IGT=IGB-IB+IT
   WRITE (6,95) J,XI,(G(L),L=IGB,IGT)
   WRITE (6,94) (HYP,L=1,LM),VERT
   IB=IB+INTRVL
   ITOLD=IT
   IT=IT+INTRVL
   IF (ITOLD.LT.IMAX) GO TO 1
   WRITE (6,93)
   FORMAT (1H1//,
99  THE ARRAY OF INPUT DATA (G), OBTAINED BY GARRAY,
   MODE ',I1,', FOR Z=',F7.3,', CM: ')
   FORMAT (//,11X,'I=',15I7)
98  FORMAT (//,11X,'X=',15F7.3)
97  FORMAT (//,11X,'XI=',15F7.3)
96  FORMAT (//,11X,'J=',15I7)
95  FORMAT (//,11X,'I=',15I7)
94  FORMAT (//,11X,'I=',15I7)
93  FORMAT (//,11X,'I=',15I7)
92  FORMAT (//,11X,'I=',15I7)
   RETURN
   END
C000014
C

```

SUB000740
 SUB000750
 SUB000760
 SUB000770
 SUB000780
 SUB000790
 SUB000800
 SUB000810
 SUB000820
 SUB000830
 SUB000840
 SUB000850
 SUB000860
 SUB000870
 SUB000880

```

C  SUBROUTINE GPUNCH (Z,XO,YO,PHS,NOF,IMX,JMX,G)
C  GPUNCH PUNCHES OUT THE FIRST NON-SYMMETRIC PORTION OF GARRAY
C  (OR WRITES IT ON FILE 7 IN CMS VERSION)
C  COMMON /SYM/ ISM,JSM,MSM,FCU,IMS,JMS,QSM
C  DIMENSION G(IMX,JMX)
C  WRITE (7,39) NOF,IMX,JMX,ISM,JSM,IMS,JMS
39  WRITE (7,38) ((G(I,J),I=1,IMS),J=1,JMS)
38  FORMAT(10I5)
   RETURN
   END
C000015
C

```

SUB000890
 SUB000900
 SUB000910
 SUB000920
 SUB000930
 SUB000940

```

C  SUBROUTINE READ (Z,XO,YO,PHISYM,NOF,IMAX,JMAX,G)
C  READS THE NON-SYMMETRIC PORTION OF THE GARRAY AND EXPANDS IT TO AN
C  ORTHOGONAL SET. NOTE, INSURE SUFFICIENT DIMENSIONS IN MAIN PROGRAM.
C  COMMON /SYM/ ISYM,JSYM,MSYM,FCU,IMS,JMS,QSYM

```



```

COMMON / IO/ CMS, IN1, IN2, IN4
DIMENSION G(IMAX,JMAX)
READ (IN1,39) NOF, IMAX, JMAX, ISYM, JSYM, IMS, JMS
READ (IN1,38) Z, XO, YO, PHISYM
READ (IN1,38) ((G(I,J), I=1,IMS), J=1,JMS)
WRITE(6,37) NOF, Z, XO, YO, PHISYM, IMAX, JMAX, JSYM
RJM=JMAX
MSYM=JSYM
IF ((MSYM.EQ.0).OR.(MSYM.GT.JMAX)) MSYM=1
FCU=ISYM*JMAX
IF (JSYM.GT.JMAX) FCU=JMAX
QSYM=FCU/RJM
DO 4 J=1,JMS
IF (ISYM.EQ.1) GO TO 2
DO 1 I=1,IMS
II=IMAX+1-I
G(II,J)=G(I,J)
GO TO 4
J2=JMAX/2+1-J
J3=JMAX/2+J
J4=JMAX+1-J
DO 3 I=1,IMAX
II=IMAX+1-I
G(II,J2)=G(I,J)
G(II,J3)=G(I,J)
G(II,J4)=G(I,J)
CONTINUE
FORMAT(10I5)
FORMAT(10F7.3)
FORMAT(//,' MODE 3 READS GARRAY DIRECTLY: NOF=',I4,'
1,' , XO=',F7.3,' , YO=',F7.3,' , JSYM=',F7.3,' ,
2,' , JMAX=',I4,' , Z=',F7.3,
RETURN
END
C000016
C
C
C
C
SUBROUTINE MAP (IM,JM,A,N,Z,BAND)
MAP CALLS SUBROUTINE MIMPII AND PLOTS A CONTOUR MAP OF THE ARRAY
DIMENSION A(IM,JM),T(24)
DATA BL/1H /
DO 1 I=1,24
T(I)=BL
ICON=1
IF(BAND.LT.0.) ICON=0
SUB009950
SUB009960
SUB009970
SUB009980
SUB009990
SUB010000
SUB010010
SUB010020
SUB010030
SUB010040
SUB010050
SUB010060
SUB010070
SUB010080
SUB010090
SUB010100
SUB010110
SUB010120
SUB010130
SUB010140
SUB010150
SUB010160
SUB010170
SUB010180
SUB010190
SUB010200
SUB010210
SUB010220
SUB010230
SUB010240
SUB010250
SUB010260
SUB010270
SUB010280
SUB010290
SUB010300
SUB01310
SUB01320
SUB01330
SUB01340
SUB01350
SUB01360
SUB01370
SUB01380
SUB01390
SUB01400

```


SUB01410
 SUB01420
 SUB01430
 SUB01440
 SUB01450
 SUB01460
 SUB01470
 SUB01480
 SUB01490
 SUB01500
 SUB01510
 SUB01520

```

IF(BAND.LT.O.) BAND=--BAND
AMIN=0.
IJT=0
AZ=1.
BZ=0.
WRITE(6,49) N,Z
CALL MTMPII (A, IM, JM, T, BAND, AZ, BZ, AMIN, IJT, ICON)
FORMAT (1H1//, THE FUNCTION SURFACE, TEST NO.,I3, Z='F5.3//)
RETURN
END
49
C000017
C

```

SUB01530
 SUB01540
 SUB01550
 SUB01560
 SUB01570
 SUB01580
 SUB01590
 SUB01600
 SUB01610
 SUB01620
 SUB01630
 SUB01640
 SUB01650
 SUB01660
 SUB01670
 SUB01680
 SUB01690
 SUB01700
 SUB01710
 SUB01720
 SUB01730
 SUB01740
 SUB01750
 SUB01760
 SUB01770
 SUB01780
 SUB01790
 SUB01800
 SUB01810
 SUB01820
 SUB01830
 SUB01840
 SUB01850
 SUB01860

```

SUBROUTINE GPLOT (G, GA, JMS)
C
C GPLOT PRINTS A ROUGH PLOT OF THE LINE INTEGRAL FUNCTIONS IN GARRAY.
C
COMMON IMAX, JMAX, IIMX, JIMX, IJMX, ALPHA, SIZE, EPS, MODE, BOX, SD, IX, Z
COMMON /TAB/ INDEX(7), JSYM, ISYM
COMMON /TAB2/ IPT, KPT, LPT, MPT, REST(5)
DIMENSION G(IMAX, JMAX), GA(IMAX, JMAX), ROW(101)
DIMENSION A(201), B(101), C(201), D(101)
JM=101
DATA BL, PL, ST, DH, EX/1H, 1H+, 1H*, 1H-, 1H-/
JMS2=JMAX/2+1
IF(ISYM.EQ.2) JMS2=1
JMS3=JMS2+JMS-1
DO 8 J=JMS2, JMS3
WRITE(6,67) (ST, I=1, 120)
DO 1 I=1, IMAX
A(I)=G(I, J)
C(I)=GA(I, J)
AS=.5
BS=.0
CALL INTERP (A, IMAX, AS, B, JM, BS)
CALL INTERP (C, IMAX, AS, D, JM, BS)
WRITE (6,69) J
BIG=0.
SMALL=0.
DO 2 I=1, IMAX
IF(A(I).GT.BIG) BIG=A(I)
IF(C(I).GT.BIG) BIG=C(I)
IF(A(I).LT.SMALL) SMALL=A(I)
IF(C(I).LT.SMALL) SMALL=C(I)
RANGE=BIG-SMALL
RINK=RANGE/80.
TOP=BIG+RINK

```


SUB01870
 SUB01880
 SUB01890
 SUB01900
 SUB01910
 SUB01920
 SUB01930
 SUB01940
 SUB01950
 SUB01960
 SUB01970
 SUB01980
 SUB01990
 SUB02000
 SUB02010
 SUB02020
 SUB02030
 SUB02040
 SUB02050
 SUB02060
 SUB02070
 SUB02080
 SUB02090
 SUB02100
 SUB02110
 SUB02120
 SUB02130
 SUB02140
 SUB02150
 SUB02160
 SUB02170
 SUB02180
 SUB02190
 SUB02200
 SUB02210

```

CEN=BIG
BOT=BIG-RINK
KC=0
DO 7 K=1,41
  IC=0
  DO 6 I=1,101
    ROW(I)=BL
    IF((I.EQ.1).OR.(I.EQ.51).OR.(I.EQ.101)) ROW(I)=PL
    IF((K.EQ.1).OR.(K.EQ.41)) ROW(I)=PL
    IF((TOP.GE.0).AND.(BOT.LE.0)) ROW(I)=DH
    IF((IC.EQ.0.5) GO TO 3
  GO TO 4
  IC=0
  IF(KC.EQ.10) ROW(I)=PL
  IF(KPT.LE.2) GO TO 5
  IF((D(I).LE.TOP).AND.(D(I).GE.BOT)) ROW(I)=ST
  IF((B(I).LE.TOP).AND.(B(I).GE.BOT)) ROW(I)=EX
  IC=IC+1
  IF(KC.EQ.5) KC=0
  IF(KC.NE.0) WRITE (6,65) (ROW(I),I=1,101)
  IF(KC.EQ.0) WRITE (6,68) CEN,(ROW(I),I=1,101)
  TOP=CEN-2.*RINK
  BOT=CEN-2.*RINK
  KC=KC+1
  WRITE (6,66) (ST,I=1,120)
  FORMAT (1X,F8.3,1X,101A1)
  FORMAT (1H1,121A1)
  FORMAT (10X,101A1)
  RETURN
  END

```

C000018
 C

SUB02220
 SUB02230
 SUB02240
 SUB02250
 SUB02260
 SUB02270
 SUB02280
 SUB02290
 SUB02300
 SUB02310
 SUB02320

```

SUBROUTINE INTERP (A,IM,AS,B,JM,BS)
  INTERP CONVERTS A REGULAR VECTOR A OF IM POINTS TO A REGULAR VECTOR
  B OF JM POINTS. OS=.5 FOR A VECTOR WITH POINTS DEFINED IN THE
  CENTER OF THE INTERVAL, AS AND BS ARE THE % OF AN INTERVAL FROM THE
  EDGE OF THE FIELD TO THE FIRST POINT (.0 OR .5 FOR EDGE OR CENTER
  DEFINED POINTS)

```

```

  DIMENSION A(IM),B(JM)
  RIM=IM
  RJM=JM

```

C
 C
 C
 C
 C
 C

SPL00340
 SPL00350
 SPL00360
 SPL00370
 SPL00380
 SPL00390
 SPL00400
 SPL00410
 SPL00420
 SPL00430

DETERMINE THE COEFFICIENTS TO BE USED IN PERFORMING THE
 INTERPOLATIONS. SEARCH FOR BRACKETING ABSCISSA VALUES IS
 ALWAYS MADE FROM THE REFERENCE LAST USED IN INTERPOLATING.

REFERENCE
 PENNINGTON, RALPH H., "INTRODUCTORY COMPUTER METHODS AND
 NUMERICAL ANALYSIS", THE MACMILLAN COMPANY, NEW YORK, 1965

SPL00440
 SPL00460
 SPL00470
 SPL00480
 SPL00490
 SPL00500
 SPL00510
 SPL00520
 SPL00530
 SPL00540
 SPL00550
 SPL00560
 SPL00570
 SPL00580
 SPL00590
 SPL00600
 SPL00610
 SPL00620
 SPL00630
 SPL00640
 SPL00650
 SPL00660
 SPL00670
 SPL00680
 SPL00690
 SPL00700
 SPL00710
 SPL00720

```

SUBROUTINE SPLINE(X, Y, M, XINT, YINT)
DIMENSION X(M), Y(M), C(4,300)
CALL SPLICO(X, Y, M, C)
K=1
ENTRY SPLINN(X, Y, M, XINT, YINT)
IF(XINT-X(I)) 70,1,2
3 70 K=1
GO TO 7
1 YINT=Y(I)
RETURN
2 IF(XINT-X(K+1)) 6,4,5
4 YINT=Y(K+1)
RETURN
5 K=K+1
71 IF(M-K) 71,71,3
GO TO 7
6 IF(XINT-X(K)) 13,12,11
12 YINT=Y(K)
RETURN
13 K=K-1
GO TO 6
7 PRINT 101, XINT
FORMAT(8H0XINT = E18.9,32H, OUT OF RANGE FOR INTERPOLATION)
101 YINT=(X(K+1)-XINT)*(X(K+1)-XINT)**2+C(3,K))
11 YINT=YINT+(XINT-X(K))*C(2,K)*(XINT-X(K))**2+C(4,K)
RETURN
END
  
```

SPL00730
 SPL00750
 SPL00760
 SPL00770
 SPL00780
 SPL00790

```

SUBROUTINE SPLICO(X, Y, M, C)
DIMENSION X(M), Y(M), C(4,300), D(300), P(300), E(300), A(300,3), B(300),
1Z(300)
MM=M-1
DO 2 K=1,MM
D(K)=X(K+1)-X(K)
  
```

CC
 CC
 CC
 CC
 CC
 CC
 CC

CC

MET00130
MET00140
MET00150
MET00160
MET00170
MET00180
MET00190
MET00200
MET00210
MET00220
MET00230
MET00240
MET00250
MET00260
MET00270
MET00280
MET00290
MET00300
MET00310
MET00320
MET00330
MET00340
MET00350
MET00360
MET00370
MET00380
MET00390
MET00400
MET00410
MET00420
MET00430
MET00440
MET00450
MET00460
MET00470
MET00480
MET00490
MET00500
MET00510
MET00520
MET00530
MET00540
MET00550
MET00560
MET00570
MET00580
MET00590
MET00600

DESCRIPTION OF PARAMETERS

Y -- THE ARRAY TO BE CONTOURED. DIMENSIONED Y(N,M)
 N -- NUMBER OF ROWS IN Y.
 M -- NUMBER OF COLUMNS IN Y.
 T -- ARRAY FOR PLOT TITLE.
 BND -- BANDWIDTH FOR THE CONTOURING. IF BND IS ZERO
 A BANDWIDTH WILL BE CALCULATED AS FOLLOWS
 BND=(MAX(Y)-MIN(Y))/15.
 AZ -- A LINEAR TRANSFORMATION MAYBE PERFORMED ON
 THE ARRAY Y OF THE FOLLOWING FORM AZ*Y+BZ.
 IF AZ=0 THEN AZ WILL BE COMPUTED SUCH THAT
 MAX(|MAX(Y)|,|MIN(Y)|) WILL BE LESS THAN 1,
 AND BZ WILL BE LEFT AS INPUT.
 BZ -- SEE UNDER AZ
 AMIN -- THE LEVEL AT WHICH COUTOURING WILL BEGIN. IF
 AMIN > MIN(Y) THEN AMIN WILL BE CALCULATED
 TO BE WITH REFERENCE AT ZERO, THE NEXT LOWER
 CONTOUR LEVEL FROM MIN(Y) AS DETERMINED BY
 BND.
 IJT -- IF IJT=0 AMIN WILL BE CALCULATED AS DESCRIBED
 ABOVE.
 ICON -- IF ICON=0 NO CONTOURING WILL BE DONE BUT THE
 ARRAY Y WILL BE PRINTED IN THE PLOT FORMAT.

REMARKS

MTMPII REQUIRES A PRINTER WITH 132 PRINT POSITIONS.
 IF NECESSARY THE MAP WILL BE SEGMENTED COLUMNWISE.
 THE ROWS AND COLUMNS ARE NUMBERED ALONG THE EDGES SO
 THAT A SEGMENTED MAP MAYBE EASILY JOINED TOGETHER.
 ONLY THREE SIGNIFICANT FIGURES WILL BE PRINTED AT
 EACH POINT. THE POSITION OF THE FIRST SIGNIFICANT
 DIGIT WILL BE DETERMINED BY MAX(|MAX(Y)|,|MIN(Y)|).
 THE PLOT WILL BE PRODUCED ON A INCH INCH GRID. IT
 WILL BE ASSUMED THAT THE SPACING BETWEEN POINTS IN
 BOTH DIRECTIONS IS THE SAME AND EQUAL FOR ALL POINTS

SUBROUTINES REQUIRED

NONE

METHOD

THE CONTOUR LEVELS ARE DETERMINED BY SIMPLE LINEAR
 INTERPOLATION FROM THE FOUR SURROUNDING PIONTS.

MTMPII SUBROUTINE FOR ONE-INCH GRID SPACING

C OAKES CODE 5105 15 JAN 69

MET00610
MET00620

SUBROUTINE MTPJ1(Y,N,M,T,BND,AZ,BZ,AMIN,IJT,ICON)
REAL*4 IH,KG,ITJZ
DIMENSION A(140),B(140),C(140),D(140),IH(20),Y(N,M),IP(10),TPX(10)
Z,TPM(10),XMT(10),BTM(10),BTX(10),BT(10),KG(10),T(24)
DIMENSION E(140),F(140),G(140),H(140)

MET00630
MET00640
MET00650
MET00660
MET00670
MET00680
MET00690
MET00700
MET00710
MET00720
MET00730
MET00740
MET00750
MET00760
MET00770
MET00780
MET00790
MET00800
MET00810
MET00820
MET00830
MET00840
MET00850
MET00860
MET00870
MET00880
MET00890
MET00900
MET00910
MET00920
MET00930
MET00940
MET00950
MET00960
MET00970
MET00980
MET00990
MET01000
MET01010
MET01020
MET01030
MET01040
MET01050
MET01060

DATA DUE/4H /,EPL/4H+ /,EMI/4H- /,IH/1H0,1H,1H1,1H,1H2,
1H3,1H4,1H5,1H6,1H7,1H8,1H9,1H /,KG/
21H0,1H1,1H2,1H3,1H4,1H5,1H6,1H7,1H8,1H9/,BLK/4H

MET00740
MET00750
MET00760
MET00770
MET00780
MET00790
MET00800
MET00810
MET00820
MET00830
MET00840
MET00850
MET00860
MET00870
MET00880
MET00890
MET00900
MET00910
MET00920
MET00930
MET00940
MET00950
MET00960
MET00970
MET00980
MET00990
MET01000
MET01010
MET01020
MET01030
MET01040
MET01050
MET01060

YMIN=Y(1,1)
YMAX=Y(1,1)
DO 20 I=1,M
DO 10 J=1,N
YMIN=AMINI(YMIN,Y(J,I))
YMAX=AMAXI(YMAX,Y(J,I))
CONTINUE

MET00740
MET00750
MET00760
MET00770
MET00780
MET00790
MET00800
MET00810
MET00820
MET00830
MET00840
MET00850
MET00860
MET00870
MET00880
MET00890
MET00900
MET00910
MET00920
MET00930
MET00940
MET00950
MET00960
MET00970
MET00980
MET00990
MET01000
MET01010
MET01020
MET01030
MET01040
MET01050
MET01060

10 CONTINUE
20 DELY=YMAX-YMIN
IF(BND) 25,25,30
25 BND=DELY/15.0
30 IF (AMIN-YMIN) 31,31,32
31 IF (IJT) 33,32,33
32 PD=YMIN/BND
PF=ABS(PD-INT(PD))
IF (YMIN) 2,1,1
1 AMIN=YMIN-PF*BND
GO TO 33

MET00740
MET00750
MET00760
MET00770
MET00780
MET00790
MET00800
MET00810
MET00820
MET00830
MET00840
MET00850
MET00860
MET00870
MET00880
MET00890
MET00900
MET00910
MET00920
MET00930
MET00940
MET00950
MET00960
MET00970
MET00980
MET00990
MET01000
MET01010
MET01020
MET01030
MET01040
MET01050
MET01060

2 AMIN=YMIN-(1.0-PF)*BND
3 AHLD=AZ
33 IF(AZ) 55,35,55
35 SM=AMAX1(ABS(YMIN),ABS(YMAX))
NS=0
40 NS=NS+1
SM=10.0*SM
IF(SM-1.0) 40,50,45
45 NS=NS-1
SM=SM/10.0
IF(SM-1.0) 50,50,45
50 AHLD=10.0**NS
55 HBND=BND/2.0
PRINT 70
PRINT 6,T

MET00740
MET00750
MET00760
MET00770
MET00780
MET00790
MET00800
MET00810
MET00820
MET00830
MET00840
MET00850
MET00860
MET00870
MET00880
MET00890
MET00900
MET00910
MET00920
MET00930
MET00940
MET00950
MET00960
MET00970
MET00980
MET00990
MET01000
MET01010
MET01020
MET01030
MET01040
MET01050
MET01060


```

6  FORMAT(5X,24A4,/)
   PRINT 57,AHLD,BZ
57  FORMAT(1H0,65H THE FOLLOWING TRANSFORMATION WAS PERFORMED ON THE IN
   INPUT MATRIX /5X,1H(,E12.5,8H*Y(I,J)+,E12.5,1H) //2X,73HAND THREE
   2 DIGITS TO THE RIGHT OF THE DECIMAL POINT ARE PRINTED IN THE MAP )
C
   PRINT 54,YMAX,YMIN
54  FORMAT(/4X,5HYMAX=,E15.7,5X,5HYMIN=,E15.7)
   IF (ICON)5,58,5
5   PRINT 11,BND
11  FORMAT(2X,17H THE BAND WIDTH IS,E12.5,6H UNITS //4X,14H CONTOUR LEVE
11S
   I=0
   YTOP=AMIN
   IF (ABS(YMIN-YMAX)-100.0*BND)53,53,58
53  YB=YTOP
   YTOP=YTOP+BND
   I=I+1
   J=MOD(I,20)
   ITJZ=IH(J)
   IF(YB-YMAX)59,58,58
59  PRINT 61,YB,YTOP,ITJZ
61  FORMAT(/4X,E10.3,4H TO ,E10.3,2H =,1X,A1)
   GO TO 53
58  NCCP=0
   NCP=0
60  PRINT 70
70  FORMAT(1H1)
   PRINT 6,T
   NLINE=0
   NCCP=NCP+1
73  IF(NCP-M)80,80,75
75  NCP=M
80  CONTINUE
   J=-2
   NLINE=NLINE+1
   LLINE=NLINE+1
   UP HEADING
   IF(NCCP-1) 85,85,90
85  J = - 1
90  DO 100 I = 1,135
   A(I)=BLK
   B(I)=BLK
   H(I) = BLK
100 CONTINUE
110 DO 160 L=NCCP,NCP
   J = J+8
MET01070
MET01080
MET01090
MET01100
MET01110
MET01120
MET01130
MET01140
MET01150
MET01160
MET01170
MET01180
MET01190
MET01200
MET01210
MET01220
MET01230
MET01240
MET01250
MET01260
MET01270
MET01280
MET01290
MET01300
MET01310
MET01320
MET01330
MET01340
MET01350
MET01360
MET01370
MET01380
MET01390
MET01400
MET01410
MET01420
MET01430
MET01440
MET01450
MET01460
MET01470
MET01480
MET01490
MET01500
MET01510
MET01520
MET01530
MET01540

```


MET01550
 MET01560
 MET01570
 MET01580
 MET01590
 MET01600
 MET01610
 MET01620
 MET01630
 MET01640
 MET01650
 MET01660
 MET01670
 MET01680
 MET01690
 MET01700
 MET01710
 MET01720
 MET01730
 MET01740
 MET01750
 MET01760
 MET01770
 MET01780
 MET01790
 MET01800
 MET01810
 MET01820
 MET01830
 MET01840
 MET01850
 MET01860
 MET01870
 MET01880
 MET01890
 MET01900
 MET01910
 MET01920
 MET01930
 MET01940
 MET01950
 MET01960
 MET01970
 MET01980
 MET01990
 MET02000
 MET02010
 MET02020

```

    KI=L
    IF(KI-100) 130,120,120
    LL=KI/100
    A(J)=KG(LL+1)
    KI=KI-100*LL
    GO TO 135
    A(J)=KG(I)
    J=J+1
    IF(KI-10) 150,140,140
    LL=KI/10
    A(J)=KG(LL+1)
    KI=KI-10*LL
    GO TO 155
    A(J)=KG(I)
    J=J+1
    A(J)=KG(KI+1)
    CONTINUE
    C SETUP FIRST ROW OF ARRAY
    GO TO 260
    NLINE=NLINE+1
    LL=NL-NLINE+1
    IF(NLINE-N) 180,180,380
    DO 190 I=1,135
    A(I)=BLK
    B(I)=BLK
    C(I)=BLK
    D(I)=BLK
    E(I) = BLK
    F(I) = BLK
    G(I) = BLK
    H(I) = BLK
    CONTINUE
    IF (ICON)195,260,195
    190 NCY=NCCP-I
    J=4
    IF(NCY)200,200,210
    J=5
    NCY=NCY+1
    IF(NCY-NCP) 220,220,260
    IF(NCY-M) 230,260,260
    NLINE = NLINE - 1
    YDI = Y(NLINE,NCY) - Y(NLINE+1,NCY)
    YD2=Y(NLINE,NCY+1)-Y(NLINE+1,NCY+1)
    TP(I) = Y(NLINE,NCY)-0.125*YDI
    TPX(I)=Y(NLINE,NCY)-0.250*YDI
    TPI(I)=Y(NLINE,NCY)-0.375*YDI
    XMT(I)=Y(NLINE,NCY)-0.500*YDI
    BTM(I)=Y(NLINE,NCY)-0.625*YDI
  
```


MET02030
 MET02040
 MET02050
 MET02060
 MET02070
 MET02080
 MET02090
 MET02100
 MET02110
 MET02120
 MET02130
 MET02140
 MET02150
 MET02160
 MET02170
 MET02180
 MET02190
 MET02200
 MET02210
 MET02220
 MET02230
 MET02240
 MET02250
 MET02260
 MET02270
 MET02280
 MET02290
 MET02300
 MET02310
 MET02320
 MET02330
 MET02340
 MET02350
 MET02360
 MET02370
 MET02380
 MET02390
 MET02400
 MET02410
 MET02420
 MET02430
 MET02440
 MET02450
 MET02460
 MET02470
 MET02480
 MET02490
 MET02500

BTX(1)=Y(NLINE,NCY)-0.750*YD1
 BT(1)=Y(NLINE,NCY)-0.875*YD1
 TP(10)=Y(NLINE,NCY+1)-0.125*YD2
 TPX(10)=Y(NLINE,NCY+1)-0.250*YD2
 XMT(10)=Y(NLINE,NCY+1)-0.375*YD2
 BTM(10)=Y(NLINE,NCY+1)-0.500*YD2
 BTX(10)=Y(NLINE,NCY+1)-0.625*YD2
 BT(10)=Y(NLINE,NCY+1)-0.750*YD2
 NLINE = NLINE + 1
 D1=0.1*(TP(10)-TP(1))
 D2=0.1*(TPX(10)-TPX(1))
 D3=0.1*(XMT(10)-XMT(1))
 D4=0.1*(BTM(10)-BTM(1))
 D5=0.1*(BTX(10)-BTX(1))
 D6=0.1*(BT(10)-BT(1))
 D7=0.1*(BT(10)-BT(1))
 DO 240 I = 2,9
 TP(I)=TP(I-1)+D1
 TPX(I)=TPX(I-1)+D2
 XMT(I)=XMT(I-1)+D3
 BTM(I)=BTM(I-1)+D4
 BTX(I)=BTX(I-1)+D5
 BT(I)=BT(I-1)+D6
 BT(I)=BT(I-1)+D7
 CONTINUE
 DO 250 I=1,10
 J=J+1
 I1=MOD(IFIX((TP(I)-AMIN)/BND),20)+1
 I2=MOD(IFIX((TPX(I)-AMIN)/BND),20)+1
 I3=MOD(IFIX((XMT(I)-AMIN)/BND),20)+1
 I4=MOD(IFIX((BTM(I)-AMIN)/BND),20)+1
 I5=MOD(IFIX((BTX(I)-AMIN)/BND),20)+1
 I6=MOD(IFIX((BT(I)-AMIN)/BND),20)+1
 I7=MOD(IFIX((BT(I)-AMIN)/BND),20)+1
 A(J)=IH(I1)
 B(J)=IH(I2)
 C(J)=IH(I3)
 D(J)=IH(I4)
 E(J)=IH(I5)
 F(J)=IH(I6)
 G(J)=IH(I7)
 CONTINUE
 GO TO 210
 250
 260 NCCP-1
 J=-2
 IF(NCY) 265,265,270
 J=-1
 265

MET02510
 MET02520
 MET02530
 MET02540
 MET02550
 MET02560
 MET02570
 MET02580
 MET02590
 MET02600
 MET02610
 MET02620
 MET02630
 MET02640
 MET02650
 MET02660
 MET02670
 MET02680
 MET02690
 MET02700
 MET02710
 MET02720
 MET02730
 MET02740
 MET02750
 MET02760
 MET02770
 MET02780
 MET02790
 MET02800
 MET02810
 MET02820
 MET02830
 MET02840
 MET02850
 MET02860
 MET02870
 MET02880
 MET02890
 MET02900
 MET02910
 MET02920
 MET02930
 MET02940
 MET02950
 MET02960
 MET02970
 MET02980

```

270 GO TO 330
    NCY=NCY+1
    IF(NCY-NCP) 280,280,310
280 J=J+7
    THLD=AHLD*Y(NLINE,NCY)+BZ
    IF(THLD) 285,290,290
285 H(J)=EMI
    GO TO 295
290 H(J)=EPL
295 NUM=INT((ABS(THLD-INT(THLD)))*1000.0+0.5)
    NDS=100
    DO 300 KK=1,3
      J=J+1
      KI=NUM/NDS
      H(J)=KG(KI+1)
      NUM=NUM-KI*NDS
      NDS=NDS/10
    CONTINUE
300 GO TO 270
310 IF(NCP-M) 360,320,320
320 IF(J-127)330,330,360
330 J=J+3
      KI=NLINE
      IF(KI-100) 340,335,335
      LL=KI/100
      H(J)=KG(LL+1)
      KI=KI-100*LL
      GO TO 343
340 H(J)=KG(1)
343 J=J+1
      IF(KI-10) 350,345,345
345 LL=KI/10
      H(J)=KG(LL+1)
      KI=KI-10*LL
      GO TO 355
350 H(J)=KG(1)
355 J=J+1
      H(J)=KG(KI+1)
      J=J-5
360 IF(NLINE-1)362,362,368
362 PRINT 370,(A(I),I=1,132),(B(IP1),IP1=1,132),(H(IP2),IP2=1,132)
368 PRINT 370,(A(I),I=1,132),(B(IP1),IP1=1,132),(C(IP2),IP2=1,132),
      1(D(IP3),IP3=1,132),(E(IP4),IP4=1,132),(F(IP5),IP5=1,132),
      2(G(IP6),IP6=1,132),(H(IP7),IP7=1,132)
370 FCORMAT(132A1)
    GO TO 170
  
```



```

380 DO 390 I=1,135
    A(I)=BLK
    B(I)=BLK
    C(I)=BLK
    D(I)=BLK
    CONTINUE
390 J=-2
    IF(NCCP-1) 395,395,400
    J=-1
    DO 430 L=NCCP,NCP
    J=J+8
    KI=L
    IF(KI-100) 410,405,405
    LL=KI/100
    C(J)=KG(LL+1)
    KI=KI-100*LL
    GO TO 412
    C(J)=KG(I)
    J=J+1
    IF(KI-10) 420,415,415
    LL=KI/10
    C(J)=KG(LL+1)
    KI=KI-10*LL
    GO TO 422
    C(J)=KG(I)
    J=J+1
    C(J)=KG(KI+1)
    CONTINUE
430 PRINT 370, (B(IP1), IP1=1,132), (C(IP2), IP2=1,132)
    IF(NCP-M)60,500,500
500 RETURN
    END

```

```

C000021
C .....
C SUBROUTINE GAUSS
C .....
C PURPOSE
C COMPUTES A NORMALLY DISTRIBUTED RANDOM NUMBER WITH A GIVEN
C MEAN AND STANDARD DEVIATION
C .....
C USAGE
C CALL GAUSS(I,X,S,AM,V)
C .....
C DESCRIPTION OF PARAMETERS
C .....
GAUS 10
GAUS 20
GAUS 30
GAUS 40
GAUS 50
GAUS 60
GAUS 70
GAUS 80
GAUS 90
GAUS 100
GAUS 110
GAUS 120
GAUS 130

```



```
SUBROUTINE RANDU(IX,IY,YFL)
  IY=IX#65539
  IF(IY) 5,6,6
  5 IY=IY+2147483647+1
  6 YFL=IY
  YFL=YFL*.4656613E-9
  RETURN
END
```

```
RAND 540
RAND 550
RAND 560
RAND 570
RAND 580
RAND 590
RAND 600
```


LIST OF REFERENCES

1. Heflinger, L. O., Wuerker, R. F., and Brooks, R. E., "Holographic Interferometry," Journal of Applied Physics, Vol. 37, No. 2, pp. 642-649, February 1966.
2. Brooks R. E., Heflinger, L. O., and Wuerker, R. F., "9A9 - Pulsed Laser Holograms," IEEE Journal of Quantum Electronics, Vol. EQ-2, No. 8, pp. 275-299, August 1966.
3. Matulka, R. D., The Application of Holographic Interferometry to The Determination of Asymmetric Three-Dimensional Density Fields in Free Jet Flow, PhD Thesis, Naval Postgraduate School, June 1970.
4. Matulka, R. D., and Collins, D. J., "Determination of Three-Dimensional Density Fields From Holographic Interferograms," Journal of Applied Physics, Vol. 42, No. 3, pp. 1109-1119, March 1971.
5. Maldonado, C. D., Caron, A. P., and Olsen, H. N., "New Method for Obtaining Emission Coefficients from Emitted Spectral Intensities. Part I - Circularly Symmetric Light Sources," Journal of The Optical Society of America, Vol. 55, No. 10, pp. 1247-1254, October 1965.
6. Maldonado, C. D., and Olsen, H. N., "New Method for Obtaining Emission Coefficients from Emitted Spectral Intensities. Part II - Asymmetric Sources," Journal of The Optical Society of America, Vol. 56, No. 10, pp. 1305-1312, October 1966.
7. Jagota, R. C., The Application of Holographic Interferometry to The Determination of The Flow Field Around a Right Circular Cone At Angle of Attack, Aeronautical Engineer's Thesis, Naval Postgraduate School, December 1970.
8. Jagota, R. C., and Collins, D. J., "Finite Fringe Holographic Interferometry Applied to A Right Circular Cone At Angle of Attack," ASME Paper No. 72-APM-PP, to appear in the Journal of Applied Mechanics.
9. Heyer, R. W., Holographic Interferometry of The Flow Field Between A Fin and Flat Plate, Master's Thesis, Naval Postgraduate School, March 1972.

10. Liepmann, H. W., and Roshko, A., Elements of Gas Dynamics, p. 165, John Wiley and Sons, Inc., 1957.
11. Collier, R. J., and others, Optical Holography, sect. 10.8.4, Academic Press, 1971.
12. Sweeney, D. W., and Vest, C. M., "Reconstruction of Three-Dimensional Refractive Index Fields by Holographic Interferometry," Applied Optics, Vol. 11, No. 1, pp. 205-207, January 1972.
13. Van Houten, P. E., Analysis of Discontinuous Three-Dimensional Density Fields Using Holographic Interferometry, Aeronautical Engineer's Thesis, Naval Postgraduate School, December 1972.
14. Junginger, H. G., and van Haeringen, W., "Calculation of Three-Dimensional Refractive Index Fields Using Phase Integrals," to appear in Optics Communications.

INITIAL DISTRIBUTION LIST

	No. Copies
1. Defense Documentation Center Cameron Station Alexandria, Virginia 22314	2
2. Library, Code 0212 Naval Postgraduate School Monterey, California 93940	2
3. Professor D. J. Collins, Code 57Co Department of Aeronautics Naval Postgraduate School Monterey, California 93940	1
4. LT Robert A. Kosakoski, USN The Arches, Apt #77 1235 Wildwood Avenue Sunnyvale, California 94086	1
5. Chairman, Department of Aeronautics Naval Postgraduate School Monterey, California 93940	1

DOCUMENT CONTROL DATA - R & D

(Security classification of title, body of abstract and indexing annotation must be entered when the overall report is classified)

1. ORIGINATING ACTIVITY (Corporate author) Naval Postgraduate School Monterey, California 93940		2a. REPORT SECURITY CLASSIFICATION Unclassified	
		2b. GROUP	
3. REPORT TITLE Application of Holographic Interferometry to Density Field Determination in Transonic Corner Flow			
4. DESCRIPTIVE NOTES (Type of report and, inclusive dates) Master's Thesis; December 1972			
5. AUTHOR(S) (First name, middle initial, last name) Robert A. Kosakoski			
6. REPORT DATE December 1972		7a. TOTAL NO. OF PAGES 120	7b. NO. OF REFS 14
8a. CONTRACT OR GRANT NO.		9a. ORIGINATOR'S REPORT NUMBER(S)	
b. PROJECT NO.			
c.		9b. OTHER REPORT NO(S) (Any other numbers that may be assigned this report)	
d.			
10. DISTRIBUTION STATEMENT			
11. SUPPLEMENTARY NOTES		12. SPONSORING MILITARY ACTIVITY Naval Postgraduate School Monterey, California 93940	
13. ABSTRACT The successful application of holographic interferometry to the study of density fields around opaque bodies in wind tunnel experiments has been reported in the literature. The present report extends this technique to the study of the three-dimensional asymmetric flow fields encountered near the wing-fuselage junction of an aerodynamic model in the transonic flow regime. Finite fringe interferometry has been used to obtain fringe information about a partially transparent wind-body structure. A FORTRAN computer program was utilized to invert the fringe information and produce a plot of the density field around the model. The resulting asymmetric density field and shock wave structure are shown to be an accurate representation of the phenomena encountered in aerodynamic corner flow.			

14. KEY WORDS	LINK A		LINK B		LINK C	
	ROLE	WT	ROLE	WT	ROLE	WT
Holography						
Interferometry						
Transonic Flow						
Corner Flow						
Transparent Phase Object						
Aerodynamic Model						
Wing-Fuselage Junction						

1 MAR 74

20978

Thesis

141295

K823 Kosakoski

c.1

Application of holo-
graphic interferometry to
density field determi-
nation in transonic
corner flow.

1 MAR 74

20978

Thesis

141295

K823 Kosakoski

c.1

Application of holo-
graphic interferometry to
density field determi-
nation in transonic
corner flow.

thesK823

Application of holographic interferometr



3 2768 002 10495 2

DUDLEY KNOX LIBRARY